Human and zoonotic *Chlamydia* species interact with Golgi-dependent vesicular and non-vesicular trafficking pathways

Inaugural-Dissertation
to obtain the academic degree
Doctor rerum naturalium (Dr. rer. nat.)

submitted to the Department of Biology, Chemistry and Pharmacy
of Freie Universität Berlin

by
Sophia Edelmann
from Gera

2016

Diese Arbeit wurde von Januar 2012 bis January 2016 in der Nachwuchsgruppe "Sexuell übertragbare bakterielle Krankheitserreger" am Robert Koch-Institut unter der Leitung und Betreuung von Dr. Dagmar Heuer angefertigt.

This work was realized from January 2012 till January 2016 in the Junior Research Group "Sexually Transmitted Bacterial Pathogens" at the Robert Koch Institute, Berlin and was supervised by Dr. Dagmar Heuer.

1st Reviewer: Dr. Dagmar Heuer
2nd Reviewer: Prof. Dr. Markus C. Wahl

Date of thesis defense: **May 24, 2016**

“Indes sie forschten, röntgten, filmten, funkten, entstand von selbst die köstlichste Erfindung:der Umweg als die kürzeste Verbindung zwischen zwei Punkten.”

Erich Kästner

Zusammenfassung

Chlamydien sind gram-negative, obligat intrazelluläre Bakterien, die verschiedene Krankheiten in Menschen und Tieren auslösen. Um sich in der so genannten Inklusion, einem membranumschlossenen Kompartiment zu vermehren, nutzen Chlamydien unterschiedliche Wirtszellprozesse, die für den Nährstofftransport, im Besonderen von Sphingolipiden, verantwortlich sind. Der humanpathogene Erreger *C. trachomatis* induziert die Fragmentierung des Golgi Apparats, rekrutiert kleine Golgi Stapel und sichert somit die Versorgung mit Sphingolipiden. Die Fragmentierung des Golgi Apparats soll dabei durch eine chlamydienabhängige Spaltung von golgin-84 ausgelöst werden. Die vorliegende Arbeit zeigt, dass golgin-84, ein wichtiges Strukturprotein des Golgi Apparates und Regulierer des retrograden Transports, an die Inklusion von *C. trachomatis* rekrutiert wird. In lebenden Zellen konnte zudem durch Überexpression einer doppelt markierten golgin-84-Mutante eine mögliche Spaltung dieses Proteins gezeigt werden. Diese Daten deuten darauf hin, dass golgin-84 die Aufnahme besonders nährstoffreicher golgin-84-positiver Strukturen zu verbessert und dabei möglicherweise der bakteriellen Entwicklung dient.

Weiterhin zeitgt diese Studie, dass sogar der zoonotische Erreger *C. psittaci* eine Umorganisation des Golgi Apparats humaner Zellen auslöst. Der Phänotyp und die Verteilung der Golgi Elemente unterscheiden sich jedoch in Infektionen mit *C. trachomatis* oder *C. psittaci*. Auch die Interaktionen zwischen Bakterien und Struktur- und Transportproteinen des Golgi Apparats, erwiesen sich als artspezifisch. Dabei schien *C. psittaci* nur wenige vesikuläre Transportwege auszunutzen, wohingegen beide Bakterienarten mit dem nicht-vesikulären Ceramidtransport durch CERT interagierten. Dass CERT für die chlamydiale Entwicklung essentiell ist und mehrere Aspekte der Infektion in artspezifischer Weise beeinflusst, wurde durch Inhibitionsstudien mit dem Ceramidanalogon HPA-12 bestätigt.

Um die Bedeutung von Golgi Fragmentierung und CERT für Chlamydien zu ermitteln, wurde die Sphingolipidzusammensetzung infektiöser Partikel mittels Massenspektrometrie bestimmt. Diese umfangreiche Analyse zeigte zum ersten Mal eine artspezifische Verteilung von Sphingolipiden im humanen und im zoonotischen Erreger.

Insgesamt zeigt diese Studie, dass eine Golgi Fragmentierung in humanen Zellen sowohl die humane als auch die zoonotische Chlamydieninfektion kennzeichnet wobei die Phänotypen der Fragmentierung für die jeweilige Chlamydienart spezifisch sind. Auch die Interaktion mit vesikulären und nicht-vesikulären Transportwegen des Golgi Apparats erfolgt artspezifisch. Dabei hängt die bakterielle Entwicklung stark von der Interaktion mit CERT ab. Diese Daten, ergänzt durch quantitative Sphnigolipidanalysen, erweitern unser Wissen über chlamydiale Interaktionsmechanismen und betonen die aufsteigende Bedeutung von Sphingolipiden als Ansatzpunkt zur Entwicklung antichlamydialer Wirkstoffe.

Abstract

Chlamydia spp. are gram-negative obligate intracellular bacteria causing different diseases in humans and animals. To live inside a membrane bound vacuole, termed 'inclusion', *Chlamydia* spp. hijack diverse host cell processes, that support nutrient and in particular sphingolipid acquisition. The human pathogen *C. trachomatis* induces Golgi fragmentation, recruits Golgi ministacks and thereby ensures sphingolipid supply. *C. trachomatis*-dependent processing of golgin-84, regulator of Golgi structure and retrograde trafficking, was proposed to trigger this process. Here, a detailed mutational analysis of golgin-84 revealed that golgin-84 localizes to *C. trachomatis* inclusions and is likely to be processed in a subset of living cells. Since recruitment of golgin-84 supported bacterial development, it can be assumed that the acquisition of specific golgin-84 positive compartments that supply *C. trachomatis* with metabolites fuel bacterial development.

Golgi fragmentation is induced by various human-adapted *Chlamydia* spp. This study demonstrates that even zoonotic *C. psittaci* rearrange the Golgi apparatus in human cells. Phenotypic appearance and distribution of Golgi elements were however distinct in *C. trachomatis* and *C. psittaci* infections. Concomitant, species-specific interactions between bacteria and mediators of Golgi structure and trafficking were observed. Here, *C. psittaci* seemed to scavenge a reduced set of vesicular trafficking routes whereas the interaction with non-vesicular transport of ceramide via CERT was conserved among human and zoonotic species. Inhibitor studies, using the ceramide analogue HPA-12, further verified that CERT is required for chlamydial biogenesis and, in a species-specific manner, interferes with various aspects of chlamydial infections.

To elucidate the biological relevance of Golgi fragmentation and CERT for sphingolipid acquisition and bacterial infectivity, the sphingolipid composition of infectious chlamydial particles was determined by mass spectrometry. Here, for the first time, a comprehensive description of the sphingolipid composition of infectious EBs revealed characteristics for human and zoonotic *Chlamydia* spp.

In sum, this study shows that Golgi fragmentation in human cells is a hallmark of human and zoonotic chlamydial infections. However, phenotypes of Golgi fragmentation are species-specific. Along with this, bacteria interact with Golgi-dependent vesicular and non-vesicular transport routes in a species-specific manner. CERT-dependent ceramide transport is essential for the development of both chlamydial species. These results, together with quantitative sphingolipid analyses foster our knowledge of the pathogen's repertoire to exploit host sphingolipid trafficking and emphasize the emerging role of sphingolipids as targets for novel antichlamydial interventions.

Table of contents

1 Introduction

1.1 The pathogen *Chlamydia*

The order *Chlamydiales* comprises a variety of gram-negative obligate intracellular bacteria that infect a large range of host organisms. The human pathogen *Chlamydia trachomatis* causing ocular and genital infections is the most prominent member of this order. Other *Chlamydiales* even have zoonotic potential and, in various cases, cause severe disease in human or animals. The precise mechanisms and occasions of zoonotic transmission are not well understood and research on zoonotic chlamydial strains is nowadays still neglected (Longbottom & Coulter, 2003, Knittler & Sachse, 2015).

Despite species-specific preferences for infecting distinct hosts, all *Chlamydiales* share an exceptional biphasic developmental cycle. To establish and maintain this specialized intracellular lifestyle a close interplay with the host cell is required. Thus, these bacteria have developed complex mechanisms to interact with their hosts (Su *et al.*, 2004, Jewett *et al.*, 2006, Ying *et al.*, 2006, Aeberhard *et al.*, 2015). The intracellular lifestyle and strong host dependency were the reasons for researcher of the early years to mistake chlamydial agents for protozoans or viruses, assumptions that were just revised in the late 60's of the last century (Moulder, 1966). Within this decade, incremental improvements in electron microscopic techniques and instrumentation fueled the description of chlamydial fine structures and gave insights into their bacterial characteristics (Tamura *et al.*, 1967, Matsumoto & Manire, 1970). The description of chlamydial agents was, however, restricted to two species – the human-pathogen *C. trachomatis* and avian pathogenic *C. psittaci* (Page, 1966).

Over the years, more and more members of *Chlamydiales* were identified and the enormous advances of the genomic era finally provided access to evolutionary traits. Modern pathogenic *Chlamydiaceae* separated from their environmental relatives more than 700 million years ago (Horn *et al.*, 2004). Since then, due to the outstanding developmental cycle and the restriction to specialized intracellular niches, pathogenic *Chlamydiaceae* massively reduced their genome size. About 560 core genes are conserved among all *Chlamydiales* and encode among others proteins of a well-developed Type three secretion system (T3SS), ATP binding cassette transporters and diverse virulence factors (Stephens *et al.*, 1998, Kalman *et al.*, 1999, Collingro *et al.*, 2011). The remaining species-specific protein coding genes are most likely involved in defining host and tissue tropism.

The connection between genetic diversity, tissue tropism and disease severity is nonetheless poorly understood. To refine diagnostic and therapeutic approaches and improve treatment of medically important human, animal and zoonotic chlamydiosis, studies of specific host-pathogen interactions are urgently needed.

1.1.1 Taxonomy of *Chlamydia*

In 1998, the first genome sequence of a *C. trachomatis* strain was published and gave initial insights into the complex genetic adaptation of this pathogen (Stephens *et al.*, 1998). Today, thanks to continual improvements in whole genome sequencing techniques, the number of publicly available genomes is steadily increasing and enhances our understanding of chlamydial evolution.

The modern taxonomic classification of *Chlamydia* is based on very precise 16S rRNA sequence data as well as on relevant phenotypical and biochemical features. The family *Chlamydiaceae*, originating from the order *Chlamydiales*, encloses the genus *Chlamydia* that can be divided into 11 species, with distinct host ranges (Sachse *et al.*, 2015) (Figure 1.1).

When the first phylogenetic analyses based on 16S and 23S rRNA sequence data were published, Everett and colleagues proposed the introduction of two genera *Chlamydia* and *Chlamydophila* (Everett *et al.*, 1999, Bush & Everett, 2001) (Figure 1.1). The proposal quickly met opposition and the new classification was largely rejected by the chlamydial community (Schachter *et al.*, 2001). Indeed, analyses on a whole genome level demonstrated that gene order and content (syntheny), a large set of insertions and deletions as well as fundamental phenotypic characteristics are conserved among all *Chlamydiaceae,* which provides strong evidence for the classification of *Chlamydia* into one single genus (Griffiths *et al.*, 2006, Gupta & Griffiths, 2006). In 2009 Stephen and colleagues finally reclaimed to use the one genus classification (Stephens *et al.*, 2009). Even though an ultimate agreement on one classification system is missing, this thesis, as well as the majority of publications, refers to the classification proposed by Stephens *et al.* which was further extended by Sachse *et al.* (Stephens *et al.*, 2009, Sachse *et al.*, 2015).

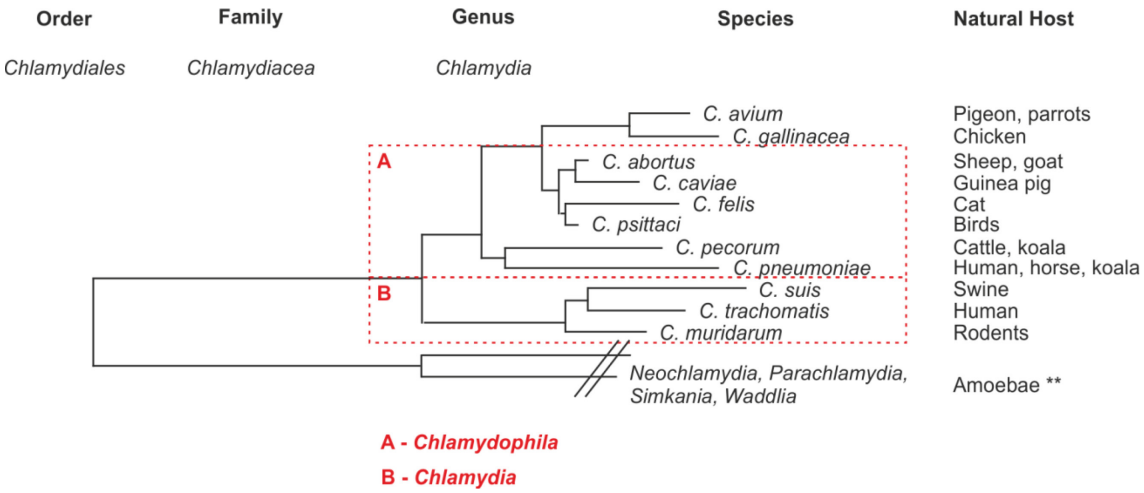

Figure 1.1 The order Chlamydiales encloses the genus *Chlamydia* that is subdivided in 11 species.
Phylogenetic reconstruction of the order *Chlamydiales,* as proposed by Sachse *et al.,* 2015 based on almost full-length 16S rRNA genes are shown. rRNA genes from type strains of established *Chlamydia* species (spp.) were used, including the recently proposed new species *C. avium* and *C. gallinacea*. Branch lengths are measured in nucleotide substitutions; slashes indicate simplification or pooling of branches. Dashed boxes enclose all species formerly divided in (A) *Chlamydophila* and (B) *Chlamydia* according to Everett *et al.,* 1999. On the right, natural hosts usually infected by respective *Chlamydia* spp. are stated; ** alternative host range possible.

1.1.2 Medical importance of *Chlamydia*

Chlamydia infections are found throughout the whole animal kingdom. The diversity of resulting clinical pictures in humans or animals is remarkable and poses a big challenge for the development of diagnostics and treatment.

In humans, *C. trachomatis* is the causative agent of preventable blindness and one of the most common sexually transmitted bacterial pathogens worldwide (WHO, 2012). Ocular infections are caused by *C. trachomatis* subspecies, called serovars, A to C and lead to a scaring of the eyelid. With repeated episodes of infection, eyelids and the cornea become severely scarred which in long term leads to blindness. As the lack of hygienic standards is the primary reason for ocular infections, they are predominantly found in rural Asia and Africa and South and Latin America (WHO, 2012). In industrialized countries, urogenital tract infections caused by *C. trachomatis* serovars D to K are major reasons for acquired infertility. In women urogenital infections are often asymptomatic favoring the unnoticed spread of the pathogen. Here, these undetected chronic infections consequently increase the risk of long term complications such as pelvic inflammatory disease, tubal infertility or ectopic pregnancy. Furthermore, highly infectious *C. trachomatis* lymphogranuloma venereum (LGV) serovars, cause genital ulcers at the site of transmission and often disseminate to the lymph nodes where a local blocking of the lymphatic system result in severe and painful tissue swelling.

Despite the high prevalence of *C. trachomatis* infections, public awareness to this pathogen and the sequelae is alarmingly low and improvements of informative campaigns are essentially needed to reduce *C. trachomatis* cases (BZGA, 2014).

C. pneumoniae is another chlamydial pathogen of high medical importance, tested seropositive in up to 70% of people (Grayston, 2000). In humans, *C. pneumoniae* infects the lungs thereby causing acute pneumonia that can develop into chronic respiratory illness like bronchitis or asthma (Blasi *et al.*, 2009). Moreover, *C. pneumoniae* is likely involved in reactive arthritis and might contributes to coronary heart disease (Zeidler & Hudson, 2014, Grayston *et al.*, 2015). Beside the capability to infect humans, *C. pneumoniae* has zoonotic potential and has already been isolated from marsupials, amphibians and reptiles (Myers *et al.*, 2009).

The third species of *Chlamydia* that is an important threat to human health is *C. psittaci*. Although originating from avian species, *C. psittaci* can be found in a wide range of other hosts. Disease outcome of *C. psittaci* infections is very diverse, in some individuals zoonotic transmission from birds to humans causes fatal cases of respiratory tract infections; in others no symptoms occur (Gaede *et al.*, 2008). Interestingly, the zoonotic agent *C. psittaci* is found in 2.1% of community-acquired pneumonia cases, more often than *C. pneumoniae* (Dumke *et al.*, 2015). Because of its high infectious potential and the facile transmission by contaminated aerosols *C. psittaci* is classified as a bioterrorism agent in the US (CDC, 2009).

Reported cases of zoonotic transmission of other *Chlamydia* spp. are very rare. Human infections with *C. abortus* can cause flu like illnesses and increase the risk abortions in pregnant women (Longbottom & Coulter, 2003). Transmissions of *C. felis* to human individuals might cause eye infections or lead to atypical pneumoniae (Hartley *et al.*, 2001). Despite the relatively low impact on human health, animal chlamydioses caused by these pathogens are considerable problems in veterinary medicine and animal husbandry.

1.1.3 The developmental cycle of *Chlamydia*

A hallmark shared by all *Chlamydiaceae* is their unique biphasic developmental cycle that involves functionally and morphologically distinct bacterial forms (Figure 1.2).

The elementary body (EB), around 0.3 µm in size, is the environmentally resistant but metabolically idle developmental form that initiates the infection. To meet demands on temporal existence in an extracellular space, EBs are structurally very stable. This stability is promoted by a functional peptidoglycan layer and the cross-linking of outer membrane proteins that promote a reduction of the bacterial surface area which further goes along with a histone-mediated condensation of the chromosome (Hatch *et al.*, 1986, Barry *et al.*, 1993, Liechti *et al.*, 2014).

To invade non-phagocytic host cells, EBs attach to the host cell surface and induce their uptake into a specialized phagocytic compartment (Jewett *et al.*, 2006, Hybiske & Stephens, 2007). *Chlamydia*-derived proteins then support a rapid modification of the parasitophorous vacuole that matures to a so-called “inclusion” and escapes the phagolysosomal pathway to avoid degradation (Scidmore *et al.*, 2003). Moreover, Chlamydiae protect their intracellular habitat by modifying host signaling pathways which otherwise would support premature apoptotic and necrotic cell death (Ying *et al.*, 2007). Inside the inclusion which is rerouted to the microtubule organizing center, EBs differentiate into larger (1 - 1.5 µm) reticulate bodies (RBs), the metabolically active and replicative (Grieshaber *et al.*, 2003). As RBs multiply the inclusion expands and bacteria heavily interact with host trafficking pathways to acquire essential nutrients (Hackstadt *et al.*, 1996, Carabeo *et al.*, 2003, Beatty, 2006). Finally, towards the end of the infection cycle, RBs asynchronously re-differentiate into EBs and have to be released to initiate new cycles of infection. In most cases, a sequence of membrane and inclusion permeabilization leads to cell lysis and subsequent EB egress. Alternatively, a packed release mechanism called extrusion has been described, where the inclusion is partially pinched off and emitted in a cell membrane envelope, while host cells are left intact (Hybiske & Stephens, 2007).

Under conditions of nutrient starvation or antibiotic pressure the developmental cycle can be interrupted and RBs differentiate to enlarged viable but non-cultivable aberrant bodies (ABs) (Raulston, 1997, Gieffers *et al.*, 2004). However, upon removal of the stress factor ABs can revert to normal development.

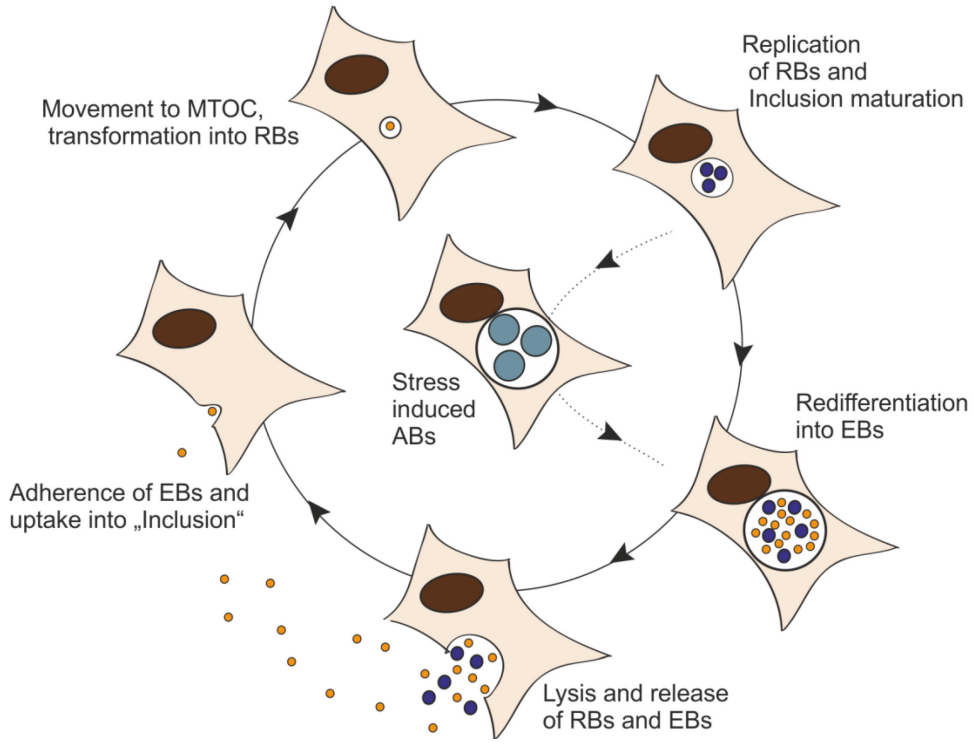

Figure 1.2 The developmental cycle of *Chlamydia*.
Schematic illustration of the chlamydial developmental cycle. Infection of a host cell is initiated by the attachment and invasion of an elementary body (EB) that resides in a membrane bound "inclusion". Within the inclusion EBs differentiate to metabolically active reticulate bodies (RBs) that interact with the host cell to ensure reproduction. When a sufficient number of RBs has formed, they re-differentiate into EBs. EBs are released by cell lysis or by extrusion of the inclusion and can start a new cycle of infection. Poor growth conditions can induce a reversible arrest of growth whereupon RBs transform into enlarged aberrant bodies (ABs).

1.1.4 The chlamydial inclusion as a platform for host-pathogen interactions

To maintain and improve the obligate intracellular lifestyle *Chlamydia* developed a rich repertoire of mechanisms to interact with the host cell (Figure 1.3).

Initiation of chlamydial host cell invasion is supported by the secretion of bacterial effector proteins. Using the T3SS EBs make contact to the host cell and secrete effectors into the host cytosol that subsequently induce reorganization of the host cytoskeleton and thereby promote bacterial uptake into a nascent inclusion (Clifton *et al.*, 2004, Carabeo *et al.*, 2007, Thalmann *et al.*, 2010, Nans *et al.*, 2014). This nascent inclusion escapes the degradative endolysosomal pathway but instead assembles host motor proteins to travel along host microtubules to the microtubule organizing center (MTOC), a hub of protein and lipid trafficking (Grieshaber *et al.*, 2003, Scidmore *et al.*, 2003). At the same time, EBs start to differentiate into RBs. The T3SS already used for invasion, is reassembled in RBs and plays a central role for inclusion biogenesis. By the secretion of effector proteins, in particular hydrophobic inclusion membrane proteins (Incs), the inclusion obtains its characteristic interface which enable *Chlamydia* to selectively interact with host proteins (Subtil *et al.*, 2001, Belland *et al.*, 2003, Dehoux *et al.*, 2011).

Just after invasion, *Chlamydia* interferes with host trafficking pathways to scavenge essential sphingolipids (Hackstadt *et al.*, 1996). Moreover, *Chlamydia* successfully acquires other lipids

such as cholesterol, glycerophospholipids and neutral lipids which contribute to bacterial development and progeny formation (Scidmore *et al.*, 1996, Carabeo *et al.*, 2003, Beatty, 2006, Kumar *et al.*, 2006). Beside lipids, host cell ATP generated at mitochondria and amino acids resulting from lysosomal degradation supply the parasite with energy and nutrients (Derre *et al.*, 2007, Ouellette *et al.*, 2011, Fisher *et al.*, 2013).

Effective nutrient transportation to the inclusion is essential for *Chlamydia* and is therefore sustained by vesicular and non-vesicular trafficking pathways. This becomes apparent by the observation that several Inc proteins bind to and interact with Rab GTPases, mediators of vesicular trafficking. One example, CT229 binds to active Rab4 which usually modulates early and recycling endosomal trafficking (Rzomp *et al.*, 2003, Rzomp *et al.*, 2006). Another example is given by Cpn0585 which selectively recruits Rab1A, Rab11A and Rab10 to *C. pneumoniae* inclusions (Cortes *et al.*, 2007). In both cases the interactions with Rab trafficking pathways promote functional sphingomyelin uptake and iron acquisition to bacteria (Rejman Lipinski *et al.*, 2009, Ouellette *et al.*, 2011). Further, selected species interfere with a non-vesicular ceramide transport route, mediated by ceramide transport protein CERT to ensure RB replication and progeny formation (Derre *et al.*, 2011, Elwell *et al.*, 2011, Dumoux *et al.*, 2012). In case of *C. trachomatis* the inclusion protein IncD is responsible for the interaction between inclusion and CERT (Derre *et al.*, 2011, Agaisse & Derre, 2014).

Recently performed holistic approaches revealed extended insights into the proteome of mid-cycle inclusions and the human interactome of various Inc proteins, and thereby confirmed most of the so far known interaction partners of chlamydial proteins (Aeberhard *et al.*, 2015, Mirrashidi *et al.*, 2015). Beyond a considerable number of yet unknown infection-connected proteins were found which opens the door for new fields in chlamydial research.

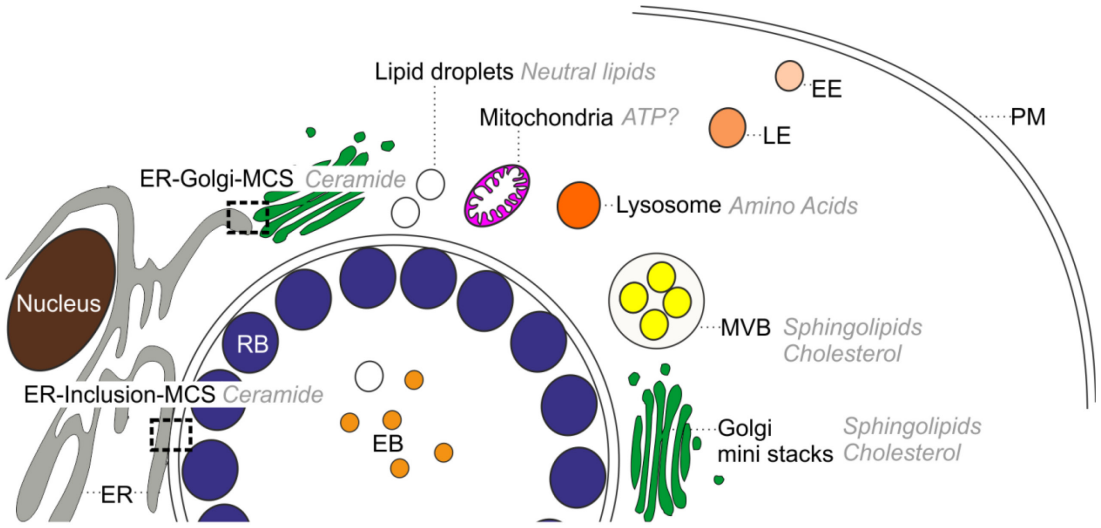

Figure 1.3 *Chlamydia* hijacks diverse host cell functions
Summary of selected interactions of *Chlamydia* with the host cell. Chlamydia reside in a specialized inclusion, characterized by a set of effector proteins (Incs). During RB replication the inclusion expands and Inc proteins recruit and bind various host proteins to facilitate nutrient acquisition from vesicular or non-vesicular pathways. Uptake of lipids is ensured by interactions with Golgi-derived vesicles, multivesicular bodies (MVBs), lipid droplets (LDs) and via membrane contact sites (MCS) to the endoplasmic reticulum (ER). Interactions with lysosomes might provide essential amino acids and some strains further exploit mitochondria as energy sources. Modified from Bastidas *et al.*, 2013.

1.1.5 Diversity of Inc proteins

Inc proteins are involved in interactions between *Chlamydia* and their host cells and are expected to show similarity among different *Chlamydia* spp. (Dehoux *et al.*, 2011, Lutter *et al.*, 2012). Surprisingly, nucleotide and amino acid sequences of Inc proteins are just poorly conserved among different species (Bannantine *et al.*, 2000, Dehoux *et al.*, 2011). However, all Inc proteins have a conserved secondary structure motif, a bilobed hydrophobic domain of 40 to 60 amino acids with non-hydrophobic residues in its middle, which is hardly found in other bacteria (Bannantine *et al.*, 2000). Based on this structural motif, bioinformatic predictions including structural, phylogenetic, and functional features identified numerous Inc proteins in seven *Chlamydia* spp. While the absolute numbers of Inc proteins varied from 92 in *C. pneumoniae* to 54 in *C. muridarum*, a core of 23 Incs was shared by all species (Lutter *et al.*, 2012). The proportion of shared and species-specific Inc proteins might contribute to the respective host tropisms. Nevertheless, functions of predicted Inc proteins are not very well characterized and their existence is not even validated in all strains examined. Furthermore, studies that include zoonotic strains such as *C. psittaci* or *C. abortus* are still missing.

1.2 *Chlamydia* interacts with the host Golgi apparatus

The Golgi apparatus has a central role for protein and lipid trafficking within mammalian cells. It is positioned juxtanuclear at the MTOC and is composed of disk-like membrane cisternae arranged in polarized stacks. Proteins and lipids synthesized in the endoplasmic reticulum (ER) enter the *cis*-face of the Golgi apparatus and, while passing through cisternae, become

posttranslationally modified and sorted (De Matteis & Luini, 2008, Brandizzi & Barlowe, 2013, Lavieu *et al.*, 2013). Mature proteins and lipids then exit the Golgi apparatus at the *trans*-side of the organelle and are further transported to their final intracellular destination or packed for secretion into the extracellular space (De Matteis & Luini, 2008, Lavieu *et al.*, 2013). Concurrently, cargo from the plasma membrane arrives at the *trans*-Golgi or the *trans*-Golgi network (TGN) where it can be processed for recycling (Franch-Marro *et al.*, 2008, Pfeffer, 2009, Fisher *et al.*, 2013). In general, transport from and to the Golgi apparatus can be mediated by vesicles or via non-vesicular pathways (Yamaji & Hanada, 2015).

As the Golgi apparatus is the major distributor of proteins and lipids it is a popular target for intracellular pathogens to acquire nutrients or modulate host cell signaling. From the protozoan *Leishmania* or *Toxoplasma* to the bacterial agents *Legionella*, *Shigella* and *Chlamydia* interactions at different stages of Golgi mediated trafficking pathways have been described (Canton & Kima, 2012, Hilbi & Haas, 2012, Mounier *et al.*, 2012). The pathogens *Shigella* and *Chlamydia* not only interfere with Golgi trafficking events but even rearrange the Golgi apparatus to promote their intracellular survival (Heuer *et al.*, 2009, Mounier *et al.*, 2012).

1.2.1 The structure of the mammalian Golgi apparatus

Due to the constant turnover of proteins and lipids the Golgi apparatus is a highly dynamic organelle. In mammals the flattened cisternae of the Golgi apparatus can be laterally interconnected by tubular structures to form a Golgi ribbon. The ribbon structure itself is a dynamic state and can be temporarily dispersed during mitosis or apoptosis (Colanzi & Corda, 2007, Mukherjee *et al.*, 2007). Defined by their enzymatic composition Golgi cisternae are divided into distinct regions, namely the *cis*- , *medial*- or *trans*-Golgi, which act on distinct steps of the anterograde secretory pathway (Klumperman, 2011). At the *cis*- and the *trans*-faces of the Golgi apparatus, complex tubular networks (*cis*-Golgi-Network = CGN; *trans*-Golgi-Network = TGN) foster the intense communication with adjacent organelles. Together, the high organization of the mammalian Golgi apparatus comprises very defined environments for effective and precise protein and lipid processing and sets the precondition for cell polarity (Puthenveedu *et al.*, 2006, Yadav *et al.*, 2009).

The family of golgin coiled-coil proteins that act in concert with small GTPases maintain this complex structure of the Golgi apparatus. The scaffold of golgins and small GTPases is discussed to form a stable matrix that shapes cisternae and encloses Golgi enzymes (Seemann *et al.*, 2000). At the cytoplasmic surface of Golgi membranes different golgins form homodimeric parallel coiled-coils that promote stability and serve as membrane tethers (Munro, 2011). Three main types of golgins distinguished by different modes of membrane binding are described. A number of golgins contain C-terminal transmembrane domains that directly span the Golgi membrane (Figure 1.4, B1). Some are bound via GRASP adaptor proteins (GRASP = Golgi reassembly stacking proteins) (Figure 1.4, B2) while others contain structural motifs as a GRIP or GRAB domain that bind to small GTPases (Figure 1.4, B3) (Munro, 2011).

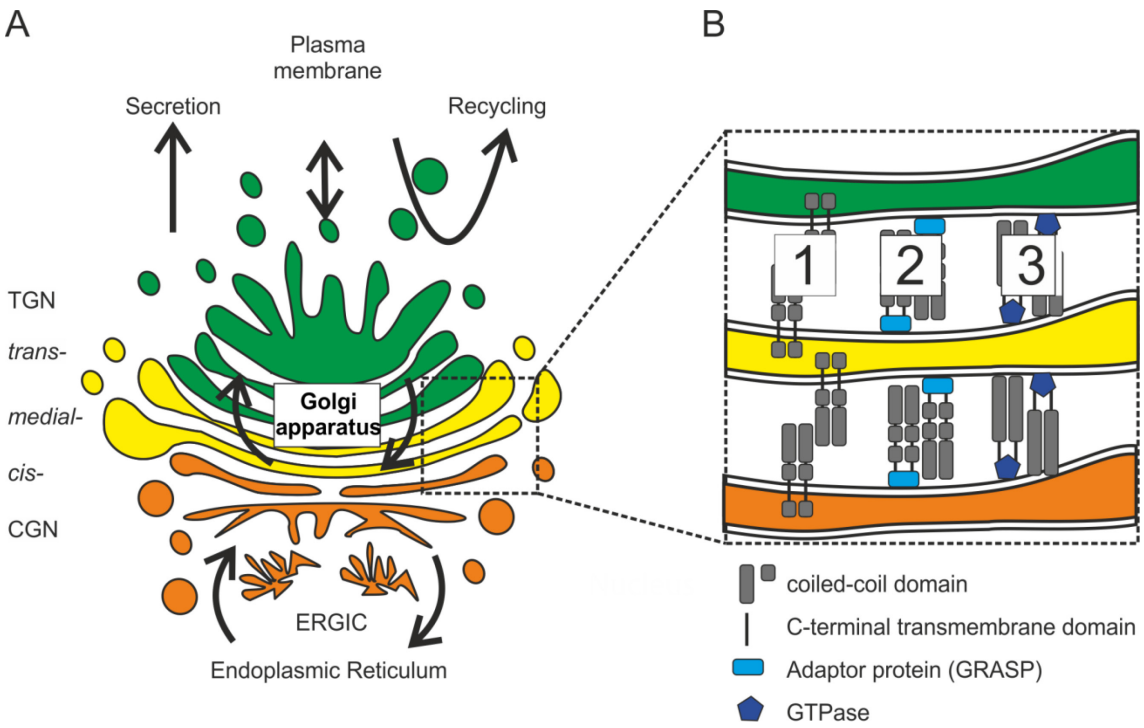

Figure 1.4 The Golgi apparatus is a key organelle for sorting and secretion and is organized in a complex structure.
Schematic representation of the mammalian Golgi apparatus which is composed of cisternae that are laterally connected and form the Golgi ribbon. Cargo destined for secretion enters the Golgi at the *cis*-face, passes through the stack where it is posttranslationally modified and exits at the *trans*-Golgi. The tubular structures at the *cis*- and *trans*-face (*cis*-Golgi-Network = CGN; *trans*-Golgi-Network = TGN) promote communication with adjacent organelles (A). Golgi structure is maintained by golgin-coiled coil proteins that are C-terminally linked to the the Golgi surface where they form homodimers. Golgins are bound via a transmembrane domain (B1), via GRASP adaptor proteins (B2) or via direct interaction of a GRIP or GRASP domain with small GTPases (B3).

1.2.2 *Chlamydia* induces Golgi fragmentation

Golgins are crucial components of the Golgi matrix and both excess and depletion result in unlinking of the Golgi ribbon and formation of Golgi ministacks (Diao *et al.*, 2003, Munro, 2011). Such rearrangements are commonly seen in apoptotic cells or during mitosis when Golgi enzymes are distributed to daughter cells (Colanzi & Corda, 2007, Mukherjee *et al.*, 2007).

Interestingly, infections with the intracellular pathogen *Chlamydia* also lead to a drastic reorganization of the Golgi apparatus (Scidmore *et al.*, 1996, Heuer *et al.*, 2009). In the course of *C. trachomatis* infections, the normal Golgi ribbon structure disperses and Golgi-ministacks align around the inclusion at around 16 h *post infectionem* (*p.i.*). At this time, chlamydial replication strongly depends on efficient sphingolipid uptake. Hence, the close proximity to intact Golgi ministacks, where sphingolipids are synthesized and sorted, facilitates sphingolipid uptake to the chlamydial inclusion. In sum, Golgi fragmentation and recruitment of Golgi ministacks to the inclusion are essential mechanisms to ensure bacterial replication and formation of infectious progeny. Nevertheless, the underlying molecular mechanisms are insufficiently defined.

1.2.3 Golgin-84, Rab6A and Rab11A in *Chlamydia*-induced Golgi fragmentation

Golgi stability which is maintained by a scaffold of golgins and small GTPases is severely affected by *C. trachomatis* infections. The Golgi matrix protein golgin-84, which is involved in maintenance of Golgi structure and vesicular Golgi trafficking, was proposed to occupy a central position within this process (Diao *et al.*, 2003, Satoh *et al.*, 2003, Malsam *et al.*, 2005). Here, *in vitro* studies indicated that proteolytic processing of golgin-84 goes along with *Chlamydia*-induced Golgi fragmentation. The interdependence of golgin-84 processing and Golgi breakdown is however not completely solved.Which factors are involved in protein processing, in particular whether golgin-84 is directly processed by a chlamydial protease, by an indirect caspase-dependent mechanism or due to some unknown processes is another open question. Initial studies proposed that the chlamydial protease-like activity factor (CPAF) determines golgin-84 cleavage (Christian *et al.*, 2011). This finding, however, was recently challenged by different research groups that claimed that different experimental procedures, including different methods of cell lysis, might lead to inconclusive or even artificial results (Chen *et al.*, 2012, Snavely *et al.*, 2014, Johnson *et al.*, 2015). Yet, by using alternative methods, the role and biological background of golgin-84 processing in *C. trachomatis* infections need to be reinvestigated.

Beside golgin-84 two other host proteins, Rab6A and Rab11A are key players in the regulation of *Chlamydia*-induced Golgi fragmentation and associated sphingolipid uptake (Rejman Lipinski *et al.*, 2009). In uninfected cells, Rab6A participates in diverse steps of intra-Golgi trafficking and regulates entry and exit of transport vesicles (Martinez *et al.*, 1997, Grigoriev *et al.*, 2007). The entry of transport vesicles to the Golgi apparatus from Rab11A positive recycling endosomes is regulated by Rab6A interacting protein 1 which binds to both Rab6A and Rab11A and in this way co-ordinates their modes of action (Miserey-Lenkei *et al.*, 2007). In *C. trachomatis* infected cells, Rab6A and Rab11A are recruited to and accumulate around the chlamydial inclusion (Rzomp *et al.*, 2003, Rejman Lipinski *et al.*, 2009, Aeberhard *et al.*, 2015). Their functions in regulated vesicle transport might contribute to the acquisition of sphingolipids to *Chlamydia*, indicated by a strong reduction of sphingolipid uptake upon siRNA mediated knockdown of Rab6A or Rab11A (Rejman Lipinski *et al.*, 2009). Interestingly, by a yet unknown mechanism both proteins lead to a stabilization of the Golgi ribbon and interfere with *C. trachomatis* induced golgin-84 dependent Golgi fragmentation thereby affecting sphingolipid uptake and bacterial development. The coordinated interplay of these three proteins is of specific interest to unravel the mechanism of *Chlamydia*-induced Golgi fragmentation and the related mechanism of sphingolipid acquisition.

1.3 *Chlamydia* interacts with the host endoplasmic reticulum

The ER is the largest intracellular endomembrane system in eukaryotic cells that covers numerous enzymes for protein-, lipid- and carbohydrate synthesis. Particularly, transmembrane proteins are translocated to the ER where they fold, mature and after quality control are further

sorted towards their intracellular destinations (Ellgaard & Helenius, 2003, Braakman & Bulleid, 2011). Beyond, the enlarged surface of the ER integrates this organelle in an extensive network of intra- and intercellular communication (Berridge, 2002, Zhang & Kaufman, 2008). Because of these outstanding functions, various intracellular pathogens from viruses to protozoa to bacteria have evolved strategies to interact with the ER (Roy *et al.*, 2006).

1.3.1 Biology and functions of the ER

As the key organelle for the biosynthesis of cellular molecules, the ER participates in the maintenance of various cell functions. Firstly, the ER lumen provides an optimal oxidizing environment for protein folding and maturation and additionally holds enzymes for the synthesis of membrane lipids (Hwang *et al.*, 1992, Kim & Arvan, 1995). To avoid ER chaos resulting from inefficient or incorrect protein folding or from an imbalance in biomolecule levels, quality and homeostasis are tightly controlled as is biomolecule export and distribution (Walter & Ron, 2011).

Starting from the ER newly synthesized molecules are transported to the Golgi apparatus, directly to the plasma membrane or to different endosomal compartments. To ensure efficient transportation, alternative pathways have evolved including vesicular and non-vesicular routes. Export of packed vesicular cargo occurs at functional ER exit sites that are connected to tubular structures which form the ER-Golgi intermediate compartment (ERGIC) (Appenzeller *et al.*, 1999). Moving along the ERGIC vesicles are directed to the Golgi apparatus where cargo can be posttranslationally modified and sorted (Ben-Tekaya *et al.*, 2005).

In addition to vesicles, non-vesicular transport of biomolecules at membrane contact sites (MCS) has been shown to bridge intra-membrane gaps of 10-25 nm between the ER and mitochondria, the plasma membrane, the Golgi apparatus or endosomes (Levine, 2004, Levine & Loewen, 2006). These MCS serve predominantly to transfer and exchange lipids and moreover coordinate Ca^{2+} signaling (Liou *et al.*, 2007, Helle *et al.*, 2013)(Liou *et al.*, 2007, Helle *et al.*, 2013)(Liou *et al.*, 2007, Helle *et al.*, 2013)(Liou *et al.*, 2007, Helle *et al.*, 2013)(Hanada *et al.*, 2003, Baumann *et al.*, 2005, Liou *et al.*, 2007, Helle *et al.*, 2013).

The sensing of Ca^{2+} levels and respective signal transduction is another central function met by the ER that in normal cells contains elevated levels of Ca^{2+} compared to the cytosol. Under physiological conditions that provoke an accumulation of unfolded proteins within the ER, the increased stress leads to Ca^{2+} release which consequently affects mitochondrial integrity (Zhang & Kaufman, 2008). Subsequently, the amount of reactive oxygen species (ROS) increases and might translate ER stress to an inflammatory response (Naik & Dixit, 2011). Therefore, this mechanism of inflammatory activation is another interesting target for intracellular pathogens that aim to protect their niche.

1.3.2 *Chlamydia* assembles a synapse to the ER

Given its functions in biomolecule processing and in the secretory pathway the ER is an attractive target for intracellular *Chlamydia*. Initial evidence for an intimate association of the chlamydial inclusion with the ER was given by Giles and Wyrick who showed that in infected cells, chlamydial antigens are frequently found in ER structures (Giles & Wyrick, 2008). Soon, the nature of this ER-inclusion connection was described as a novel type of MCSs which form a patchwork around the inclusion of *C. trachomatis* and closely related genital strains (Derre *et al.*, 2011, Dumoux *et al.*, 2012). Strikingly, the environmental strain *Simkania nervergensis* is not only surrounded by an ER patchwork but almost entirely enveloped with ER structures (Pilhofer *et al.*, 2014). The close proximity to the ER is thought to facilitate the vital exchange of proteins and lipids thus promoting transport of host derived nutrients to inclusions and simultaneously allowing ER modification by proximal *Chlamydia* and secreted effector proteins. Actually, close contact between *Chlamydia* and the ER, which is actively established by bacteria, is essential for bacterial growth and development (Dumoux *et al.*, 2012, Shima *et al.*, 2015). In case of *C. pneumonia,* this close contact is not only observed in productive infections but is even maintained after interferon-γ (IFN-γ) induced growth arrest (Shima *et al.*, 2015). Whether ER-inclusion MCS are functionally altered after IFN-γ treatment is still an open question.

As demonstrated by proteomic analyses the inclusion of *C. trachomatis* contains an intriguing amount of ER resident proteins at 24 h *p.i.*, even though it is not known if they originate from ER-inclusion MCS (Aeberhard *et al.*, 2015). Aside from that, only few functional consequences of ER-inclusion MCS which affect chlamydial development are described in detail. As an example *C. trachomatis* uses ER contact sites to recruit the non-vesicular ceramide transport protein CERT via IncD (see section 1.1.4) implying direct transport of *de novo* synthesized ceramide to the inclusion. Moreover, the important Ca^{2+} sensor STIM1, usually found at MCS of ER and plasma membrane, is highly enriched at the inclusion membrane and might be used to interfere with Ca^{2+}-related regulatory responses (Aeberhard *et al.*, 2015, Agaisse & Derre, 2015). In the future further investigations on other ER proteins will complement our recent understanding regarding ER-inclusion MCSs.

1.3.3 CERT and non-vesicular ceramide transport

One considerable participant of ER-inclusion MCS is the cytosolic lipid transport protein CERT that directly binds the ER and *C. trachomatis* inclusions. In uninfected cells, CERT extracts *de novo* synthesized ceramide from ER membranes and transports it along MCS to the *trans*-Golgi for conversion into sphingomyelin (Hanada *et al.*, 2003). To fulfill this role CERT contains an N-terminal pleckstrin-homology (PH)-domain recognizing phosphatidyl-inositol 4-monophosphate (PI4P) in the *trans*-Golgi, an FFAT motif within a coiled-coil region, mediating binding to the ER associated protein VAPB and a StAR-related lipid transfer (START)-domain for ceramide binding

that act in concert. Moreover, a serine rich (SR)-domain has been described where phosphorylations by protein kinase D (PKD) and casein kinase 1 isoform γ2 (CK1γ2) regulate protein activity (Figure 1.5) (Fugmann *et al.*, 2007, Tomishige *et al.*, 2009).

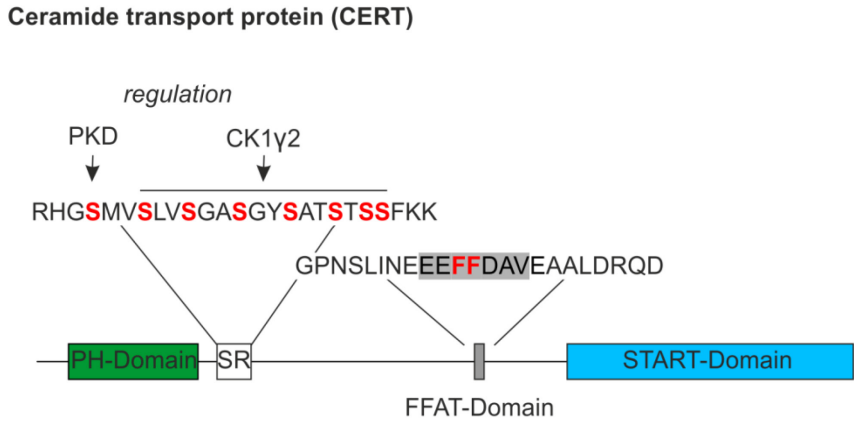

Figure 1.5 CERT contains distinct structural motifs for regulated non-vesicular ceramide transport.
The scheme shows important protein motifs of CERT. CERT contains an N-terminal PH domain responsible for PI4P-binding and resulting *trans*-Golgi localization, a SR domain where regulation by phosphorylation occurs, a FFAT domain mediating binding to the ER and a C-terminal START domain, that covers ceramide binding activity. Important functional amino acids are depicted in red; PKD – protein kinase D, CK1γ2 – casein kinase 1 isoform γ2.

CERT binding to the *C. trachomatis* inclusion is dominated by the CERT-PH domain which binds to IncD *in vitro* (Derre *et al.*, 2011, Agaisse & Derre, 2014). Henceforth, a functional link between inclusion association and chlamydial development has been shown by siRNA mediated knockdown of CERT that significantly reduces the development of infectious chlamydial progeny. Surprisingly, ceramide uptake to *C. trachomatis* is not affected, indicating that CERT plays a currently unknown role in this process. How exactly CERT-mediated ceramide transport contributes to *C. trachomatis* development and if these principles are transferrable to other *Chlamydia* spp. are worthwhile questions to address.

1.4 *Chlamydia* relies on host cell sphingolipids

Sphingolipids are a class of complex lipids first described by the American biochemist Herbert E. Carter in 1947 (Carter *et al.*, 1947). Basically sphingolipids are composed of a sphingoid base backbone which is linked to a fatty acid and a polar head group. Complex sphingolipids serve as integral components of the mammalian cell membrane where they, together with cholesterol, assemble in specific rigid subdomains called “rafts” thereby defining membrane structure (van Meer *et al.*, 2008). Moreover, sphingolipids and their metabolites have impacts on various signal transduction pathways that affect cellular functions like cell proliferation or secretion (Hannun & Obeid, 2008). Hence, imbalances in sphingolipid homeostasis are closely connected to the pathophysiology of cancer, immunity and infectious diseases (Ogretmen & Hannun, 2004, Hanada, 2005, Maceyka & Spiegel, 2014).

Bacterial or viral microorganisms rarely produce their own sphingolipids but have evolved sophisticated strategies to intervene in host sphingolipid processes to ensure efficient infections.

1.4.1 Sphingolipid metabolism – focus on sphingomyelin

Sphingolipid synthesis is initiated by the enzymatic action of serine palmitoyl transferases that use serine and palmitoyl-CoA to generate sphingoid bases. This reaction, taking place at the cytoplasmic leaflet of the ER, is rate limiting for all classes of higher sphingolipids. The reaction product 3-ketodihydrosphingosine is further reduced, acylated and desaturated to generate ceramide, still located at the ER. Ceramide is then used as the central precursor for numerous sphingolipids including sphingomyelin, lactosyl-, galactosyl- and glycosylceramides or ceramide-1-phosphate.

Enzymes that catalyze the reactions of ceramide to complex sphingolipids are located at different organelles. Sphingomyelin is the most abundant sphingolipid and is preferentially scavenged by *Chlamydia* (Moore *et al.*, 2008). This lipid is generated through the transfer of the phosphocholine head group from phosphatidylcholine to ceramide. This reaction is catalyzed by two enzymes, sphingomyelin synthase 1 and 2 (SMS1 and SMS2) (Huitema *et al.*, 2004). SMS1 mainly localizes to the *trans*-Golgi, whereas SMS2 is predominantly found in the plasma membrane but also within the Golgi apparatus (Tafesse *et al.*, 2007). In both cases ceramide, synthesized at the endoplasmic reticulum has to be transported to the respective enzyme to get converted. Transport is primarily mediated by the non-vesicular transport via CERT and, although experimental evidence is still vague, by vesicular ATP-dependent traffic (Hanada *et al.*, 2003, Giussani *et al.*, 2008). In Figure 1.6 CERT-dependent ceramide transport and sphingomyelin synthesis in uninfected cells are schematically summarized.

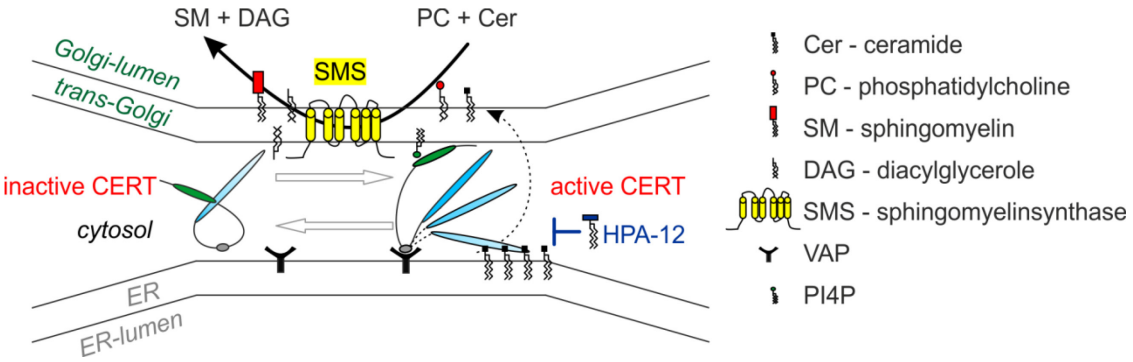

Figure 1.6 Ceramide is transported to the *trans*-Golgi where it is converted to sphingomyelin by sphingomyelin synthase.
Schematic model of CERT-mediated lipid transport and sphingolipid synthesis. Inactive CERT is activated by dephosphorylation and while connected to the ER and the Golgi apparatus, extracts ceramide for transport to the *trans*-Golgi. There, ceramide together with phosphatidylcholine is enzymatically converted to sphingomyelin and diacylglycerole by sphingomyelin synthase. Inactivation of CERT is mediated by phosphorylation or by chemical inhibition with the ceramide analogue HPA-12. Modified from *Yamagi & Hanada, 2015.

1.4.2 *Chlamydia* acquires sphingolipids

Sphingolipids are highly abundant in mammalian cells and are of great importance for chlamydial development. 20 years ago, pioneering work performed by Ted Hackstadt and colleagues showed that *Chlamydia* acquires fluorescently labeled sphingolipids from the host cell (Hackstadt *et al.*, 1996). They further demonstrated that purified EBs exclusively contain fluorescent sphingomyelin and concluded that bacteria gather Golgi-derived sphingomyelin instead of its precursor ceramide. Until today, there is no evidence that any other ceramide derivatives are delivered to *Chlamydia* (Moore *et al.*, 2008).

To ensure selective acquisition of sphingomyelin *Chlamydia* hijack a subpopulation of Golgi-derived exocytic vesicles, while endocytic vesicles from the plasma membrane are not targeted (Hackstadt *et al.*, 1996, Moore *et al.*, 2008, Elwell *et al.*, 2011). Although vesicular transport of sphingomyelin is essential for inclusion biogenesis and fusion, it is dispensable for infectious progeny formation. Additionally to vesicular pathways, *Chlamydia* intercepts the non-vesicular ceramide transport by direct binding to CERT. The temporal and mechanistic interplay of these pathways might thereby contribute to compensate fluctuations in lipid access.

While vesicular sphingolipid trafficking is essential for various *Chlamydia* spp., the alternative interaction with CERT has only been shown for *C. trachomatis* and *C. muridarum* (Derre *et al.*, 2011, Elwell *et al.*, 2011). Future investigations are needed to understand how individual *Chlamydia* spp. accomplish sphingolipid acquisition.

1.5 Aim of this study

Chlamydia spp. have evolved a rich repertoire of mechanisms to interact with the host cell and maintain their intracellular lifestyle. To acquire essential nutrients bacteria exploit diverse trafficking pathways of the host and in particular intercept Golgi related trafficking routes. The human pathogen *C. trachomatis* rearranges the Golgi apparatus and recruits resulting ministacks to the chlamydial inclusion. This process is essential for efficient sphingolipid acquisition and progeny formation. The nature and function of *C. trachomatis*-induced Golgi ministacks, defined by the mode of ministack formation, are however poorly described.

In a first part of this thesis, the dynamics of resident Golgi enzymes in *C. trachomatis*-induced Golgi ministacks were analyzed via live-cell imaging in order to link Golgi structure with Golgi functionality. Golgin-84 was recently proposed as a key player in *C. trachomatis*-dependent Golgi fragmentation and associated sphingolipid acquisition. To further investigate and specify its relevance in *C. trachomatis* infections, golgin-84 and functional mutants were analyzed by microscopic means using transiently expressed mutants of the protein. Consequences of golgin-84 function on *C. trachomatis* infectivity were further addressed in golgin-84 knockdown cells transiently expressing relevant mutants.

So far, Golgi fragmentation was only described for human chlamydial strains neglecting zoonotic *C. psittaci*. Therefore, the second part of this thesis addressed the question if the zoonotic agent *C. psittaci* also interferes with Golgi morphology and exploits Golgi-related trafficking pathways to establish an infection in a human cell. Microscopic analyses upon staining or transient expression of relevant Golgi matrix and trafficking proteins intended to investigate species-specific features and preferences of this zoonotic pathogen.

Since *C. trachomatis* and *C. psittaci* have distinct interaction profiles and seemed to share few selected interaction partners to acquire sphingolipids, the conserved interaction with CERT became of particular interest to develop strategies to intervene both infections. Therefore, the relevance of non-vesicular CERT-dependent ceramide transport for human or zoonotic agents was further determined by inhibitor studies that considered molecular, morphological or biochemical means.

Finally, to investigate whether conserved and species-specific mechanisms of sphingolipid acquisition determine the endogenous-sphingolipid composition of infectious EBs, a customized approach of quantitative sphingolipid analysis based on rapid resolution liquid chromatography MS/MS was developed. Resulting data could reveal important information to design sphingolipid-based antichlamydial strategies.

2 Materials and Methods

2.1 Materials

2.1.1 Organisms

Cell lines

Table 2.1 Cell lines

Name	Origin	Source
HeLa	human cervix carcinoma	ATCC: CCL-2
HeLa sh luciferase	human cervix carcinoma	(Heuer *et al.*, 2009)
HeLa sh golgin-84	human cervix carcinoma	(Heuer *et al.*, 2009)
HeLa229	human cervix carcinoma	ATCC: CCL-2.1
DF-1	chicken embryo fibroblast	ATCC: CRL-12203

Bacteria

Table 2.2 Bacteria

Species	Strain	Origin	Source
C. trachomatis	L2	lymphatic isolate 434 Bu	ATCC: VR-902B
C. trachomatis	D	human cervix isolate UW-3/Cx	ATCC: VR-885
C. trachomatis	A	human conjunctiva isolate HAR-13	ATCC: VR-571B
C. psittaci	02DC15	bovine isolate	(Schofl *et al.*, 2011)
C. psittaci	01DC11	ovine isolate	(Schofl *et al.*, 2011)
C. psittaci	08DC60	human isolate	(Schofl *et al.*, 2011)
Escherichia coli	BIOBlue	-	Bioline USA Inc.

2.1.2 Nucleic Acids

Primer for cloning

Table 2.3 Primer for cloning

Gene product	Primer sequence (5'-3')	Direction	Restric-tion site
Golgin-84 (aa 1-x)	CAATGAATTCTGATGTCTTGGTTTGTTGATCTTG	fw	EcoRI
Golgin-84 (aa x-730)	CTTAGGATCCCGTTTGCCATATGGTTGGTCGTGG	rv	BamHI
Golgin-84 (aa 159-x)	CAATGAATTCTGATGTCTGTGAACCCCAGTGTAACC	fw	EcoRI

Golgin-84 (aa x-698)	CAATGGATCCCGTCGCGCTATGGGGTATCTTCG	rv	BamHI
Golgin-84 (aa x-148)	CAATGGATCCCGAGGTGTCTTGCCTTTTTCCTTTC	rv	BamHI
GFP	TATTGTCGACATGGTGAGCAAGGGCGAGGAGC	fw	SalI
CERT (aa 1-x)	GATAAAGCTTTATCGGATAATCAGAGCTGGAACT C	fw	HindIII
CERT (aa x-598)	GATAGAATTCGAACAAAATAGGCTTTCCTGCAG	rv	BamHI
CERT (FF322AA)	GTCTGATTAATGAAGAAGAGGCCGCTGATGCTGT TGAAGCTGCTC	fw	-
CERT (FF322AA)	GAGCAGCTTCAACAGCATCAGCCGCCTCTTCTTC ATTAATCAGAC	rv	-
CERT (G67E)	GTATGGCTGCAGAGAATCCATCTGTCTTAG	fw	-
CERT (G67E)	CTAAGACAGATGGATTCTCTGCAGCCATAC	rv	-

Primer for quantitative real-time PCR (qPCR)

Table 2.4 Primer for qPCR

Target sequence	Primer sequence (5'-3')	Direction	Reference
c16S rDNA	CCGCCAACACTGGGACT	fw	(Lienard *et al.*, 2011)
c16S rDNA	GGAGTTAGCCGGTGCTTCTTTAC	rv	(Lienard *et al.*, 2011)

Expression plasmids

Table 2.5 Expression plasmids

Gene product	Vector backbone	Source	Reference
Golgin-84-GFP (1-730)	pEGFP-N1	this work	-
Golgin-84-GFP (159-730)	pEGFP-N1	this work	-
Golgin-84-GFP (1-698)	pEGFP-N1	this work	-
Golgin-84-GFP (159-698)	pEGFP-N1	this work	-
Golgin-84-mCherry (1-148)	pmCherry-N1	this work	-
GFP-Golgin-84 (1-148)	pEGFP-C3	this work	-
GFP-Golgin-84 (1-730)	pEGFP-C1	Heuer, D.	-

GFP-CERT (1-598)	pEGFP-C1	this work	-
GFP-CERT (FF322AA)	pEGFP-C1	this work	-
GFP-CERT (G67E)	pEGFP-C1	this work	-
GFP-Rab1	pEGFP-C1	Roy, C.	(Ingmundson *et al.*, 2007)
YFP-Rab3D	pEYFP-C1	Gerke, V.	(Knop *et al.*, 2004)
GFP-Rab4	pECFP-C2	Zerial, M.	(Sonnichsen *et al.*, 2000)
GFP-Rab5	pECFP-C1	Zerial, M.	(Sonnichsen *et al.*, 2000)
myc-Rab6A	pEGFP-C2	Goud, B.	(Monier *et al.*, 2002)
GFP-Rab7	pECFP-C1	Helenius, A.	(Vonderheit & Helenius, 2005)
GFP-Rab8a	pECFP-C1	Gerlich, D.	(Guizetti *et al.*, 2011)
GFP-Rab11A	pEGFP-C2	Zerial, M.	(Sonnichsen *et al.*, 2000)
GFP-Rab21	pECFP-C1	Simpson, J. C.	(Simpson *et al.*, 2004)
GFP-Rab35	pECFP-C1	McPherson, P.	(Allaire *et al.*, 2013)
CFP-GalT	pECFP-C1	Clontech	-
YFP-ManII	pEYFP-C1	Clontech	-
GFP-p115	pEGFP-C1	Hesso, F.	-
GFP-ERGIC53	pEGFP-C1	Hauri, A.	(Ben-Tekaya *et al.*, 2005)
GFP	pEGFP-C1	Clontech	-
mCherry	pmCherry-N1	Clontech	

2.1.3 Media and solutions

Cell culture media

Table 2.6 Cell culture media

Application	Composition	Source
Cell growth (HeLa)	RPMI 1640	Gibco
	10% FCS, heat inactivated	Biochrom
	1 mM sodium pyruvate	Gibco
	5 mM L-glutamine	Gibco
Infection (HeLa)	DMEM high glucose (4.5 g/l)	Gibco
	5% FCS, heat inactivated	Biochrom
	1 mM sodium pyruvate	Gibco
	5 mM L-glutamine	Gibco
Transfection	OptiMEM	Gibco
Passaging	Trypsin-EDTA (0.25%), phenol red	Gibco
E. coli culture (liquid)	LB medium:	RKI, Berlin
	10 g/l trypton, 5 g/l yeast extract, 5 g/l NaCl	
E. coli culture (solid)	10 g/l trypton, 5 g/l yeast extract, 5 g/l NaCl, 1.5% bacto agar	RKI, Berlin

Buffers and Solutions

Table 2.7 Buffer and Solutions

Buffer	Composition
PBS	137 mM NaCl, 2.7 mM KCl, 10 mM Na_2HPO_4 + 2 H_2O, 1.76 mM KH_2PO4
TBS	137 mM NaCl, 10 mM Tris/HCl
TBS-T	TBS, 0.05% Tween 20
WB blocking buffer	TBS-T, 3% milk powder
5X Stacking gel SDS-PAGE buffer	1.5 M Tris/HCl pH 6.7, 0.4% SDS
5X Separating gel SDS-PAGE buffer	0.5 M Tris/HCl pH 8.8, 0.4% SDS
6X SDS-PAGE loading buffer (Lämmli)	375 mM Tris/HCl pH 6.8, 48% glycerol, 9% β-mercaptoethanol, 6% SDS, 0.03% bromphenol blue
SDS-PAGE running buffer	25 mM Tris/HCl, 192 mM glycine, 0.1% SDS
WB wet transfer buffer	25 mM Tris/HCl, 192 mM glycine, 0.1% SDS, 20% methanol
PFA solution	4% PFA, 4% sucrose in PBS
IF blocking buffer	0.2% BSA in PBS

IF permeabilisation buffer	0.2% BSA, 0.2% Triton X-100 in PBS
Mowiol mounting medium	2.4 g Mowiol 4-88, 6 g glycerol, 6 ml H_2O, 12 ml 0.2 M Tris/HCl pH 8.5
SPG buffer	250 mM sucrose in PBS
10X HBS	100 mM HEPES, 1.45 M NaCl
Liquid overlay medium	0.01% (w/v) 140 DEAE-Dextran, 0.05% (w/v) $NaHCO_3$, 5% (v/v) FCS, 0.6% (w/v) Avicel microcrystalline cellulose (RC-581, 141 FMC BioPolymer) in DMEM

2.1.4 Antibodies

Primary antibodies

Table 2.8 Primary antibodies

Antigen	Species	Dilution (IF / WB)	Source
IncA (*C. trachomatis*)	rabbit	1:500 / 1:2000	self-made, (Banhart *et al.*, 2014)
IncB (*C. psittaci*)	rabbit	1:250 / 1:2000	HKI, Jena, (Bocker *et al.*, 2014)
Hsp60 (A57E4)	mouse	- / 1:5000	Alexis
Hsp60 (A57B9)	mouse	1:600 / -	Alexis
Gpp130	rabbit	1:250 / 1:100	Convance
GM130	mouse	1:100 / 1:1000	BD Bioscience
p230	mouse	1:100 /1:1000	BD Bioscience
Giantin	rabbit	1:500 / -	Covance
CERT	chicken	1:400/ -	Sigma
β-actin	mouse	- / 1:4000	Sigma
myc (9E10)	mouse	1:100 / 1:1000	Santa Cruz

Secondary antibodies

Table 2.9 Secondary antibodies

Name	Application	Source
IgG-Cyanine dye (goat anti-mouse/ -rabbit/ -chicken)	IF (1:100 / 1:200)	Amersham Biosciences
IgG-Alexa dye (goat anti-mouse/ -rabbit)	IF (1:100 / 1:200)	Amersham Biosciences
IgG-Horseradish peroxidase (goat anti-mouse/ -rabbit)	WB (1:4000)	Dianova

2.1.5 Chemicals

Table 2.10 Chemicals

Name	Source
Methanol ROTIPURAN® ≥99,9 %, p.a., ACS	Roth
DMSO	Roth
HPA-12 (*1R,3S*)	Synthesized and provided by Christoph Arenz, AG Organic and Bioorganic chemistry, HU Berlin, (Saied et al., 2014)
Nocodazole	Sigma
Brefeldin A in DMSO	Sigma
Ampicillin	Sigma
Kanamycin	Sigma
Ammonium persulfate	Sigma
Tetramethylethylenediamine	Roth

2.1.6 Kits

Table 2.11 Kits

Name	Source
Lipofectamine2000	Qiagen
QuantiTect SYBR Green PCR Kit	Qiagen
QIAGEN Plasmid Midi Kit	Qiagen
Invisorb Spin Plasmid mini Two	STRATEC Molecular GmbH
Wizard SV Gel and PCR Clean-Up System	Promega
BCA Protein Assay Reagent Kit	Pierce
Cytotoxicity Detection Kit^{PLUS} (LDH)	Roche

2.1.7 Consumables

Labware

Table 2.12 Labware

Name	Source
Cell culture flasks/dishes	TPP
Live cell dishes	Ibidi
Cell scrapers	Biochrom
Sterican 26 G, 24 G	Braun
Glass beads 2.2 mm	Roth
Reaction containers	Sarstedt

Microscopy slides	Roth
Glass cover slips	Marienfeld
Imobilon-P (PVDF-membranes)	Millipore
X-ray films	Kodak
Parafilm	Pechiney

Enzymes and others

Table 2.13 Enzymes and others

Name	Source
Phusion High-Fidelity PCR Master Mix with HF Buffer	Thermo Scientific
Restriction enzymes (EcoRI, BamHI, HindIII)	New England Biolabs
T4 DNA Ligase	New England Biolabs
GeneRuler 1kb ladder	Thermo Scientific
Page Ruler Plus Prestained	Thermo Scientific

2.1.8 Equipment

Experiments were done using standard modern laboratory equipment.

Microscopes

Table 2.14 Microscopes

Name	Configuration
Zeiss LSM780	Plan-Apochromat 100x/1.40 Oil Ph3 M27
	Plan-Apochromat 63x/1.40 Oil DIC M27
Zeiss Observer-Z1	LD Plan-Neofluar 40x/0.6 Corr Ph1 Ph2- M27
Zeiss Axiovert 40 CLF	LD Plan-Neofluar 40x/0.6 Corr Ph2 M27

2.1.9 Software

Table 2.15 Software

Name	Source
Geneious 7.0.6	Biomatters
Zen2010, black edition (microscopy software)	ZEISS
ImageJ	US National Institute of Health, Bethesda
FRAPAnalyzer	University of Luxembourg
CorelDraw Graphics Suite X6	Corel GmbH
Excel	Microsoft
Graph Pad Prism 5	GraphPad Software

2.2 Methods

2.2.1 Cell culture

Experiments with the intracellular bacterium *Chlamydia* put high requirements on quality in cell culture to gain reliable and reproducible results. Cell culture is generally performed without antibiotics and contaminations of *Mycoplasma* were routinely excluded by central laboratory quality management via PCR. To culture the cell lines HeLa and HeLa229 RPMI cell culture medium was used. Cells were generally grown in 75 cm^2 culture flasks for 2 to 3 days until they reached confluence. To passage confluent cells in fresh culture vessels, cells were washed once with PBS, enzymatically detached using Trypsin-EDTA at 37 °C for 2 to 5 min and cells were diluted in fresh RPMI. Appropriate volumes of cell dilutions with concentrations of 0.8 – 2 x 10^5 cells/ml were seeded in new vessels including flasks, 6-, 12-, 24- or 96-well plates and kept in a humidified incubator providing 37 °C, 5% CO_2. Cells were cultured for up to ten passages.

DF-1 chicken embryonic fibroblasts were cultured in DMEM containing 10% FCS, 10 mM L-glutamine and 1 mM sodium pyruvate. Cells were split in a ratio of 1:8 or 1:10 and incubated at 37 °C, 5% CO_2 for 2 to 3 days to reach confluence.

Plasmid DNA transfection

To study short-term alterations of ectopically expressed proteins, HeLa cells were transiently transfected with plasmid DNA encoding genes of interest. Therefore, HeLa cells were seeded in 12 well plates and grown for 24 h to a density of 70%. Two mixtures, one containing 0.5 µg of plasmid DNA, one 1 µg of Lipofectamine2000 were prepared in 50 µl OptiMEM each and incubated for 5 minutes at room temperature. Both mixtures were pooled, briefly vortexed and incubated at room temperature for 15 to 20 min to allow formation of liposome-nucleic acid complexes. Cells were washed with PBS, 400 µl of fresh RPMI was added and liposome complexes were dripped to the cells. Transfection was followed by an incubation time of at least four hours before additional experimental steps were started.

Cytotoxicity assay

In the course of this work the cytotoxic potential of the ceramide analogue HPA-12, synthesized by Christoph Arenz and colleagues, was tested by a LDH cytotoxicity assay (Saied *et al.*, 2014). The assay was performed according to manufacturer's instructions (Cytotoxicity Detection Kit^{PLUS}). Briefly, cells were seeded in 96-well plates, were left uninfected or were infected with *Chlamydia* using a multiplicity of infection of 0.5 or 2 (MOI, see Titer Determination). 8 h *p.i.* samples were treated with different concentrations of compound. At 48 h *p.i.* lysis buffer was added to positive control cells for 15 min. Afterwards cell supernatants were collected, diluted 1:10 in DMEM and incubated with 100 µl of the supplied reaction mixture at room temperature for 10 min. To stop the reaction, 50 µl of stop solution was added and resulting absorbance at 492 nm

was measured using an Infinite 200 PRO plate reader (Tecan). Values were corrected for background and normalized to positive control.

2.2.2 Infection with *Chlamydia*

Two infection models were mainly employed in this study: the human pathogen *C. trachomatis* serovar L2 and the zoonotic agent *C. psittaci* isolate 02DC15. For simplification the terms *C. trachomatis* and *C. psittaci* refer to these strains unless noted otherwise.

All infections were performed in DMEM infection medium at 35 °C, 5% CO_2 in a humidified incubator. One day before infection cells were grown to 80 – 90% confluence. Stock solutions of chlamydial EBs were diluted in infection DMEM to yield an appropriate MOI (see Titer Determination). The inoculum was distributed on cells previously washed with PBS and infections were incubated at 35 °C, 5% CO_2. Infection volume corresponds to 50% of culture volume usually used. After incubation for 2 h, infected cells were washed with PBS and incubated in standard volume of fresh DMEM infection medium. For efficient infections with *C. psittaci* an additional centrifugation step was required during incubation with inoculum. After 30 min of pre-incubation in standard conditions, infected cells were centrifuged at 600 x *g*, room temperature for 30 min and subsequently incubated for 1 h in a humidified incubator. The same procedure was essential to establish infections with *C. trachomatis* serovar D, *C. trachomatis* serovar A and *C. psittaci* isolate 01DC11 or *C. psittaci* isolate 08DC60.

Preparation of Chlamydia stock solutions

To prepare stock solutions of *C. trachomatis* HeLa cells were grown in 150 cm^2 culture flasks to a confluence of 80 - 90% and infected with an MOI of 3. 48 h *p.i.*, after one ideal developmental cycle, cells were scraped and collected in Falcon tubes containing sterile glass beads. To release bacteria, cells were mechanically lysed by vortexing for 3 min. Lysates were diluted 6 to 10 times in fresh DMEM and used as inoculum for a secondary infection of fresh naïve HeLa cells. Again, infected cells were incubated for 48 h and were subsequently harvested by scraping. Cell suspensions, collected in Falcon tubes with sterile glass beads were mechanically lysed by vortexing for 3 min. Cell debris was separated by centrifugation at 500 x *g*, 4 °C for 10 min, supernatants were transferred to new tubes, EBs were enriched by centrifugation at 48,000 x *g*, 4 °C for 60 min. Pelleted EBs were washed and resuspended in cold SPG buffer. Suspensions were homogenized by passing through 24 G and 26 G syringes and small aliquots were stored at -80 °C until use.

Stock solutions of *C. psittaci* (and others) were prepared in 75 cm^2 culture flasks which allow the obligatory centrifugation step for initial infection. All other experimental steps were identical to those performed for *C. trachomatis*.

Titer Determination

HeLa cells were seeded and grown to 80 - 90% confluence in 24 well plates containing glass coverslips. Cells were infected with serial dilutions of *Chlamydia* and fixed 24 h later with 2% PFA solution at room temperature for 30 min. Subsequently bacterial Heat shock protein 60 (Hsp60) was immunostained (see Immunofluorescence staining) and developed inclusions were counted in at least ten fields of view per dilution using a Zeiss Axiovert 40 CFL microscope with 40x magnification. The following calculation was used to determine the number of inclusion forming units (IFU) per milliliter:

$$IFU/ml = \tilde{x}\ inclusions\ per\ field\ of\ view\ \times 454\ \times dilution\ factor\ \times 4$$

The calculation includes the factor 454 to correct for the number of HeLa cells visible in a microscopic section at 40 x magnification and the factor 4 to correct for the infectious volume of 250 µl.

As the unit IFU describes the absolute number of bacteria per milliliter, the unit MOI describes the ratio of bacteria per cell. Accordingly, 3 IFUs per cell correspond to an MOI of 3.

Reinfection assay

Chemical treatment or knockdown of host genes can influence chlamydial progeny formation. The reinfection assay was used to determine changes in IFU production under certain treatment conditions. Therefore, cells were infected with equal infectious doses of *C. trachomatis* or *C. psittaci* using MOI 0.5 or MOI 2. 48 h *p.i.*, cells were mechanically detached and lysed by vortexing for 3 min with glass beads. Fresh naïve cells were infected with serial dilutions and IFU was determined as described above (Titer Determination). For cells transiently expressing proteins the reinfection was usually started 32 h post primary infection to diminish cell death related effects induced by enhanced levels of transiently expressed protein.

Plaque Assay

Beside the reinfection assay, infectious outcome after chemical treatment can be determined by a plaque assay. For liquid overlay medium-based plaque assays, HeLa229 cells were seeded in 48-well plates to reach 70% confluence the next day. Cells were infected with low MOI (approximately 0.001) in 100 µl inoculum for 2 h, followed by two washing steps. 350 µl of liquid overlay medium containing chemical compound as indicated were added to the cells and incubated at 35 °C, 5% CO_2 for 5 days.

For immunofluorescence staining cells were carefully washed with PBS (removal of the overlay medium), fixed with 2% PFA for 30 min and permeabilized with 0.2% Triton X-100 in PBS for 15 min. Immunofluorescence staining of bacterial Hsp60 was performed directly in the culture dish

as described in the section "Immunofluorescence staining". After a final washing step with dH_2O, fluorescent signals were detected using an Odyssey Infrared Imaging System.

Morphology assay

The morphology of different chlamydial developmental forms was observed by transmission electron microscopy (TEM). Cells were cultured in 6 well plates, infected with *C. trachomatis* or *C. psittaci* and treated as indicated. After at least 2 h of fixation in 2.5% glutaraldehyde, 50 mM HEPES samples were scraped and further processed as pellets. A second fixation step with 1% osmium tetroxide cells was performed, followed by block contrasting with tannin and dehydration in an increasing dilution series of ethanol. The samples were infiltrated with propylenoxide and embedded in Epon resin, which was allowed to polymerize at 60 °C for 48 h. The procedure of TEM analysis is described below (see Transmission electron microscopy).

Different morphological forms of bacteria from randomized pictures were manually defined and counted. For statistical reasons at least 1500 bacteria from three independent biological experiments were included in the analysis.

Purification of elementary bodies for lipid analysis

To quantitatively analyze the sphingolipid composition of EBs, I adapted a protocol for EB isolation and purification based on previous work (Newhall *et al.*, 1986). Each condition started with four 75 cm^2 flasks of HeLa229 cells, infected with *C. trachomatis* or *C. psittaci* (MOI 2). As a background control uninfected cells were used. 48 h *p.i.* cells were washed in ice-cold PBS, scraped and transferred to reaction tubes containing glass beads for mechanical lysis. Crude lysates were pre-cleared by centrifugation at 500 x *g*, 4 °C for 10 min. The supernatants, containing EBs, RBs and residual cell debris, were transferred to centrifugation tubes and centrifugation was performed at 30,000 x *g*, 4 °C for 30 min. The resulting pellets were resupended in 16 ml 33% (vol/vol) Percoll/HBS each and centrifuged again at 30,000 x *g*, 4 °C for 30 min. 200 µl of the gradient bottom fraction, highly enriched in EBs, were removed, transferred to a fresh tube and washed in 1.5 ml HBS (21,000 x *g*, 4 °C, 30 min). Supernatants were removed up to 100 µl, 300 µl of ice-cold methanol was added and samples were stored at -80 °C until lipid isolation and mass spectrometric analysis.

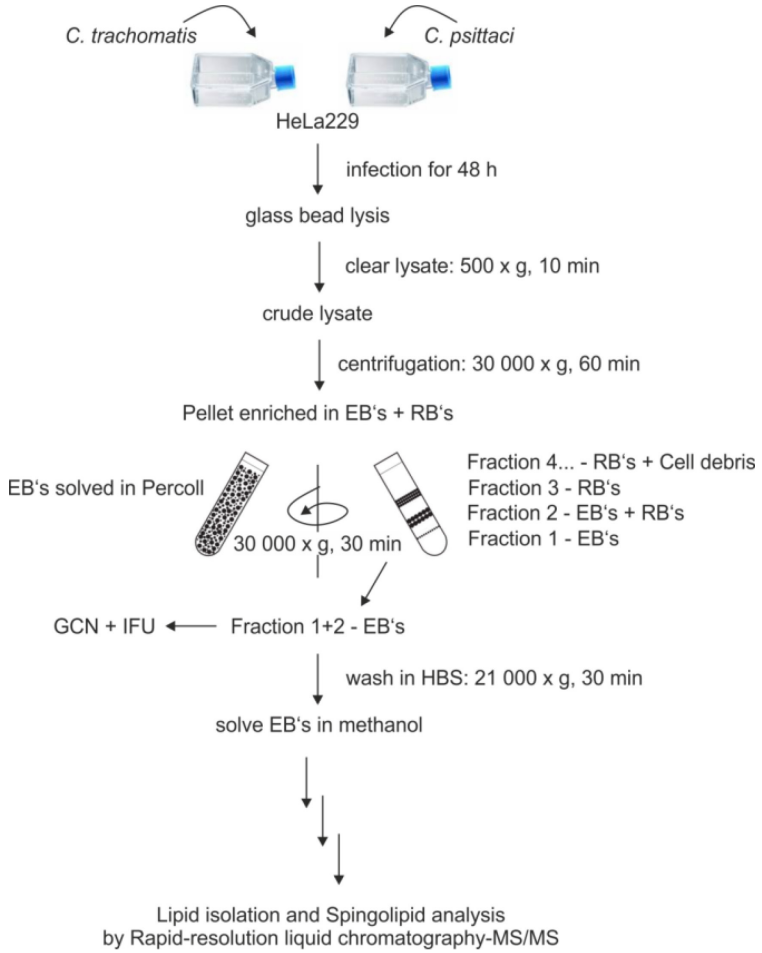

Figure 2.1 Workflow of EB purification and lipid analysis

Sample quality was assessed based on the washing fraction considering the relative content of chlamydial genomes (see Quantitative real-time PCR (qPCR)), IFUs and TEM.

2.2.3 Microscopy

Immunofluorescence staining

Cells were cultured in 12- or 24-well plates on glass coverslips. At the indicated time, cells were washed with PBS and fixed with 2% PFA at room temperature for 30 min. PFA was removed and cells were blocked and permeabilized in IF permeabilization buffer at room temperature for 20 - 25 min. Primary antibodies were diluted in IF blocking buffer and 25 µl or 40 µl droplets were placed on a parafilm. Coverslips were placed face down on top followed by incubation in a wet chamber at room temperature for 1 h. Cells were washed with PBS three times for 10 min and incubated with fluorophore-coupled secondary antibodies and DAPI in the dark for 1 h. Coverslips were washed with PBS three times for 10 min, mounted on a slide with Mowiol and dried for at least 16 h prior to microscopic analysis.

Phase contrast and epifluorescence microscopy

Phase contrast microscopy was performed with a Zeiss Axiovert 40 CLF microscope and served for the constant quality control of cell culture conditions and infections. Moreover, phase contrast

and epifluorescence microscopy were used in combination to determine the number of infectious progeny (see Reinfection assay) or measurement of bacterial inclusion size.

Laser scanning confocal microscopy

Laser scanning confocal microscopy was applied on immunostained samples using a Zeiss LSM 780 laser scanning confocal microscope (LSCM) equipped with Zeiss Zen software. Images were processed and corrected (brightness / color / contrast) with Zen2010 black where necessary and figures were assembled in Corel Draw Graphic Suite X6.

Live cell microscopy, Fluorescence Recovery After Photobleaching (FRAP)

For live cell microscopy cells were cultured and infected in live cell dishes with optimized optical properties. Experiments were performed with the Zeiss LSM780 in a preheated live cell chamber (35 - 37 °C, 5% CO_2).

A FRAP assay was developed to examine lateral diffusion in between Golgi elements. Cells were transiently transfected with plasmids encoding fluorescently labeled Golgi proteins (*cis*-Golgi: YFP-manII, *trans*-Golgi: CFP-GalT) and mock infected or infected with *C. trachomatis*. A part of the Golgi was bleached with a single laser pulse and images were acquired every 10 s using laser scanning confocal microscopy with pinhole wide open to simulate epifluorescence microscopy. Fluorescence values in the bleached and adjacent non-bleached area were measured using Zeiss Zen2010 software.

Transmission electron microscopy

Epon embedded samples were sliced with a Leica UC7 ultramicrotome in slices of approximately 60 nm. Sections were stained with uranyl acetate for 20 min, 2% lead citrate for 3 min and examined with a FEI Tecnai12 TEM operating at 120 kV. Image acquisition was performed with OSIS Megaview III Camera.

2.2.4 Nucleic acids

Polymerase Chain reaction

Fragments of DNA were amplified by polymerase chain reaction (PCR). For all DNA applications dedicated to cloning a Phusion High-Fidelity PCR Master Mix, matching primer and template DNA were used. The reaction mix was prepared as shown in Table 2.16 and reactions were run in a Jena Biosciences Flexcycler thermocycler.

Table 2.16 Standard reaction mixture for PCR

Reagent	50 µl reaction	Final concentration
2X Phusion Master Mix	25 µl	1X
10 µM Forward Primer	2,5 µl	0,5 µM
10 µM Reverse Primer	2,5 µl	0,5 µM
Template DNA	1 µl	< 250 ng
Nuclease-free water	19 µl	-

Polymerase chain reactions were performed with the standard protocol below, taking in consideration the melt temperature of the primer and product length:

Table 2.17 Standard cycling protocol for PCR

Reaction step	Time	Temperature	Cycle
Initial denaturation	10 min	95 °C	-
Denaturation	10 s	95 °C	
Annealing	30 s	50 - 58 °C	30 - 35x
Elongation	30 s / kb	68 °C	
Final elongation	10 min	68 °C	-

PCR products were separated by agarose gel electrophoresis to examine products obtained.

Cloning by restriction enzyme digestion and ligation

For cloning by restriction digestion and ligation, relevant PCR amplicons were purified directly from solution or gel purified using the Wizard SV Gel and PCR Clean-Up System following the manufacturer's instructions. In general, 500 ng of purified PCR product or 1 µg of pure destination vector plasmid were digested with appropriate restriction enzymes and buffers for 1 h at 37 °C. Digested DNA was subsequently purified and ligation reactions with T4 DNA Ligase were prepared using a 1:3 molar ratio of vector:insert. After ligation at 12 °C overnight, BioBlue chemically competent *E. coli* were transformed with 2 - 5 µl of the reaction mixture.

Clones were selected on LB Agar with antibiotics and insertion of DNA was verified by control restriction digestion. DNA sequences of positive tested clones were verified by Sanger sequencing in the Robert Koch Institute sequencing facility.

Quick change mutagenesis

DNA modifications were introduced by the quick change mutagenesis method (Zheng *et al.*, 2004). Primer containing mutations were designed with the tool PrimerX (http://www.bioinformatics.org/primerx/index.htm). The reaction mixture was prepared as described previously (Table 2.16), using 50 ng of template DNA. Cycling parameters for mutagenesis PCR are listed in Table 2.18.

Table 2.18 Cycling protocol for mutagenesis PCR

Reaction step	Time	Temperature	Cycle
Initial denaturation	5 min	95 °C	-
Denaturation	30 s	95 °C	
Annealing	30 s	50 °C	16 x
Elongation	1 min / kb + 1min	68 °C	
Final elongation	10 min	68 °C	-

After PCR, 1 µl of DpnI enzyme was directly added and incubated at 37 °C for 1h to destroy parental DNA. Products were purified and 3 µl were used for transformation. Resulting mutants were verified by Sanger sequencing of isolated plasmid DNA.

Quantitative real-time PCR (qPCR)

Relative amounts of chlamydial DNA in a sample were analyzed by quantitative real-time PCR. Reactions were prepared with QuantiTect SYBR Green RT-PCR kit (Qiagen) according to the manufacturer's instructions. Dilutions of heat inactivated cell-culture samples were used as template DNA. All reactions were run on a Stratagene Mx3000P thermocycler (Agilent Technologies).

2.2.5 Proteins

SDS-PAGE and Western blot analysis

5 x 10^5 cells grown in 12 well cell culture dishes were directly collected in 100 µl hot SDS-sample buffer and lysed by boiling at 95 °C for 10 min. 20 µl of sample per lane were loaded onto 10% or 15% denaturing SDS-gels depending on the molecular weight of proteins to be analyzed. Protein separation by electrophoresis was performed according to standard procedures (http://www.molecularcloning.com/index.php).

For Western Blot analysis (WB), separated proteins were transferred to an activated PVDF-membrane by standard wet blot procedure (200 mA for 2 h). Membranes were blocked at room temperature for at least 1 h in WB blocking buffer. Primary antibody diluted in WB blocking buffer was added to incubate under continuous agitation at 4 °C overnight. Membranes were washed with TBS-T 3 x 10 min and incubated with HRP-coupled secondary antibody at room temperature for 1 h. After 3 x 10 min washing steps, ECL solution was added and the resulting chemiluminescent signal was detected by exposure of X-ray films. Films were developed in an Agfa Citrix 60 developer and scanned for digitalization.

BCA-Assay

Protein concentrations of cell lysates were determined colorimetrically using a BCA Protein Assay Kit. Cells were lysed in PBS supplemented with 1% Triton X-100 on ice for 30 min, cell debris was spun down (600 x *g*, 4 °C for 10 min) and lysates were subsequently mixed with

prepared BCA working solution. After incubation at 37 °C for 30 min or 2 h absorption at 562 nm was measured using a Tecan infinite 200 device. Protein concentrations were calculated in relation to diluted albumin standards.

2.2.6 Lipids

Lipid extraction

Total lipid extracts from HeLa cells were generated as previously described (Yatomi *et al.*, 1995, Ruwisch *et al.*, 2001, Fayyaz *et al.*, 2014).

In brief, 0.5 - 1 x 10^6 HeLa cells were used. Cells were washed once with ice cold PBS, scraped and pelleted by centrifugation at 20,000 x *g*, 4 °C, 10 min. Cell pellets were suspended in ice cold methanol. 1/400 volume of HCl was added to each sample and solutions were complemented with C17-ceramide as internal standard. Then, 1 ml chloroform and 1 ml 1 N NaCl were added and samples were alkalized by addition of 100 µl 3 N NaOH solution. Samples were spun at 300 x *g* for 5 min to separate phases. The alkaline aqueous phase was transferred to a new vial whereas the organic phase was reextracted with 0.5 ml methanol, 0.5 ml 1 N NaCl and 50 µl 3 N NaOH. Aqueous phases were acidified with 100 µl concentrated HCl and extracted twice with 1.5 ml chloroform. Organic phases were combined, evaporated in a vacuum system and dried lipids were resolved in 275 µl methanol/0.07 M K_2HPO_4 by rigorous vortexing and sonication on ice.

Rapid-resolution liquid chromatography-MS/MS

Sample analysis was carried out by rapid-resolution liquid chromatography-MS/MS using a Q-TOF 6530 mass spectrometer (Agilent Technologies, Waldbronn, Germany) operating in the positive ESI mode (Fayyaz *et al.*, 2014, Pewzner-Jung *et al.*, 2014). The precursor ions of SPH (m/z 300.289), C17-SPH (m/z 286.274), and ceramides (C16-ceramide (m/z 520.508), C17-ceramide (m/z 534.524), C18-ceramide (m/z 548.540), C18:1-ceramide (m/z 546.524), C20-ceramide (m/z 576.571), C22-ceramide (m/z 604.602), C24-ceramide (m/z 632.634), C24:1-ceramide (m/z 630.618)) were cleaved into the fragment ions of m/z 282.280, m/z 268.264, and m/z 264.270, respectively. Quantification was performed with Mass Hunter Software (Agilent Technologies).

2.2.7 Computational methods

Determination of Golgi area

Golgi elements were immunostained with an antibody directed against GM130 and fluorescence images were taken with Zeiss LSM780 microscope using Plan-Apochromat 100x/1.40 Oil Ph3 M27 objective. Determination of Golgi area was performed with ImageJ. The smallest area enclosing all Golgi elements was manually determined and the measure command was used for data determination. Same procedure was applied to determine cell sizes. A minimum of 30 Golgi

apparatus and cells were included for each condition and Golgi areas are expressed as ratios of Golgi area / cell size.

FRAP analysis using FRAPAnalyser

The program FRAPAnalyser was provided by the University of Luxembourg (http://actinsim.uni.lu/eng/Downloads) and used for modelling and fitting of data from FRAP experiments. Data tables generated with Zen2010 software were imported as .txt files. Fluorescence recovery was calculated, and is represented as the ratio of the bleached to the adjacent areas, normalized to the pre-bleach and immediate post-bleach values. For each condition, a minimum of 30 cells was analyzed and included in the calculation.

In silico cloning, sequence alignment

For in silico cloning the software Geneious 7.1.4 was used. DNA sequences were imported from NCBI databases and all modification and alignments were performed with Geneious algorithms. Sequence alignments were performed with the Geneious Alignment option using the type of global alignment with free end gaps. For comparative sequence analysis the basic logarithmic alignement tool (blast) by NCBI was used.

Protein alignments were performed with the Geneious Alignment with the blosum62 cost matrix.

2.2.8 Statistical analysis

Data from at least two biological independent experiments were taken and technical replicates were included to correct for internal variations. In the diagrams mean values and standard errors are plotted (mean ± SE). Statistical significance was determined by Student's t-test (*: p-value< 0.05; **: p-value< 0.01; ***: p-value< 0.005).

3 Results

3.1 Golgin-84 in *C. trachomatis*-induced Golgi fragmentation

3.1.1 Golgi fragmentation and effect on enzyme distribution

The Golgi apparatus regulates secretion and sorting of newly synthesized proteins and lipids. In mammalian cells, it is a highly ordered organelle composed of stacked cisternae that are laterally linked to form the Golgi ribbon. Golgi matrix proteins, like golgins or Golgi reassembly and stacking proteins (GRASPs), are key components to maintain this complex structure (Barr & Short, 2003). Changes in the Golgi matrix composition often result in breakdown of Golgi structure accompanied by dispersal of Golgi elements (Diao *et al.*, 2003, Hu *et al.*, 2005, Mukherjee *et al.*, 2007).

Infections with *C. trachomatis* induce fragmentation of the Golgi apparatus in mammalian cells thereby lateral cisternal contact and continuity of the Golgi ribbon are impaired (Puthenveedu *et al.*, 2006, Heuer *et al.*, 2009). In *C. trachomatis*-infected cells these truncations of Golgi structure affect protein secretion and lead to reduced lipid transport to bacteria (Heuer *et al.*, 2009). However, data indicate that functionality of Golgi ministacks in protein and lipid transport strongly depend on the mode of ministack formation (Cole *et al.*, 1996, Puthenveedu *et al.*, 2006). Also enzyme distribution and enzyme dynamics within Golgi ministacks rely on ministack characteristics (Puthenveedu *et al.*, 2006).

The questions of enzyme distribution and dynamics in *C. trachomatis*-induced Golgi fragments were addressed using a live cell FRAP approach. In uninfected or *C. trachomatis*-infected HeLa cells, fluorescent Golgi enzymes YFP-ManII (*cis*-Golgi) and CFP-GalT (*trans*-Golgi) were transiently expressed and localizations were monitored over time. Golgin-84 knockdown cells, carrying a fragmented Golgi apparatus, were further analyzed to compare C*hlamydia*- and knockdown-related effects. In uninfected HeLa cells both Golgi enzymes located in distinct *cis*- or *trans*-Golgi cisternal compartments that formed an intact Golgi ribbon (Figure 3.1, A). In cells infected with *C. trachomatis* for 26 h, the Golgi apparatus was fragmented and recruited to the bacterial inclusion as previously reported. YFP-ManII and CFP-GalT accumulated in ordered compartments within ministacks indicating that *cis*- to *trans*-Golgi organization was still present. In all cases observed, the *cis*-Golgi faced the chlamydial inclusion (Figure 3.1, A). Ministacks induced by golgin-84 knockdown also comprised Golgi membrane proteins in discrete *cis*- and *trans*-Golgi compartments (Figure 3.1, A).

By introducing a strong laser pulse, fluorescent signals were selectively bleached and fluorescence recovery was monitored over time (FRAP). Loss of fluorescence rapidly recovered in uninfected cells that contained an intact Golgi ribbon. Although enzyme distribution was not obviously impaired in either infected or golgin-84 knockdown cells, we detected a decrease in fluorescence recovery of Golgi markers upon photobleaching in both conditions (Figure 3.1, B).

In summary, fluorescence recovery of fluorescently labeled Golgi enzymes was dramatically reduced in *C. trachomatis*-induced and golgin-84-mediated Golgi ministacks, whereas enzymes moved rapidly and fluorescence recovered within an intact Golgi ribbon. These results indicate that lateral cisternal contacts were essential for trafficking of Golgi membrane proteins which is impaired in *C. trachomatis*-infected cells.

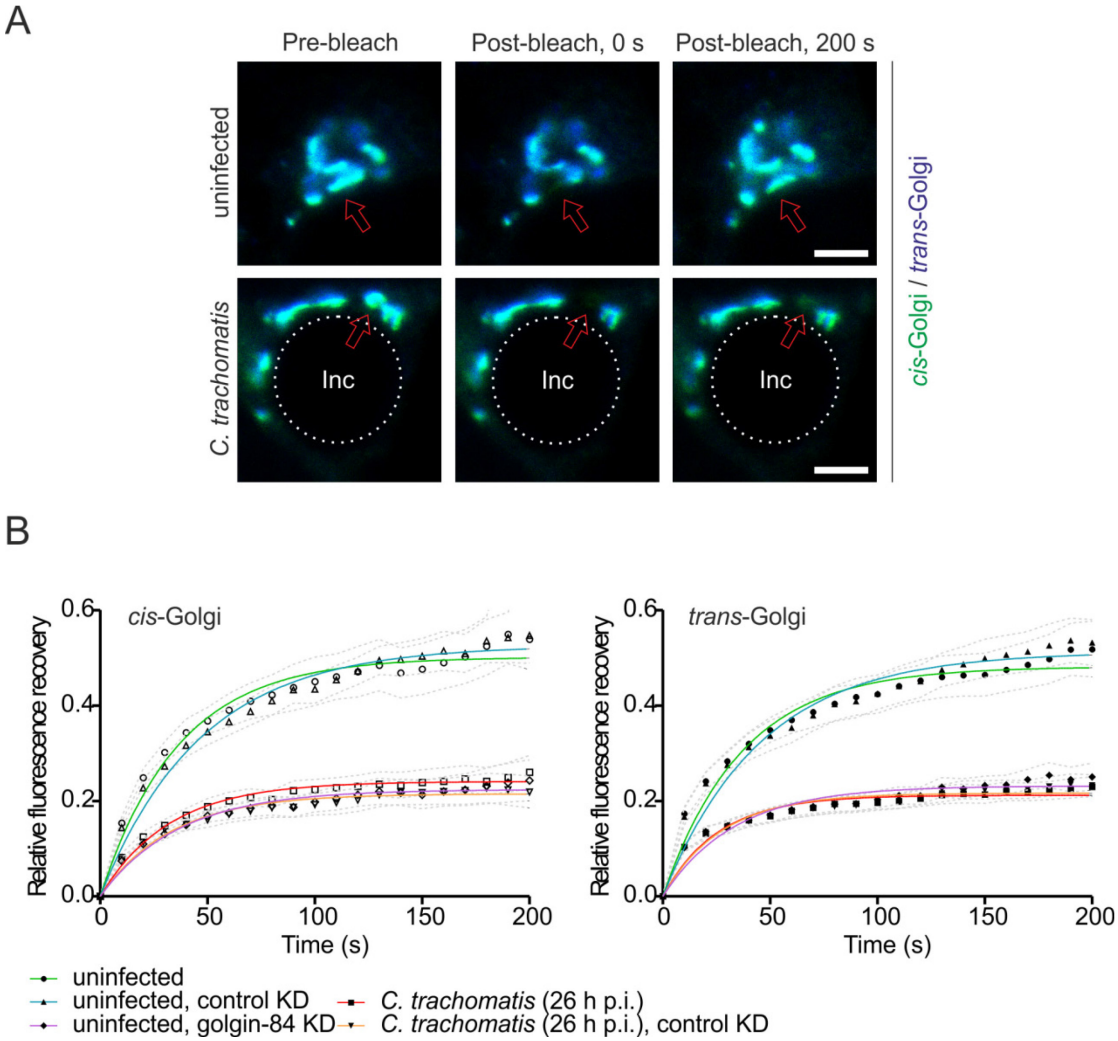

Figure 3.1 *C. trachomatis* infection reduces lateral diffusion of proteins in the Golgi apparatus.
(A) Live cell fluorescence images before and after selective photobleaching of Golgi markers expressed in infected HeLa cells. Cells were infected with *C. trachomatis* (MOI 1) and transfected for transient expression of *cis*- and *trans*-Golgi markers (*cis*-Golgi, eYFP-mannosidase II; *trans*-Golgi, eCFP-galactosyl-transferase). 26 h *p.i.* a region of fluorescence (2 µm) was selectively photobleached and fluorescence recovery was monitored over time. Chlamydial inclusions (Inc) are marked by a dashed circle, red arrows indicate area of photobleaching. Scale bar, 3 µm. (B) Quantification of the relative fluorescence recovery in the *cis*- and *trans*-Golgi, respectively. Dashed lines indicate standard error of the mean (SEM; n > 30 from 3 independent experiments).

3.1.2 Role of the Golgi matrix protein golgin-84 in *C. trachomatis*-infected cells

C. trachomatis development strongly depends on Golgi fragmentation. In cells depleted for different Golgi membrane proteins (including golgin-84, p115, Gpp130, Giantin) Golgi structure is impaired and production of infectious progeny is boosted compared to control cells (Heuer *et al.*, 2009, Rejman Lipinski *et al.*, 2009) Golgin-84 was put into spotlight when mass spectrometric

analyses revealed that concurrently to *C. trachomatis*-induced Golgi fragmentation, golgin-84 processing occurs. Inhibition of specific proteases, thus preventing *C trachomatis*--mediated processing of golgin-84 and Golgi fragmentation, resulted in the reduction of chlamydial progeny (Heuer *et al.*, 2009). However, the precise molecular mechanism behind golgin-84 processing is still an open question. Today, the circulation of conflicting data gained by different methods, demands for further clarification (Chen *et al.*, 2012, Snavely *et al.*, 2014). Therefore, since in particular different methods of cell lysis revealed inconsistent results, studies that use alternative experimental procedures are needed.

C. trachomatis extensively interacts with the host secretory pathway and exploits retrograde transport routes to ensure nutrient uptake to the inclusion which promotes bacterial development (Scidmore *et al.*, 1996, Aeberhard *et al.*, 2015). As golgin-84 is involved in retrograde trafficking and mediates Golgi structure its role for *C. trachomatis* development was further examined and experiments were performed in cell culture thereby omitting cell lysis related effects.

Localization of transiently expressed golgin-84-GFP

To examine the localization of golgin-84 in *C. trachomatis* infected cells, I generated a set of golgin-84 fusion proteins that considered functional features described in literature (Figure 3.2). Due to a possibility in protein-cleavage, the fluorescent GFP tag was fused to the C-terminus of the proteins.

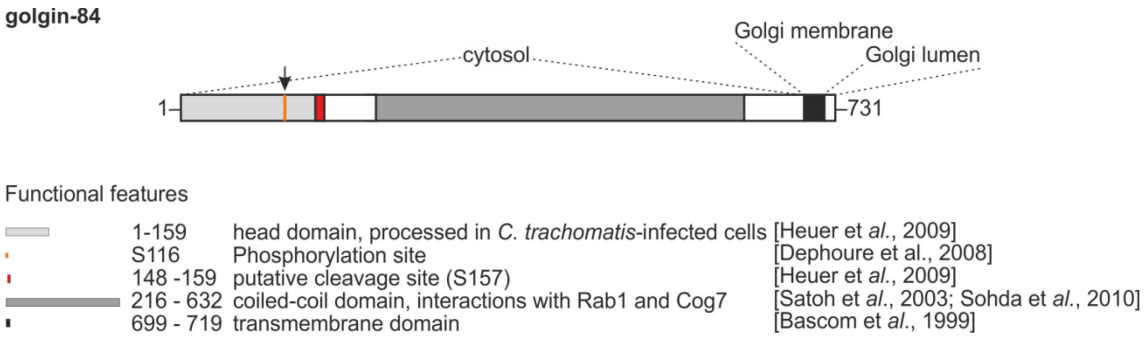

Figure 3.2 Golgin-84 is an integral Golgi protein with a cytoplasmic coiled-coil domain.
Schematic illustration of golgin-84 protein structure. Golgin-84 contains a large cytoplasmic coiled-coil domain responsible for interactions with Rab1 and Cog7 and a transmembrane achor for Golgi localization. During mitosis, phosphorylation at S116 occur. In *C. trachomatis*-infected cells, N-terminal amino-acids are removed by putative cleavage at S157. References of respective work are annotated.

To analyze protein localizations, HeLa cells transiently expressing golgin-84-GFP fusion proteins were infected with *C. trachomatis* or left uninfected. 24 h *p.i.*, cells were fixed and selected Golgi markers and DNA were stained prior to laser scanning confocal microscopy (Figure 3.3). In uninfected HeLa cells, transiently expressed golgin-84-GFP wildtype (1-731) localized to the Golgi apparatus and completely co-localized with endogenous GM130, another *cis*-Golgi marker. Golgi localization was also observed in *C. trachomatis*-infected cells. Moreover, *C. trachomatis* partially recruited the full length protein and a rim-like localization around the bacterial inclusion was observed (Figure 3.3, first panel). Deletion of the N-terminal head (amino

acids 1-148) did not change localization of golgin-84-GFP in uninfected cells. In infected cells, Golgi localization was not affected, but protein recruitment to *C. trachomatis* was no longer detectable (Figure 3.3, second panel).Transiently expressed golgin-84 (1-698) (cytosolic domain) showed, beside its localization to the Golgi apparatus, enhanced distribution throughout the cytosol. In infected cells protein recruitment of this mutant to *C. trachomatis* was even enhanced (Figure 3.3, third panel). Deletion of both N-terminal and C-terminal fragments resulted in complete loss of Golgi localization but *C. trachomatis* was still able to recruit golgin-84-GFP (159-698) from cytoplasmic pools (Figure 3.3, right panel).

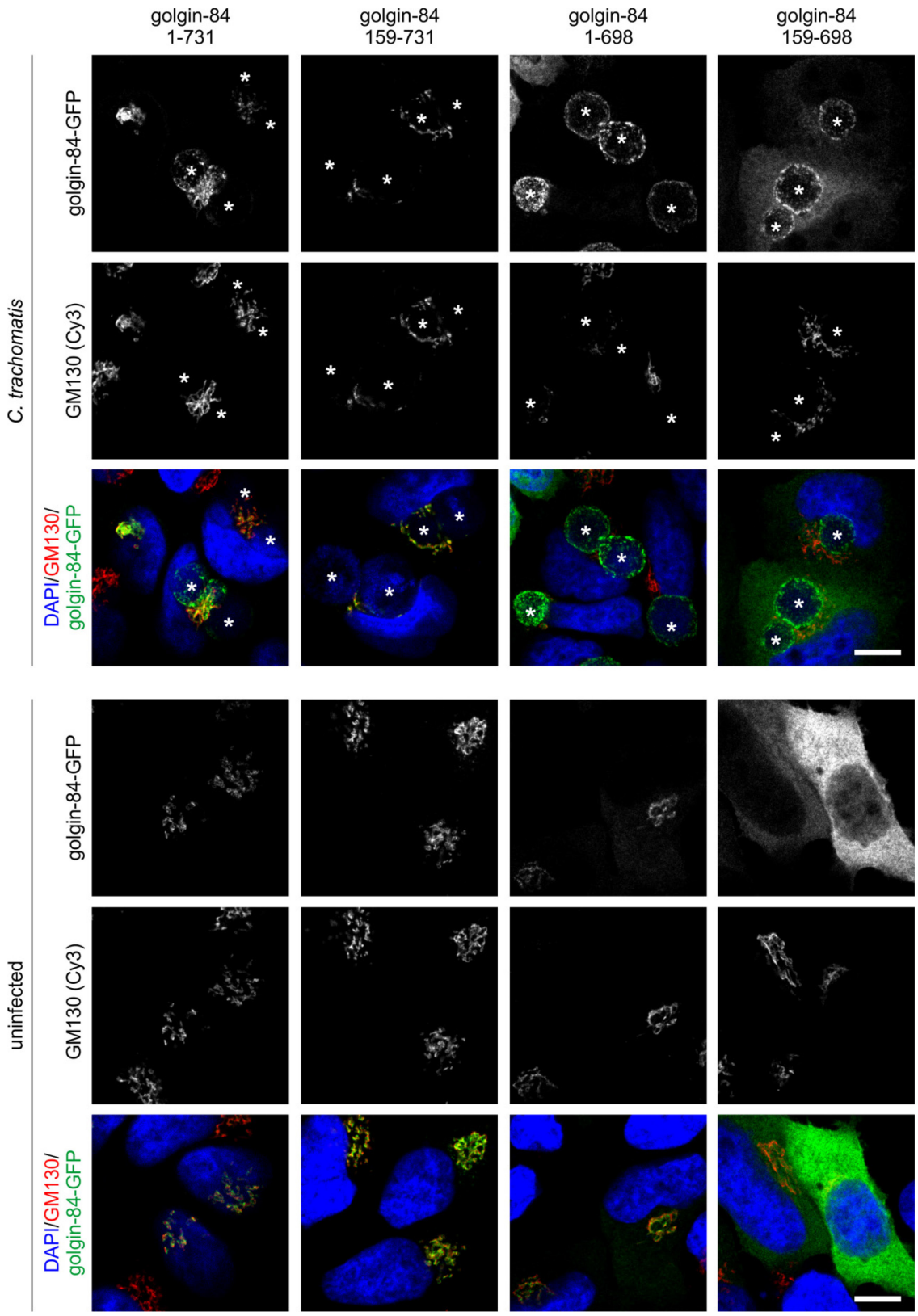

Figure 3.3 Golgin-84-GFP and several truncated versions localize to the Golgi apparatus and are recruited to *C. trachomatis* inclusions.
Representative fluorescence images of HeLa cells transiently expressing variants of golgin-84-GFP. HeLa cell transiently expressing golgin-84-GFP mutants were infected with *C. trachomatis* MOI2 for 24 h or left uninfected. Cells were fixed and Golgi elements were counterstained using an anti-GM130-antibody (Cy3). DNA was stained with DAPI. Samples were monitored by laser scanning confocal microscopy, stars indicate chlamydial inclusions. Scale bar, 10 µm; n ≥ 2 independent biological experiments.

As the N-terminal part of golgin-84 has been reported to be cleaved in the course of infection with *C. trachomatis*, and its abundance mediates recruitment to the inclusion, I tested if golgin-84 amino acids 1-148 harbor an inclusion localization signal (Heuer *et al.*, 2009). HeLa cells transiently expressing the C- or N-terminally tagged protein fragment were infected with *C. trachomatis* or left uninfected and upon staining with p230 and DNA were processed for microscopic analysis (Figure 3.4). In uninfected cells respective fluorescent signals were spread all over the cytosol without distinct accumulations. In several cells an increased fragmentation of the Golgi apparatus was detected leading to the suggestion that expression of this short fragment contributes to destabilization of the Golgi ribbon. In cells infected with *C. trachomatis*, fusion proteins were detected all over the cytosol without any indication of protein recruitment to inclusions.

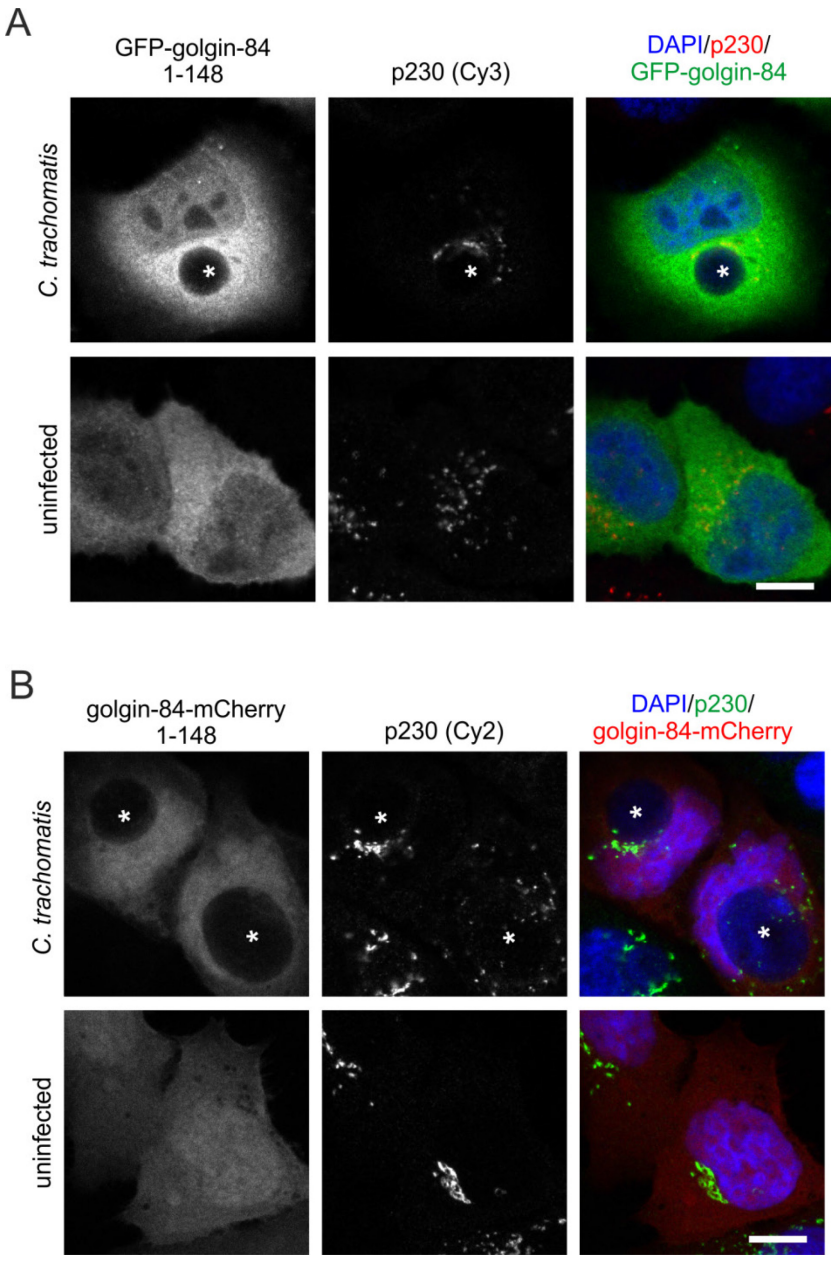

Figure 3.4 N-terminal-golgin-84 (1-148) is not recruited to *C. trachomatis* inclusion but expression increases Golgi fragmentation.
Fluorescence images of HeLa cells transiently expressing different variants of tagged N-terminal-golgin-84 (1-148). HeLa cells transiently expressing N-terminal golgin-84 mutants were infected with *C. trachomatis* MOI2 for 24 h or left uninfected. Cells were fixed and Golgi elements were counterstained using an anti-p230-antibody (Cy2 or Cy3), DNA was stained with DAPI. Laser scanning confocal microscopy was used for analysis, stars indicate chlamydial inclusions. Scale bar, 10 µm; n ≥ 2 independent biological experiments.

Localization of golgin-84-mCherry to C. trachomatis is important for progeny formation

Mutants of golgin-84 differentially localize to *C. trachomatis* inclusions. If golgin-84 localization consequently affects chlamydial progeny formation was therefore addressed by a one-step re-infection assay. To reduce effects of endogenously expressed wildtype golgin-84, experiments were performed in a cell line with stable knockdown of golgin-84 complemented with respective golgin-84-mCherry fusion proteins (Heuer *et al.*, 2009). Briefly, golgin-84 knockdown

cells transiently expressing selected mutants of golgin-84-mCherry were infected with *C. trachomatis* and 32 h *p.i.* primary infections were stopped by mechanic cell detachment and lysis. Fresh naïve HeLa cells were infected with obtained lysates and 24 h *p.i.*, these secondary infections were stopped and inclusions were immunostained and quantified. In cells, transiently expressing golgin-84 (159-731), which was not recruited to *C. trachomatis*, infectious progeny was reduced to 70% compared to cells expressing full length golgin-84 or golgin-84 (1-698) both associated with inclusions.

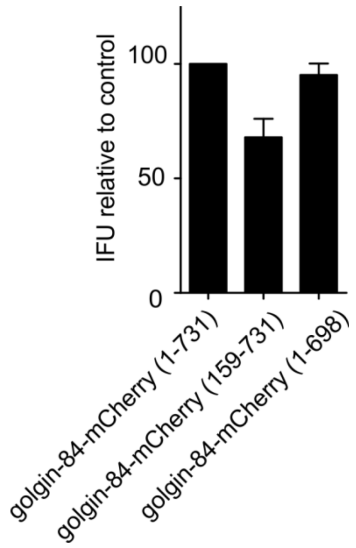

Figure 3.5 Overexpression of golgin-84-mCherry (159-731) reduces infectivity in golgin-84-knockdown cells.
Quantification of infectious progeny from *C. trachomatis* infected golgin-84 knockdown cells transiently expressing golgin-84-mCherry mutants. Samples were collected 32 h *p.i.*, titrated on fresh cells and infectious progeny was determined 24 h later after immunostaining of chlamydial Hsp60. Values were normalized to cells expressing full-length golgin-84-mCherry and data represent mean ± SEM; n = 3

Temporal analysis of golgin-84-GFP localization

C. trachomatis interactions with the host retrograde trafficking pathway are observed as soon as 1 h *p.i.* (Hackstadt *et al.*, 1996, Scidmore *et al.*, 1996). Additionally, in the course of their developmental cycle Golgi fragmentation is induced and possible golgin-84 processing occurs at 16 h *p.i.*, when bacteria are highly replicative (Hackstadt *et al.*, 1996, Heuer *et al.*, 2009). To correlate golgin-84 localization to *C. trachomatis* development (Figure 3.4, Figure 3.5), I studied spatial and temporal distribution of golgin-84-GFP in *C. trachomatis*-infected cells. Therefore HeLa cells were transfected with plasmids encoding full length golgin-84-GFP, infected with *C. trachomatis* or left uninfected and fixed at indicated times. Golgi elements and DNA were counterstained and protein localization was analyzed by laser scanning confocal microscopy. In uninfected cells, golgin-84-GFP localized to *cis*-Golgi compartments, as soon as a fluorescent signal was detectable. In HeLa cells infected with *C. trachomatis* golgin-84-GFP localized preferentially to GM130-positive structures at early times of infection. At 20 h *p.i.*, when bacterial inclusions became clearly detectable, fluorescent signals started to separate between the Golgi

apparatus and the bacterial inclusion (Figure 3.6, A). At this time, in 50% of all golgin-84-GFP expressing cells, the protein was recruited to *C. trachomatis* inclusions. 24 h *p.i.*, the proportion of golgin-84-GFP decorated *C. trachomatis* inclusions increased to 70% and remained stable over the time of analysis (Figure 3.6, B). While the ratio of golgin-84 positive inclusions remained stable over time, fluorescent signals at larger inclusions were less intense than at small early inclusions. These results suggest that a steady protein level at the inclusion was reached around 28 h *p.i.*, when homotypic fusion of bacteria was completed and re-differentiation from RBs to EBs started.

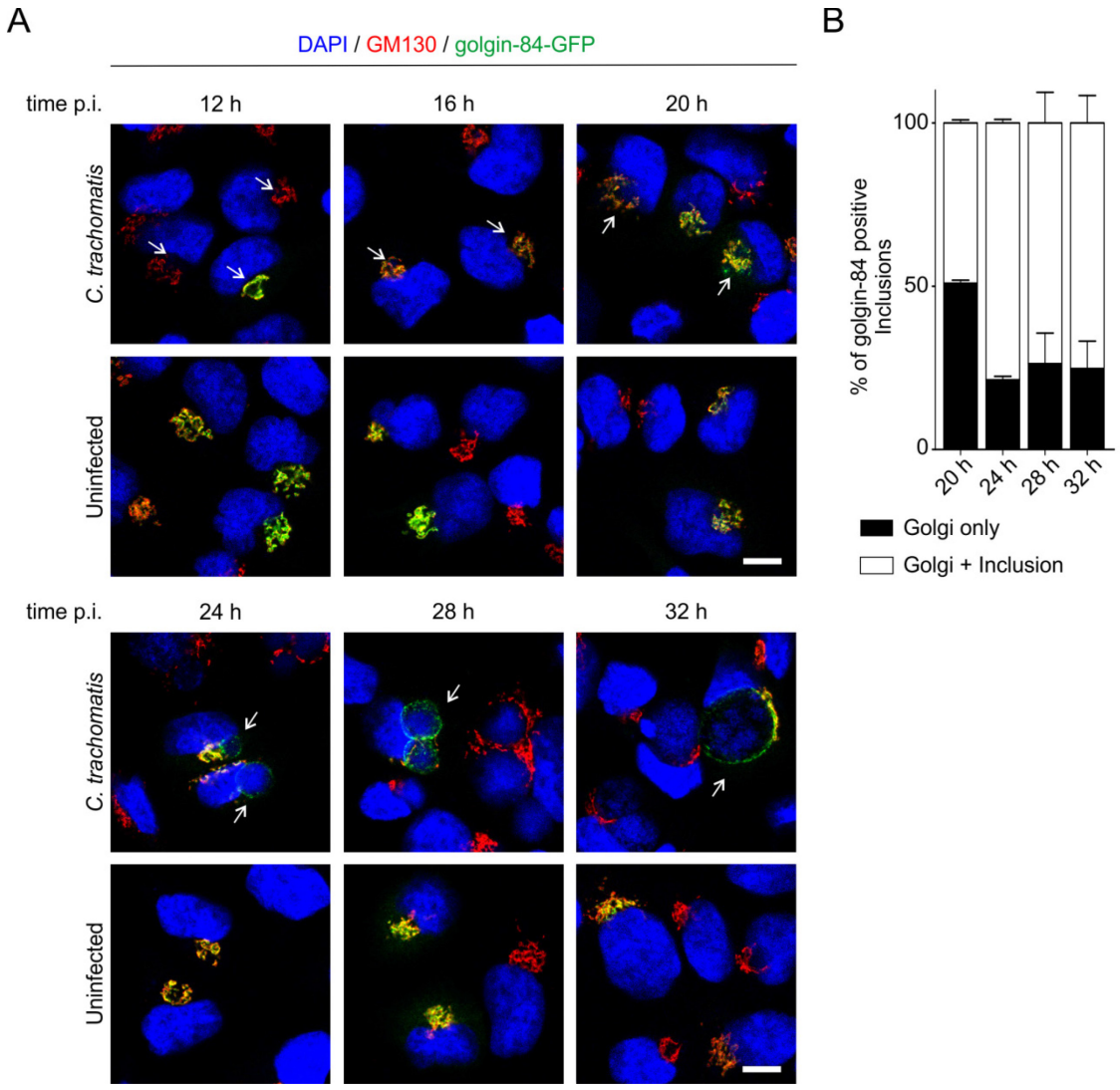

Figure 3.6 Golgin-84-GFP is recruited to *C. trachomatis* inclusions 20 h *p.i.* and stays associated over the time of analysis.
(A) Time series of fluorescence images showing HeLa cells transiently expressing golgin-84-GFP. HeLa cells transiently expressing golgin-84-GFP were infected with C. trachomatis MOI2 for indicated times or left uninfected. Cells were fixed and Golgi elements were counterstained using an anti-GM130-antibody (Cy3), DNA was stained with DAPI. Analysis was performed by laser scanning confocal microscopy, arrows indicate chlamydial inclusions. Scale bar, 10 µm. (B) Quantification of golgin-84-GFP localizations in infected cells. Values were normalized to total amount of transfected cells counted, data represent mean ± SEM; n > 60 transfected cells from 2 independent experiments.

Live cell processing of double-tagged golgin-84

Within this study, localization of golgin-84-GFP to *C. trachomatis* was shown to be influenced by the N-terminal region including amino acids 1-148 (Figure 3.3). Moreover, transient expression of golgin-84-mCherry (159-731), not localizing to *C. trachomatis* inclusions, decreased chlamydial progeny formation in golgin-84 knockdown cells (Figure 3.5). Although these results suggest a function for the N-terminal part of golgin-84 in *C. trachomatis* infections, evidence for golgin-84 processing upon chlamydial infection is still missing. Therefore, I intended to address the question of golgin-84 processing without provoking lysis related effects and came up with a set-up for live-cell microscopy. A golgin-84 construct carrying an N-terminal GFP-tag as well as a C-terminal mCherry-tag was generated (schematically show in Figure 3.7, A) and expression was tested in various cell lines (HEC-1-B, HeLa, HeLa229). In all tested cell lines the majority of transiently expressed GFP-golgin-84-mCherry localized to the Golgi apparatus in uninfected cells. In *C. trachomatis*-infected cells two distinct phenotypes of protein distribution occurred which are exemplarily shown for HeLa cells (Figure 3.7,B). Complete co-localizations of both fluorescent signals were found in a large proportion of infected cells at 24 h *p.i.* In a subset of *C. trachomatis*-infected cells the signals for GFP and mCherry were distinctly separated from each other, providing evidence for protein processing in these cells. Scatter plots showing the intensity distributions of GFP and mCherry support these qualitative observations (Figure 3.7, C).

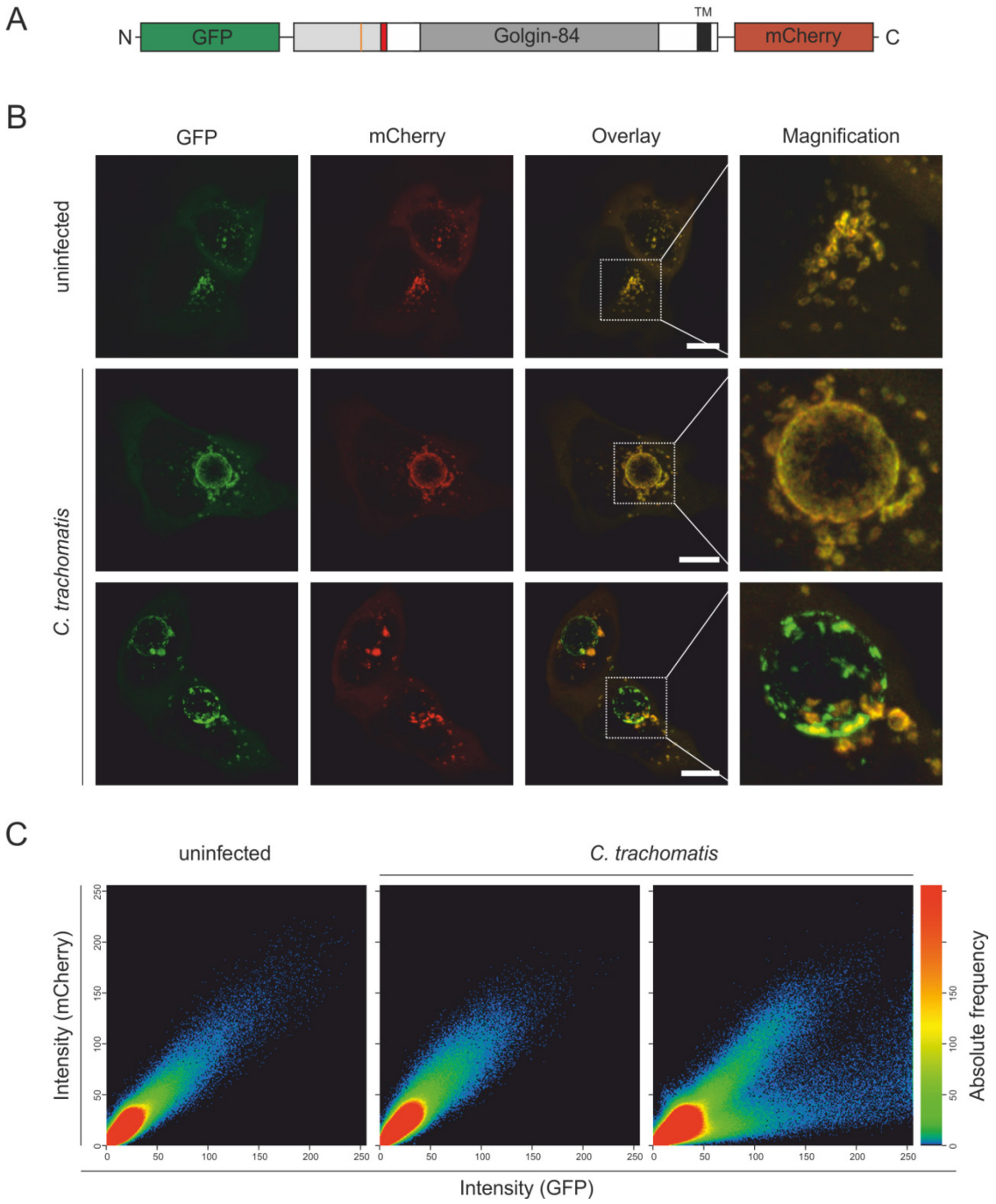

Figure 3.7 N- and C-terminus of golgin-84 display discrete localizations during *C. trachomatis* infection. (A) Schematic representation of the golgin-84 fusion protein with N-terminal GFP-tag and C-terminal mCherry-tag. (B) Representative images of live fluorescence microscopy. HeLa cells, uninfected or infected with *C. trachomatis* were transfected for transient expression of GFP-golgin-84-mCherry. 24 h *p.i.* green and red fluorescence were monitored by laser scanning confocal microscopy, micrographs were processed using maximum intensity projection of z stacks. Scale bar, 10 µm. (C) Scatter plots of GFP and mCherry signal intensities in micrographs of panel B indicating a separation of both signals at the inclusions of infected cells.

Summary

In sum, two protein domains of golgin-84 were identified that determined protein localization to *C. trachomatis* inclusions. Starting 20 h *p.i.*, transiently expressed full-length golgin-84 was tightly associated with *C. trachomatis* inclusions. N-terminal residues 1-158 were thereby essential for

protein recruitment to *C. trachomatis* inclusions, while golgin-84 residues 159-698, enclosing the coiled-coil domain, only participated in recruitment of golgin-84 from cytosolic pools. Furthermore, it was demonstrated that impaired localization of golgin-84 to *C. trachomatis* goes along with a reduction in chlamydial progeny formation. Finally, live-cell microscopy revealed that golgin-84 is processed upon *C. trachomatis* infection in a subset of living cells. The combination of gained results strengthens the point that *C. trachomatis* recognizes golgin-84 via its N-terminal domain and subsequent recruitment to the inclusion combined with protein modification contributes to infectious progeny formation.

3.2 Human and zoonotic *Chlamydia* spp. induce Golgi fragmentation

Pathogen-induced fragmentation of the Golgi apparatus has been described for the human pathogens *C. trachomatis* and *S. flexneri* (Hackstadt *et al.*, 1996, Monier *et al.*, 2002, Heuer *et al.*, 2009). For both bacteria, this process is essential to establish functional interactions with the host secretory pathway and further has been suggested to influence pathogenesis. The zoonotic species *C. psittaci* infects various hosts but molecular mechanisms that contribute to the establishment of infections are poorly described (Knittler *et al.*, 2014, Knittler & Sachse, 2015). To test if Golgi alterations are also involved in infections with zoonotic *C. psittaci*, I infected a human and an avian cell line with different *C. trachomatis* and *C. psittaci* strains and analyzed Golgi structure by immunofluorescence confocal microscopy.

3.2.1 Species-specific induction of Golgi alterations in human endothelial cells

HeLa cells were previously used to analyze Golgi fragmentation induced by *C. trachomatis*. So far, the serovar *C. trachomatis* L2, a lymphogranuloma venereum serovar, was primarily used to gain knowledge on Golgi fragmentation. The existing studies for HeLa cells infected with *C. trachomatis* L2 were extended and the ocular serovar *C. trachomatis* A and the urogenital serovar *C. trachomatis* D were included in our experiments. Additionally zoonotic *C. psittaci* isolates from different hosts were analyzed, namely *C. psittaci* 02DC15 (bovine isolate), *C. psittaci* 01DC11 (ovine isolate) and *C. psittaci* 08DC60 (human isolate). To analyze Golgi structure in *Chlamydia*-infected cells, HeLa cells were infected with the respective chlamydial strains for 26 h and Golgi elements were immunostained. To determine the relative Golgi area per cell, the area of the smallest polygon enclosing all Golgi elements was determined and divided by the area of the cell.

Within the bacterial developmental cycle, Golgi fragmentation was induced by all serovars of *C. trachomatis* and fragmentation, expressed as the relative Golgi area per cell, increased depending on MOI. As described for *C. trachomatis* L2, Golgi ministacks were recruited to the inclusions of serovars A and D independent of the infectious dose (Figure 3.8, A, upper panel). Infections with the different strains of *C. psittaci* also induced Golgi fragmentation but, in contrast to *C. trachomatis*, at higher MOI, GM130 positive Golgi elements were distributed throughout the

cell and were not recruited to bacteria (Figure 3.8, A, lower panel). The strongest effect in Golgi distribution was induced by the bovine isolate *C. psittaci* 02DC15 but was less pronounced upon infection with ovine or human isolates. However, Golgi elements induced by any *C. psittaci* strain were smaller in size compared to *C. trachomatis*.

Taken together, fragmentation was more pronounced upon *C. psittaci* infections compared to *C. trachomatis* as shown by quantitative description of the MOI dependent increase in Golgi area and decrease in Golgi particle size (Figure 3.8, B & C).

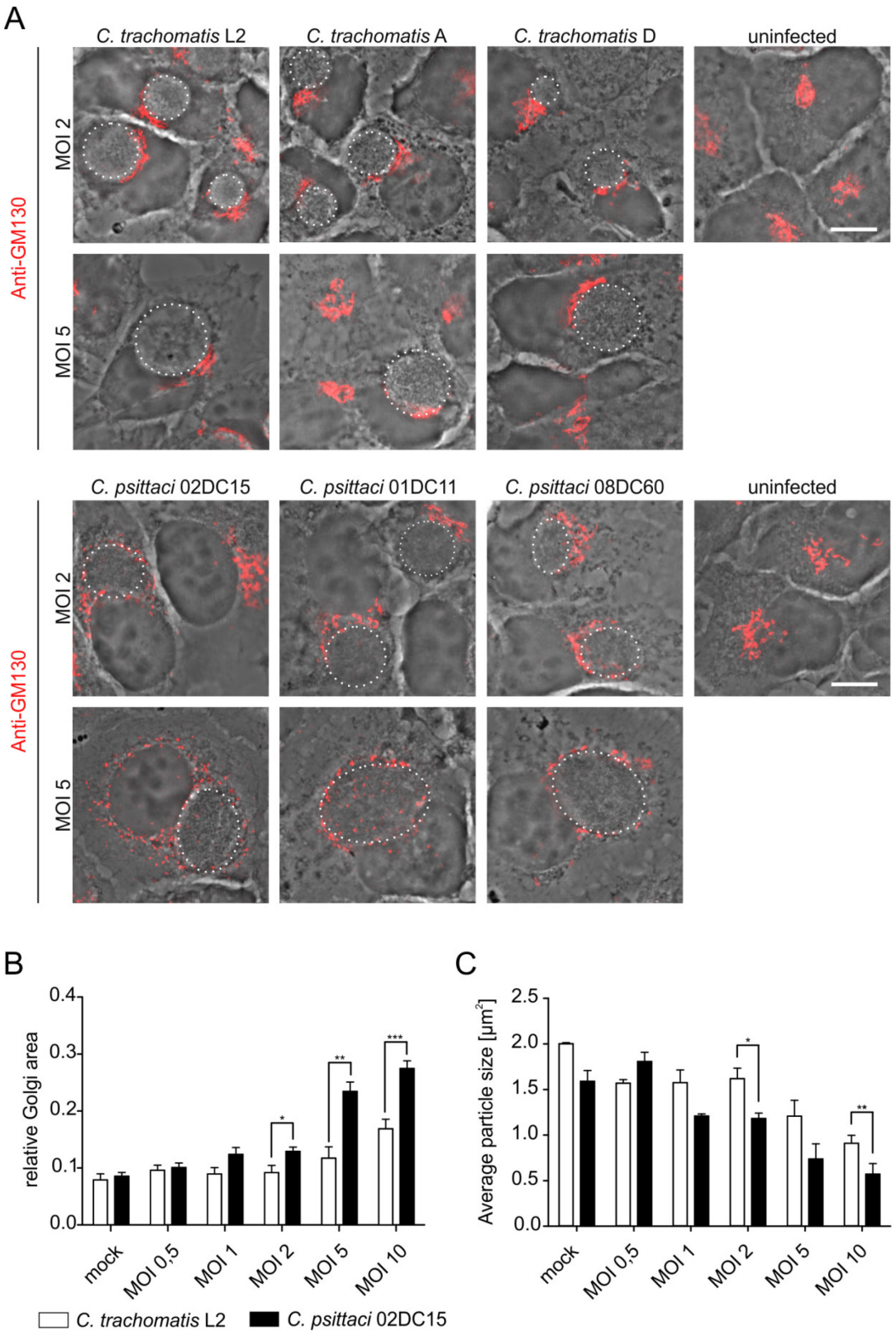

Figure 3.8 Human and zoonotic chlamydial infections induce Golgi fragmentation in HeLa cells.
Fluorescence images of HeLa cells infected with different MOI of *C. trachomatis* or *C. psittaci.* (A) HeLa cells were infected with *C. trachomatis* serovar L2, D, A or *C. psittaci* strain 02DC15, 01DC11, 08DC60 using increasing MOI (MOI 0.5 to MOI 10), uninfected cells were used as a control. Cells were fixed at 26 h *p.i.* (*C. trachomatis* L2, *C. psittaci*) or 40 h *p.i.* (*C. trachomatis* A, D) and Golgi elements were stained for GM130 (Cy3). Samples were analyzed by laser scanning confocal microscopy. White dashed lines indicate chlamydial inclusions. Scale bar 10 µm. (B) Quantification of relative Golgi area or (C) average Golgi particle size in uninfected HeLa cells or after infection with different MOI of *C. trachomatis* L2 or *C. psittaci* 02DC15. Data indicate mean ± SEM; n > 30 cells from 2 independent experiments.

3.2.2 Species-specific induction of Golgi alterations in chicken fibroblasts

Avian species, such as parrots, turkey and poultry are the predominant hosts for *C. psittaci* (Andersen & Vanrompay, 2000). We therefore asked if structural changes of the Golgi apparatus can also be induced in avian cells upon infection with *Chlamydia* spp. The chicken fibroblast cell line DF-1 was used and Golgi elements were visualized by immunostaining of GM130 (Figure 3.9). Since the antibody used in this study was raised against a C-terminal fragment of rat GM130 and was proposed to recognize GM130 homologues from other mammals, it was tested if in DF-1 cells a respective chicken antigen is recognized. Sequence alignements using blast identified a predicted Golgi protein in chicken with a high homology to the rat antigen (XP_015135031.1, score: 110 (units), query cover: 100%, sequence identity: 53%). In addition to that, a distict Golgi signal, comparable to Golgi stainings in human cells, was detected by the rat GM130 antibody in DF-1 cells.

In uninfected DF-1 cells, the Golgi apparatus localized to a perinuclear region, close to the MTOC. In sparse DF-1 cell layers, where cell-cell contacts were rare, Golgi ribbons often surrounded cell nuclei. After infection with *C. trachomatis* or *C. psittaci* (MOI 2 or MOI 5) species-specific changes in Golgi morphology were observed. In *C. trachomatis* infections, Golgi elements accumulated around the inclusion at 26 h *p.i.* but Golgi ribbon structure was almost the same as in uninfected cells. On the other side, *C. psittaci* infected cells mainly showed multiple inclusions, indicating that homotypic fusion of inclusions was impaired or delayed. Inclusions arranged around DF-1 nuclei while Golgi elements mainly surrounded nuclei.

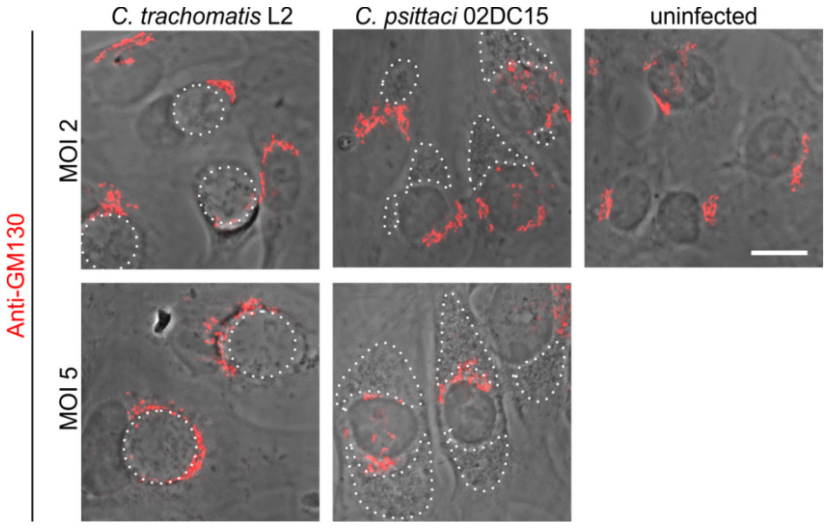

Figure 3.9 DF-1 chicken fibroblasts show distinct changes in Golgi morphology upon infection with human and zoonotic *Chlamydia* spp.
Figure shows representative fluorescence images of DF-1 cells uninfected or infected with *C. trachomatis* or *C. psittaci* (MOI 2, MOI 5). Cells were infected and fixed at 26 h *p.i.*, Golgi elements were stained for GM130 (Cy3). Red fluorescence was monitored by laser scanning confocal microscopy. White dashed lines indicate chlamydial inclusions. Scale bar, 10 µm, n = 3 independent experiments.

Together, the results show that *C. trachomatis*-induced Golgi fragmentation and recruitment of Golgi elements to the inclusion are conserved among different serovars and appear as very similar phenotypes in human or avian cell lines. Further, I showed that infections with zoonotic *C. psittaci* strains also result in Golgi fragmentation in HeLa cells but unlike *C. trachomatis*, recruitment of Golgi elements to *C. psittaci* was less pronounced. In an avian cell line, *C. psittaci* inclusions were characteristically distributed and changes in Golgi structure were induced that were distinct from HeLa cells.

3.3 Species-specific interactions of human or zoonotic *Chlamydia* spp. with Golgi-related proteins

In this study, initial experiments with *C. psittaci* showed that this zoonotic bacterium induces alterations in Golgi structure, similar to human *C. trachomatis*. Nevertheless, while Golgi fragmentation was induced by both *Chlamydia* spp., characteristics of resulting Golgi morphologies and Golgi distributions were species-specific. In the case of *C. trachomatis*, Golgi fragmentation promotes sphingolipid acquisition to chlamydial inclusions and is even essential for progeny formation. Moreover, Rab GTPases, key mediators of vesicular trafficking, participate in *C. trachomatis*-related Golgi rearrangements and support successful nutrient transport to bacteria (Rejman Lipinski *et al.*, 2009). Beside vesicular transport, *C. trachomatis* also exploits non-vesicular transport routes (Derre *et al.*, 2011, Elwell *et al.*, 2011). To further dissect species-specific properties of *C. trachomatis* and *C. psittaci* infections, I examined and compared pathogen interactions with distinct host trafficking pathways. Therefore, a series of overexpression experiments were performed in HeLa cells and localizations of Golgi resident proteins as well as other proteins involved in vesicular and non-vesicular trafficking pathways were qualitatively analyzed.

3.3.1 *Chlamydia* spp. and interactions with components of intracellular vesicular transport

Interactions with proteins of the ER-Golgi-interface

I have previously shown that golgin-84, mediator of retrograde intra-Golgi trafficking, localizes to *C. trachomatis* inclusions in HeLa cells and that localization affects infectious progeny formation (Figure 3.3, Figure 3.5). To test the role of golgin-84 in *C. psittaci* infections, I transiently expressed golgin-84-GFP in HeLa cells, and compared its localization in uninfected cells or cells infected with *C. trachomatis* or *C. psittaci*. Interestingly, unlike *C. trachomatis*, *C. psittaci* did not recruit golgin-84 and the protein completely remained in *cis*-Golgi elements (Figure 3.10). Localization of the Golgi-tether p115, a protein that similar to golgin-84 interacts specifically with a subtype of COPI vesicles, was further studied (Figure 3.10) (Malsam *et al.*, 2005). In uninfected cells, transiently expressed GFP-p115 localized to the Golgi apparatus and ER-like structures. The same localization pattern was seen in infected cells independent of the

chlamydial species. I also characterized the localization of the cargo-receptor ERGIC-53, that usually is involved in glycoprotein trafficking in the early exocytic pathway (Appenzeller *et al.*, 1999). In uninfected cells, tiny vesicular structures positive for GFP-ERGIC-53 were distributed all over the cell but highly concentrated in the Golgi region. Infections with *Chlamydia* spp. induced mild species-independent changes in protein localization; still vesicle-like distribution and accumulation in Golgi regions, here juxtaposed to inclusions were observed. Although no continuous rim-like staining to inclusions was found, inclusion association to tiny vesicular structures could not be excluded.

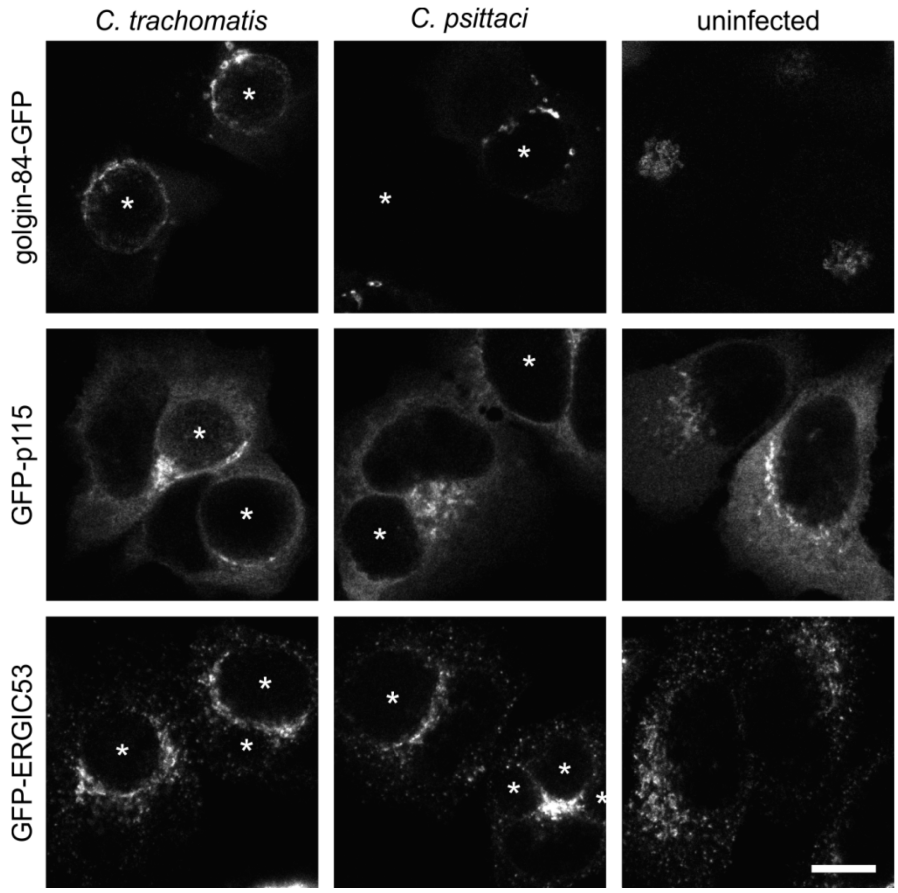

Figure 3.10 *C. trachomatis* and *C. psittaci* recruit proteins of the ER-Golgi interface in a species-specific manner.
Representative fluorescence images of HeLa cells transiently expressing GFP-fusion proteins of golgin-84, p115 or ERGIC-53. HeLa cells, transiently expressing fusion proteins were infected with *C. trachomatis*, *C. psittaci* (MOI2) or left uninfected. Cells were fixed 28 h *p.i.* and localization of fluorescent proteins was analyzed by laser scanning confocal microscopy. White stars indicate chlamydial inclusions. Scale bar, 10 µm , n ≥ 2 independent biological experiments.

In sum, localization studies indicate that *C. trachomatis* specifically intercepts golgin-84 mediated vesicular trafficking pathways whereas p115 coordinated pathways are not targeted. In contrast, no obvious recruitments of golgin-84 or p115 to *C. psittaci* inclusions were observed. Moreover, ERGIC-53 localized adjacent to the Golgi apparatus and inclusions, but was not specifically juxtaposed to one particular *Chlamydia* spp. Yet, no specific recruitment of cargo

tethering factors or receptors to *C. psittaci* inclusions could be shown, implying that the pathogen recruits nutrients via alternative routes or even acts autonomously.

3.3.2 Interactions with Golgi-coiled-coil tethering factors

Proteins of the golgin coiled-coil family are major regulators of vesicle capture at the Golgi surface. By selective tethering of cargo-laden vesicles from different origins they contribute to the organization of membrane traffic at the Golgi apparatus (Wong & Munro, 2014). As golgin-84, one member of this family was specifically related to *C. trachomatis* infections, we asked if other golgin membrane tethers can be linked to *Chlamydia* infections. It was recently demonstrated, that Golgi fragmentation due to down-regulation of golgin-84, GM130, Gpp130 and Giantin enhances *C. trachomatis* infectivity whereas knock-down of p230 does not affect infectious outcome (Heuer *et al.*, 2009). Since a connection of golgin-84 localization and *C. trachomatis* progeny formation was shown, we were further interested in the localization of golgins mentioned above. HeLa cells were infected with *C. trachomatis*, *C. psittaci* or left uninfected for 24 h. After, fixation and immunostaining samples were analyzed by laser scanning confocal microscopy. By using antibodies directed against GM130, Gpp130, Giantin and p230, I detected the localization of endogenous proteins (Figure 3.11). The peripheral *cis*-Golgi protein GM130 did not change its localization when cells were infected with *C. trachomatis* or *C. psittaci*. Golgi localizations of neither Gpp130 nor Giantin or p230 were affected by infections with *C. trachomatis* or *C. psittaci* and inclusions were not decorated with any of these tethers.

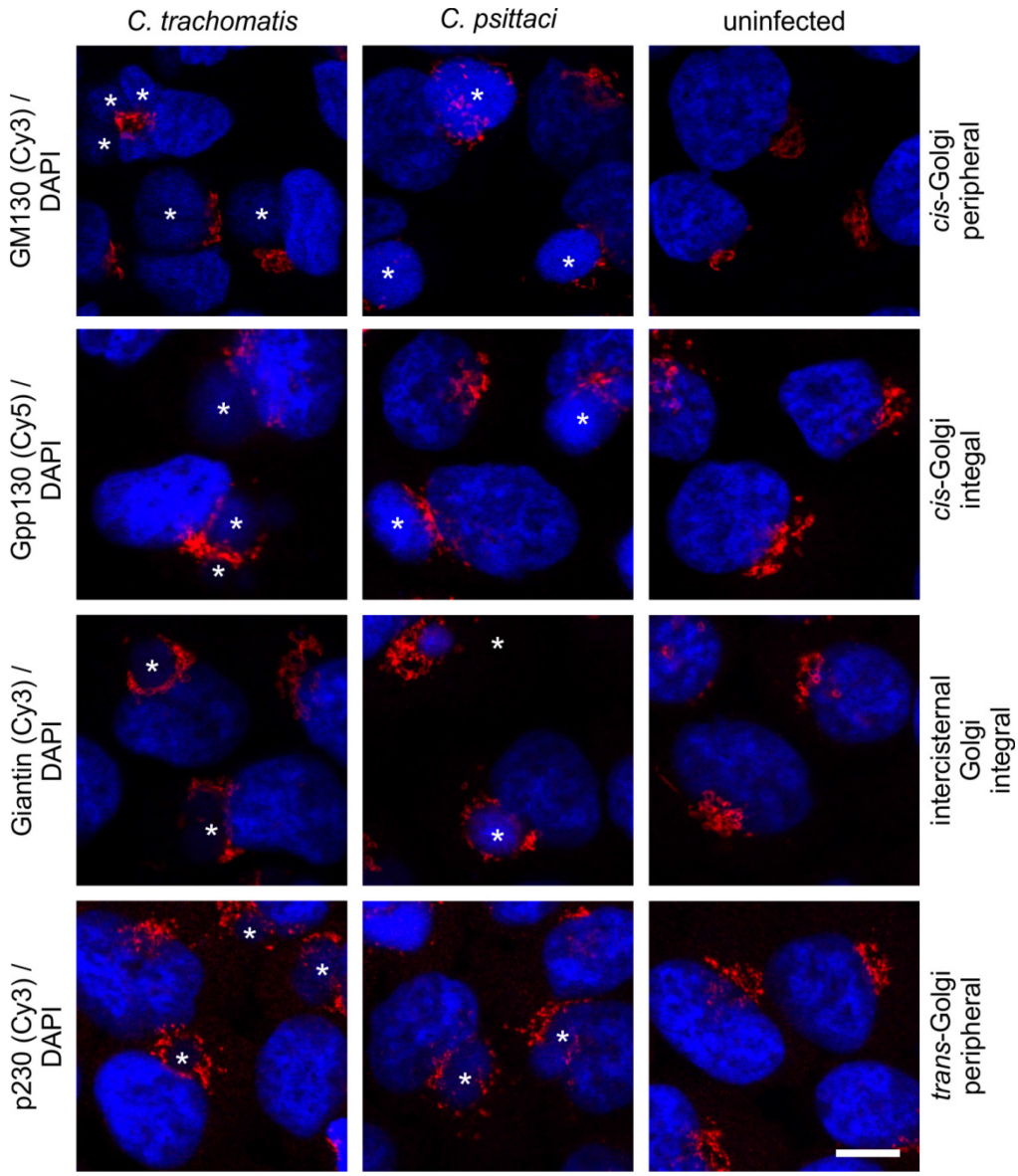

Figure 3.11 Golgin coiled-coil proteins GM130, Gpp130, Giantin and p230 are not recruited to *Chlamydia* spp. and Golgi localization is unaltered upon infection.
Representative immunofluorescence images of HeLa cells infected with *C. trachomatis* or *C. psittaci* (MOI 2) or left uninfected. 24 h *p.i.* cells were fixed and stained with antibodies against GM130, Gpp130, Giantin or p230 (all Cy3). DNA was counterstained with DAPI. Localization of fluorescently marked proteins was analyzed by laser scanning confocal microscopy. White stars indicate chlamydial inclusions. Scale bar, 10 µm, n ≥ 2 independent biological experiments.

These results strengthened the exceptional role of golgin-84 for *C. trachomatis* infections and further extended the idea of autonomy of *C. psittaci* towards tethering factors.

3.3.3 Interactions with Rab GTPases

Rab GTPases are involved in many aspects of membrane and vesicle trafficking in eukaryotic cells. In the Golgi apparatus Rab- and other small GTPases act in concert with coiled-coil golgins thereby promoting structure and identity of Golgi compartments (Short *et al.*, 2005). Beyond Golgi compartments, various other organelles participating in endocytic and secretory trafficking can be identified by their signatures of associated Rab GTPases (Zerial & McBride, 2001).

Several intracellular pathogens target and manipulate Rab GTPases to ensure reproduction and avoid lysosomal degradation (Rzomp *et al.*, 2003, Seto *et al.*, 2011, Hoffmann *et al.*, 2014). For human pathogenic *Chlamydia* spp., interactions with Rab GTPases predominantly involved in retrograde and recycling trafficking pathways have been identified (Rzomp *et al.*, 2003, Rzomp *et al.*, 2006, Cortes *et al.*, 2007). Recently published proteomic screens confirmed several of these interactions (Aeberhard *et al.*, 2015, Mirrashidi *et al.*, 2015). However, up to date, no data about possible interactions of the zoonotic agent *C. psittaci* with Rab GTPases exist.

To improve our understanding of the Rab-*Chlamydia* interplay, I transiently expressed Rab-fusion proteins in HeLa cells and analyzed their cellular distribution after infection with *Chlamydia* by laser scanning confocal microscopy.

First, I looked at Rab proteins involved in cargo transport from or to *cis*-Golgi compartments. Rab1 mediates vesicle transport from the ER to the Golgi apparatus and its association with *C. trachomatis* and other species has been previously shown (Rzomp *et al.*, 2003). I confirmed this observation for *C. trachomatis*, but on the other hand found no Rab1 signal associated with *C. psittaci* inclusions. For transiently expressed myc-Rab6A I gained an ambiguous picture. Although interactions between *C. trachomatis* and Rab6A, mediator of intra-Golgi transport, have been shown in a variety of studies, I just detected a spotty pattern surrounding *C. trachomatis* inclusions (Rzomp *et al.*, 2003, Aeberhard *et al.*, 2015). In *C. psittaci* infected cells, myc-Rab6A predominantly localized to Golgi structures and association with bacterial inclusions could neither be confirmed nor entirely excluded (Figure 3.12).

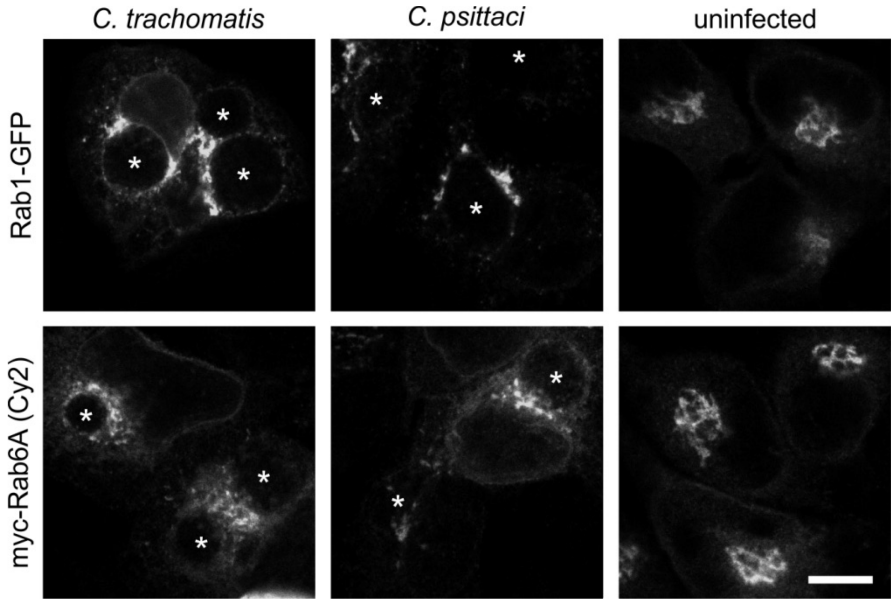

Figure 3.12 Rab proteins of the Golgi-ER interface are specifically recruited to *C. trachomatis* but not to *C. psittaci*.
Representative fluorescence images of HeLa cells transiently expressing GFP-Rab1 or myc-Rab6A. HeLa cell transiently expressing Rab fusion proteins were infected with *C. trachomatis*, *C. psittaci* (MOI 2) or left uninfected. Cells were fixed 24 h *p.i.* and, in case of Rab6A, immunostained with anti-myc antibody (Cy2). Samples were analyzed by laser scanning confocal microscopy. White stars indicate chlamydial inclusions. Scale bar, 10 µm, n ≥ 2 independent biological experiments.

Since *C. trachomatis* interferes with the host exocytic machinery, I examined the localizations of fluorescently tagged Rab11A, Rab8a and Rab35, all regulating endocytic recycling via recycling endosomes (Hackstadt *et al.*, 1996, Grant & Donaldson, 2009). Rab11A and Rab8a closely associated with *C. trachomatis* inclusions and localized in a rim-like pattern (Figure 3.13). Also Rab35 localized adjacent to *C. trachomatis* inclusions but the rim-like arrangement as previously observed was less distinct. *C. psittaci* also recruited Rab proteins from recycling endosomes to a subset of inclusions. Consistent with *C. psittaci*'s uneven inclusion morphology, fluorescent patterns were not as homogenous as those observed for *C. trachomatis*.

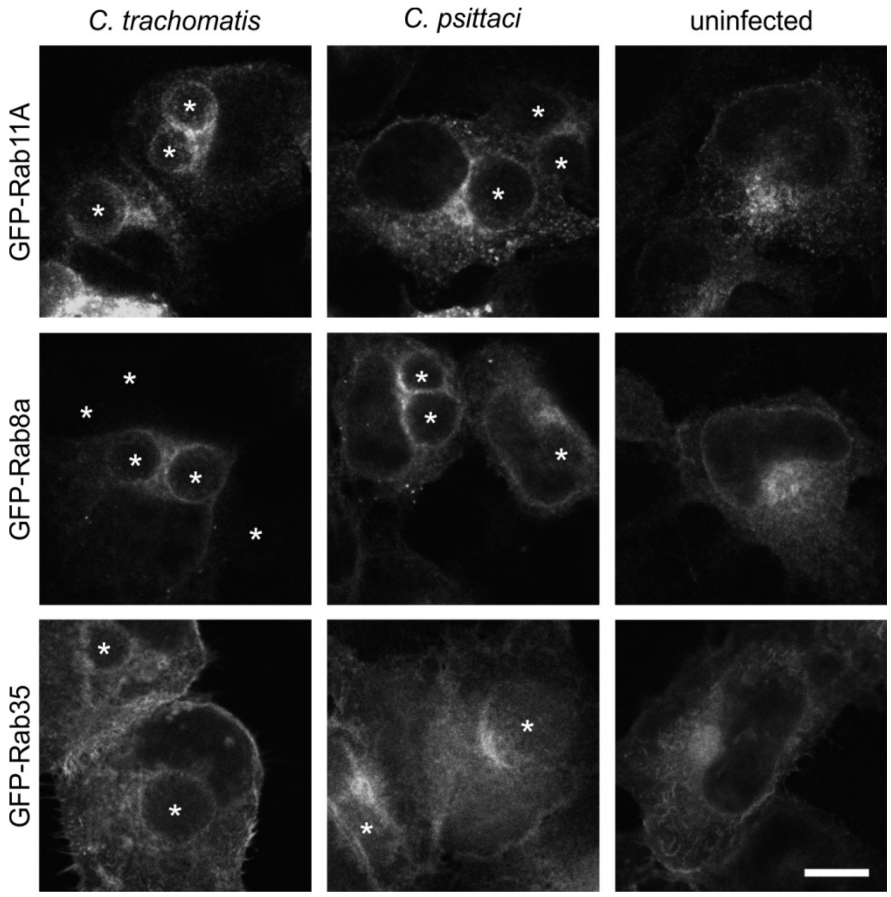

Figure 3.13 Rab mediators of recycling from late or recycling endosomes are recruited to both *C. trachomatis* and *C. psittaci* inclusions.
Representative fluorescence images of HeLa cells, transiently expressing GFP-Rab11A, GFP-Rab8a or GFP-Rab35. HeLa cells transiently expressing Rab fusion proteins were infected with *C. trachomatis* or *C. psittaci* (MOI 2) or left uninfected. 24 h *p.i.* cells were fixed and fluorescence was monitored by laser scanning confocal microscopy. White stars indicate chlamydial inclusions. Scale bar, 10 µm, n ≥ 2 independent biological replicates

Beside interactions with exocytic pathways, the regulated interplay with endo-lysosomal compartments is crucial for chlamydial inclusion maturation (van Ooij *et al.*, 1997). To prevent lysosomal degradation within the host cell, *C. trachomatis* inclusions escape from normal endosome maturation by omitting fusion with acidifying endocytic compartments (Scidmore *et al.*, 2003). Nonetheless, endosomes may still serve as nutrient reservoirs and interactions might further affect host cell signaling (Ouellette *et al.*, 2011, Palfy *et al.*, 2012).

In this experimental set-up I examined the spatial arrangement of endocytic markers Rab4, Rab5, Rab7 and Rab21 in conjunction with chlamydial infections. I confirmed that GFP-Rab4 localizes to *C. trachomatis* inclusions at 24 h *p.i.* In *C. psittaci*-infected cells, Rab4 positive vesicles accumulated in proximity to the bacterial inclusion, but continuous staining patterns, comparable to those observed for examples like Rab11A or Rab8 were just monitored in rare cases (Figure 3.14).

The endosomal markers GFP-Rab5 or GFP-Rab7, both regulating endo-lysosomal maturation, were neither found in direct contact with *C. trachomatis* nor *C. psittaci* inclusions. In both infection models small vesicular structures, although enriched at the MTOC, remained distributed all over the cytosol (Figure 3.14).

Rab21 directly controls integrin internalization and is usually found on early endosomal membranes. Rab21 activity directly affects cytokinesis and cell adhesion thus regulating cell migration (Pellinen *et al.*, 2006, Pellinen *et al.*, 2008). As *C. trachomatis* perturbs host cell migration on multiple levels GFP-Rab21 was included in the study (Heymann *et al.*, 2013). Direct spatial association of GFP-Rab21 positive vesicles and *C. trachomatis* inclusions was demonstrated. Also zoonotic *C. psittaci* recruited GFP-Rab21 and obviously accumulated Rab21 positive vesicles (Figure 3.14).

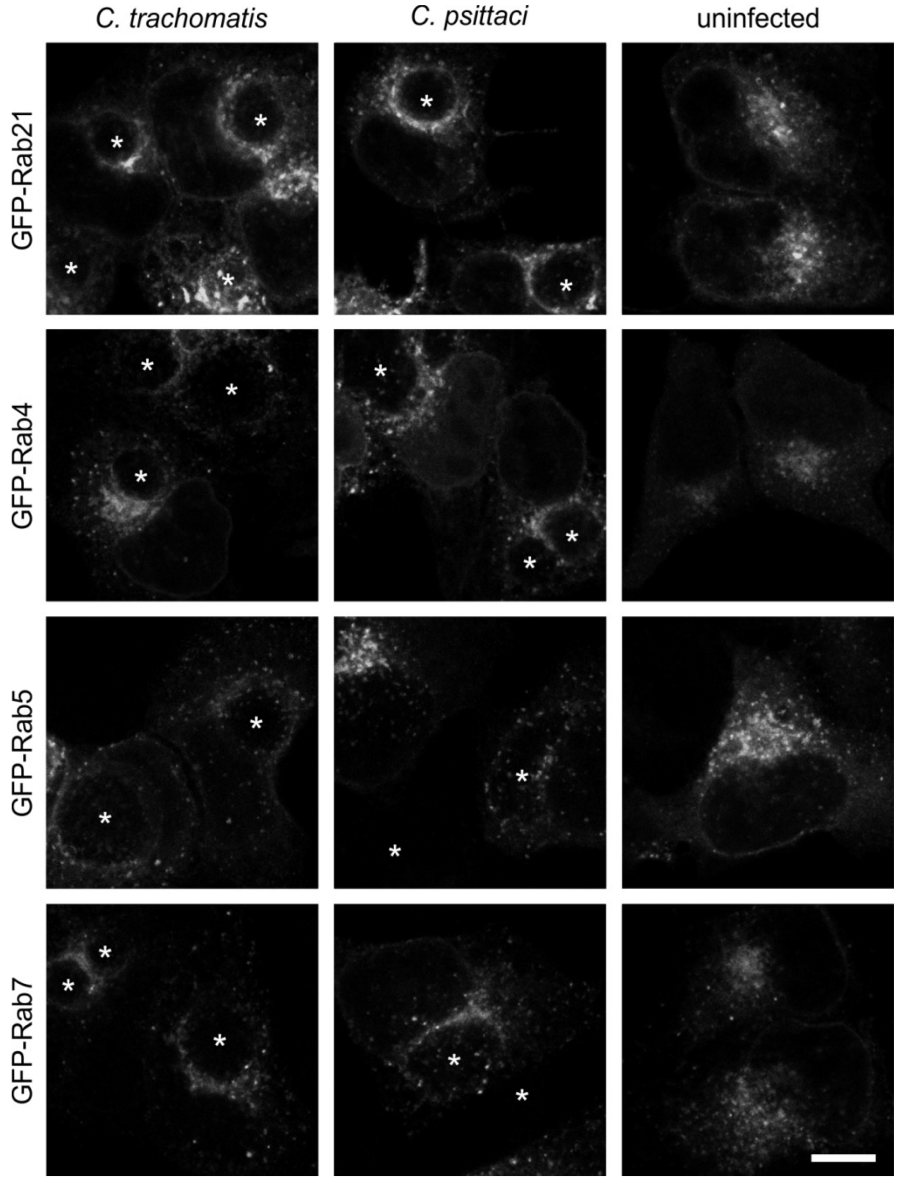

Figure 3.14 Rab proteins of early endosomal organization show no discrete localization to *C. trachomatis* or *C. psittaci* inclusions.
Representative fluorescence images of HeLa cells, transiently expressing GFP-Rab21, GFP-Rab4, GFP-Rab5 or GFP-Rab7. HeLa cells transiently expressing Rab fusion proteins were infected with *C. trachomatis*, *C. psittaci* (MOI 2) or left uninfected. Cells were fixed 24 h *p.i.* and analysis was performed using laser scanning confocal microscopy. White stars indicate chlamydial inclusions. Scale bar, 10 µm, n ≥ 2 independent biological experiments.

In a recently performed proteomic approach, Rab3D was identified as a component of the *C. trachomatis* mid-cycle inclusion (Aeberhard *et al.*, 2015). Under natural conditions the protein is found on secretory granules and directly acts on exocytic granule-membrane fusion (Knop *et al.*, 2004).

In cells infected with *Chlamydia*, transiently expressed YFP-Rab3D was found on granular structures as well as on *C. trachomatis* inclusion membranes. Fluorescence signals in cells infected with *C. psittaci* were monitored on granular as well as in ER-like structures both closely associated with the inclusion. Nevertheless, direct contact between Rab3D and *C. psittaci* was not completely clear.

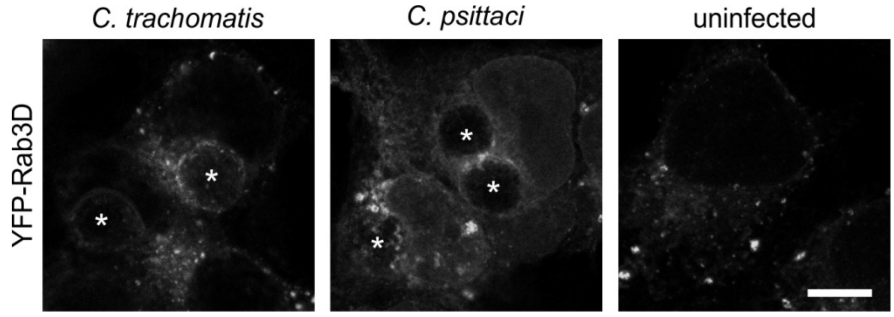

Figure 3.15 *C. trachomatis* and *C. psittaci* inclusions recruit vesicular structures of exocytic Rab3D.
Representative fluorescence images of HeLa cells, transiently expressing YFP-Rab3D. Cells were infected with *C. trachomatis*, *C. psittaci* (MOI 2) or left uninfected. 24 h *p.i.* cells were fixed and samples were analyzed by laser scanning confocal microscopy. White stars indicate chlamydial inclusions. Scale bar, 10 µm, n ≥ 2 independent experiments.

In summary, overexpression experiments demonstrate species-specific interactions of human and zoonotic *Chlamydia* spp. with distinct host Rab GTPases. Human *C. trachomatis* recruited a larger subset of Rab proteins including Rabs acting on the Golgi-ER interface, recycling endosomes and exocytic membrane fusions whereas Rab proteins responsible for phago-lysosomal maturation were excluded. Zoonotic *C. psittaci* were surrounded by a reduced subset of Rab proteins, predominantly composed of recycling endosomal Rab GTPases. Protein localizations of Rab proteins analyzed in this study are summarized in Table 3.1.

Table 3.1 Summary of GFP-Rab interactions with chlamydial inclusions
ER = endoplasmic reticulum, PM = plasma membrane, GA = Golgi apparatus, RE = recycling endosome, EE = early endosome, LE = late endosome, CCV = clathrin coated vesicle

		Inclusion localization in cells infected with		
Rab GTPase	**Membrane traffic / pathway**	***C. trachomatis***	***C. psittaci***	**uninfected**
Rab1	ER to GA, intra-GA	+	-	ER, GA
Rab6A	intra-GA	-/+	-	GA
Rab8a	RE to PM	+	+	PM, Recycling vesicles, primary cilia
Rab11A	RE to PM	+	+	GA, RE, EE
Rab35	RE to PM	-/+	-/+	PM, RE
Rab21	PM to EE	-/+	-/+	EE
Rab4	EE to PM	+	-	EE
Rab5	endosomal fusion	-	-	PM, CCV, EE
Rab7	LE to lysosome	-	-	LE, lysosomes
Rab3D	exocytosis	+	+	Secretory vesicle, PM

These results indicate that *C. trachomatis'* ability to interfere with numerous Rab-regulated trafficking pathways is a central mechanism that might have emerged during adaptation to a

specific human host cell. In contrast, *C. psittaci* interactions were limited to Rab-dependent recycling routes implying a lower level of specific adaptation. The frequent switching of hosts demands for more flexibility thereby supporting the development of alternative or autonomous mechanisms for *C. psittaci*-host interactions.

3.3.4 *Chlamydia* spp. and interactions with non-vesicular ceramide transport

Golgi-derived vesicles are important sources of sphingolipids acquired by *Chlamydia* spp. (Hackstadt *et al.*, 1995, Hackstadt *et al.*, 1996). Even though different *Chlamydia* spp. obtain host cell sphingolipids, the mechanisms of sphingolipid transport may be species- if not strain-specific (Rockey *et al.*, 1996, van Ooij *et al.*, 2000, Wolf & Hackstadt, 2001).

Beyond the interplay with sphingolipid containing vesicles, *C. trachomatis* directly interferes with non-vesicular lipid transportation along membrane contact sites. In the context of *C. trachomatis*, membrane contacts that usually bridge gaps between ER and Golgi apparatus, plasma membrane, mitochondria or endosomes, were formed between ER and the bacterial inclusion (Derre *et al.*, 2011, Dumoux *et al.*, 2012). Thus, *C. trachomatis* effector protein IncD could directly bind and interact with CERT, one functional component of ER-Golgi membrane contact sites mediating non-vesicular transport of ceramide. Indeed, CERT was highly enriched in *C. trachomatis* inclusion membranes and potentially transported *de novo* synthesized ceramide directly to bacteria (Derre *et al.*, 2011, Elwell *et al.*, 2011, Aeberhard *et al.*, 2015).

While *C. trachomatis* and *C. psittaci* recruit and interact with distinct subsets of Rab proteins the question arose if non-vesicular ceramide transport is also exploited by zoonotic *C. psittaci.* At this point, this question was addressed by analyzing localizations of endogenous CERT or transiently expressed GFP-CERT constructs in the context of *C. trachomatis* and *C. psittaci* infections.

Immunfluorescence images, using an antibody directed against endogenously expressed CERT, showed protein localization in HeLa cells that were previously infected with *C. trachomatis* or *C. psittaci* for 24 h. These confirmed CERT recruitment to *C. trachomatis* and further revealed, that *C. psittaci* inclusions also accumulate CERT to a high extend (Figure 3.16).

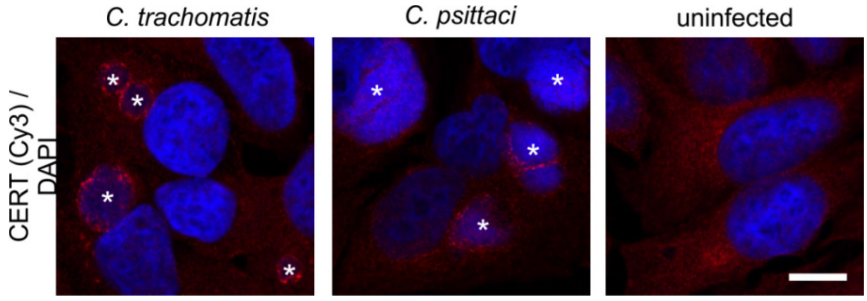

Figure 3.16 CERT localizes to *C. trachomatis* and *C. psittaci* inclusions.
Representative immunofluorescence images of infected HeLa cells. HeLa cells were infected with *C. trachomatis*, *C. psittaci* (MOI 2) or left uninfected for 24 h. Afterwards cells were fixed, CERT was immunostained (Cy3) and DNA was counterstained using DAPI. Fluorescence analysis was performed by laser scanning confocal microscopy. White stars indicate chlamydial inclusions. Scale bar, 10 µm, n ≥ 3 independent experiments.

We further questioned if *C. psittaci*, in accordance to *C. trachomatis*, recruits CERT via its Golgi-targeting PH domain or its ER-interacting FFAT peptide motif. Therefore, I generated GFP-fusion proteins of full length CERT (aa 1-158) and, based on this sequence, introduced mutations in CERT-PH (G67E) or CERT-FFAT (FF321AA) domains. HeLa cells were transfected with respective plasmid DNA, infected with *C. trachomatis*, *C. psittaci* or left uninfected and CERT localization was analyzed by laser scanning confocal microscopy.

GFP-CERT was found on both *C. trachomatis* and *C. psittaci* inclusions and fluorescent signals were distributed similar to those observed by CERT-immunostaining (Figure 3.16, Figure 3.17). Though, in uninfected cells, overexpression of GFP-CERT leads to protein accumulation in the Golgi apparatus which was barely seen upon antibody-staining. Mutations in the PH domain prevented protein recruitment to *C. trachomatis* and interestingly the same effect was seen for *C. psittaci*. In uninfected cells, PH mutants did not localize to Golgi structures any longer. On the contrary, CERT-FFAT mutants were recruited to both *Chlamydia* spp. to the same extends as the wild-type protein. In uninfected cells, CERT-FFAT mutants were strictly found in Golgi elements.

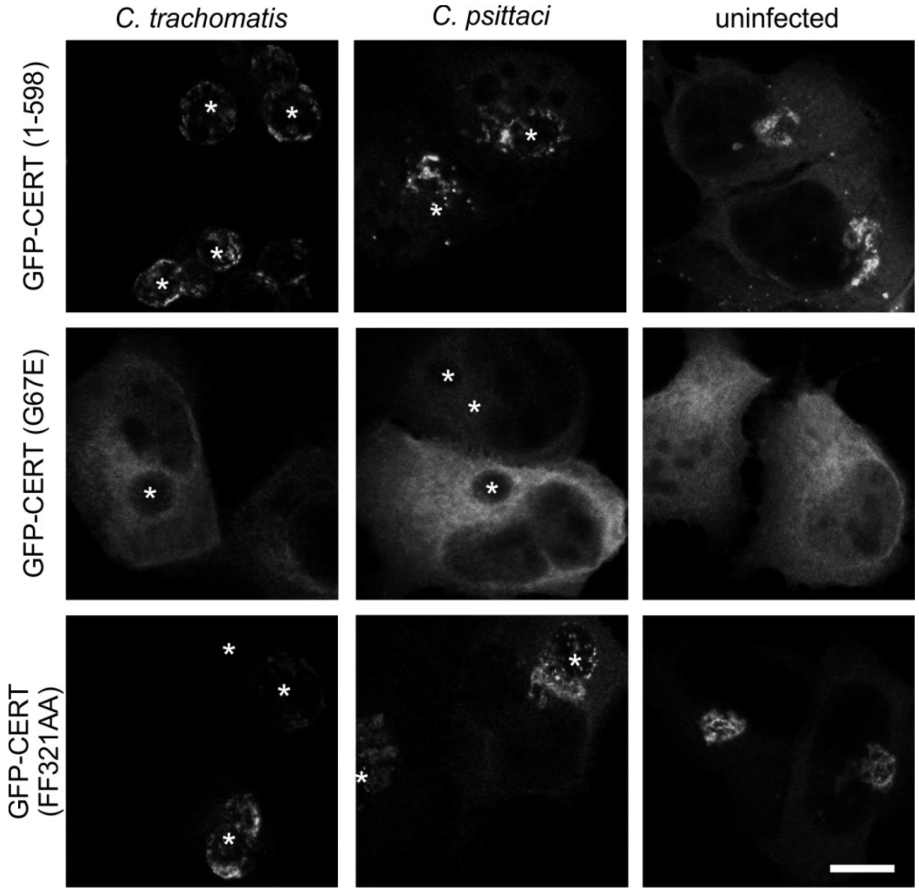

Figure 3.17 CERT-GFP localizes to *C. trachomatis* and *C. psittaci* inclusions and is recognized via its PH-domain.
Representative fluorescence images of HeLa cells transiently expressing GFP-fusion proteins of CERT, CERT PH mutant (G67E) or CERT FFAT mutant (FF321AA). Cells transiently expressing CERT-GFP mutants were infected with *C. trachomatis*, *C. psittaci* (MOI 2) or left uninfected. Cells were fixed 24 h *p.i.* and samples were analyzed by laser scanning confocal microscopy. White stars indicate chlamydial inclusions. Scale bar, 10 µm, n ≥ 2 independent experiments

CERT binding to *C. trachomatis* inclusions involves binding of the bacterial protein IncD which specifically recognizes CERT PH domain (Derre *et al.*, 2011, Agaisse & Derre, 2014). To determine if CERT binding to *C. psittaci* inclusions is mediated by a similar mode of CERT PH-Inc interaction, I checked if *C. psittaci* contains homologues to *C. trachomatis* IncD. Using blast, protein sequences with little similarities were identified. The highest score of 27.7 (units) was obtained for a hypothetical protein (WP_013462691.1: Query cover: 36%, Identity 35%) and predicted similarities were mainly found in the transmembrane region of IncD. Comparing the first 4 hits generated by blast clearly showed that sequences of *C. trachomatis* IncD and *C. psittaci* candidates varied to a very high extend. Respective alignements are found in the supplement (Figure 6.1).

Together, CERT recruitment to both *C. trachomatis* and *C. psittaci* inclusions was demonstrated whereby CERT PH domain served as essential recognition motif for both species.

3.4 Consequences of CERT-dependent ceramide transport inhibition on *Chlamydia* spp.

Recently Derré and colleagues showed that *C. trachomatis* inclusions establish close contact with the ER and form ER-inclusion MCS. The identification of CERT as one major constituent of these ER-inclusion MCSs lead to the assumption that this specialized microenvironment is built to facilitate lipid acquisition. Surprisingly, uptake of fluorescently labeled ceramide was not obviously affected by siRNA mediated knockdown of CERT that yet significantly impaired *C. trachomatis* inclusion development (Derre *et al.*, 2011). CERT was furthermore found at ER-inclusion MCS of *C. muridarum*-infected cells and was proposed to have a distinct role for bacterial replication rather than for inclusion stability (Elwell *et al.*, 2011). Although experimental procedures slightly diverged, these results together implied that CERT-mediated ceramide transport affects species-specific aspects of chlamydial development. In this thesis, CERT was shown to be recruited to both *C. trachomatis* and *C. psittaci* inclusions, indicating that the interplay between bacteria and non-vesicular ceramide transport is conserved among species. To characterize the physiological relevance of CERT-dependent ceramide transport for human and zoonotic *Chlamydia* spp. a set of inhibitor experiments were performed that addressed different aspects of chlamydial development.

3.4.1 Inhibition of CERT by HPA-12

The chemical compound HPA-12 is a ceramide analogue that inhibits CERT and thereby prevents ceramide transport from the ER to the Golgi apparatus which results in reduced levels of sphingomyelin at the plasma membrane (Kudo *et al.*, 2010, Saied *et al.*, 2014, Santos *et al.*, 2015). By exposing *C. muridarum* infected HeLa cells to 10 µM HPA-12, formation of infectious bacterial progeny decreased by 90% (Elwell *et al.*, 2011). To test how HPA-12 affects *C. trachomatis* and *C. psittaci* infections, a set of experiments were performed considering conserved and species-specific effects.

Chlamydial plaque formation in HPA-12 treated cells

For fast and robust analysis of HPA-12 treatment in *C. trachomatis* and *C. psittaci* infections a plaque assay was performed which allowed easy titration of HPA-12. Briefly, HeLa229 cells were infected with *Chlamydia* spp., incubated with a liquid overlay medium containing different concentrations of HPA-12 for five days. After immunostaining bacterial plaques were determined and quantified as previously described (Banhart *et al.*, 2014).

In untreated cell monolayers, under given conditions *C. trachomatis* formed 70 plaques on average, for *C. psittaci* a mean of 140 plaques was determined (Figure 3.18, A). Upon treatment with up to 5 µm HPA-12, these values remained nearly unaltered. Interestingly, *C. psittaci* showed species-specific sensitivity to HPA-12 at concentrations above 5 µM. To describe the species-specific effect of HPA-12 treatment in more detail, plaques formed by either *C. trachomatis* or

C. psittaci were quantified and data were expressed relative to untreated control conditions. Quantifications revealed that plaque numbers of *C. trachomatis* did not decrease after treatment with HPA-12 in the indicated dose range, but on the contrary tended to rise. Application of 10 µM HPA-12 resulted in a maximal plaque number, which was 1.5 fold higher than in untreated conditions. The use of 20 µM yet reversed this tendency. In contrast to *C. trachomatis*, 10 µM HPA-12 reduced *C. psittaci* plaque formation which was completely blocked by concentration of 20 µM HPA-12. Based on these data, the IC_{50} of HPA-12 was determined by plotting the concentrations of HPA-12 against relative plaque numbers, yielding an IC_{50} of 10.34 ± 0.19 µM for *C. psittaci* (Figure 3.18, B).

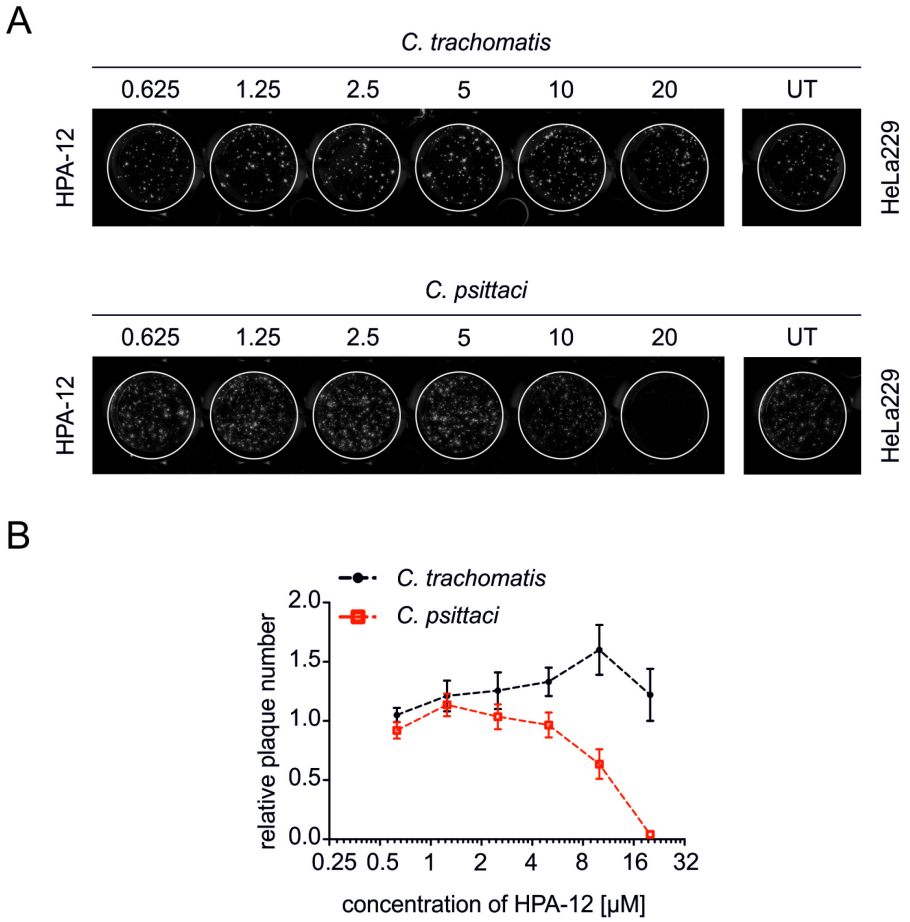

Figure 3.18 Chemical inhibition of CERT by HPA-12 reduces *C. psittaci* plaque numbers in a dose-dependent and species-specific manner.
(A) Immunofluorescence images showing plaques of *C. trachomatis* or *C. psittaci* formed in a HeLa229 cell monolayer. HeLa229 cells were infected with *C. trachomatis* or *C. psittaci* and at 8 h *p.i.* treated with indicated amounts of HPA-12 (µM). After 4 days of incubation, cells were fixed and stained for chlamydial Hsp60. UT, untreated controls. (B) Quantification of relative plaque numbers. Plaque numbers were normalized to untreated controls. Data show mean ± SEM; n = 2, *Experiments were performed by S. Banhart, RKI, Berlin*

Cytotoxic potential of HPA-12

To further investigate effects of HPA-12 treatment on host cell viability, an LDH cytotoxicity assay of uninfected and infected cells was performed using different concentrations of HPA-12. In brief, HeLa229 cells were infected with indicated infectious doses of *C. trachomatis* or *C. psittaci*

and at 8 h *p.i.* were treated with HPA-12. 48 h *p.i.* activity of LDH released from damaged cells was determined according to the manufacturer's protocol. Cytotoxicity was expressed relative to control conditions composed of chemically lysed cells.

In uninfected cells no severe signs of cytotoxicity were observed within the analyzed range of time. Even upon treatment, cytotoxicity was not elevated using up to 40 µM HPA-12.

In cells infected with *C. trachomatis*, cytotoxicity was induced in an MOI-dependent manner. While untreated cells stayed intact when infected with *C. trachomatis* MOI 0.5, infections with a higher bacterial load (MOI 2) resulted in an increased *C. trachomatis*-dependent cytolysis. Inhibitor treatment with concentration of up to 20 µM HPA-12 did not affect the cytotoxic potential of *C. trachomatis* infections, independent of the infectious dose, which correlates with previous plaque assay results. However, by introducing 40 µM HPA-12 *C. trachomatis*-dependent cytotoxicity was dramatically reduced, in case of infections with MOI 2 by 48% (Figure 3.19).

Upon infections with *C. psittaci* untreated HeLa229 cells showed an increase in cytotoxicity depending on the initial infectious dose. Here, treatment with HPA-12 interfered with the cytotoxic potential of *C. psittaci* infections. By applying concentrations of up to 5 µM HPA-12 *C. psittaci*-dependent cytolysis tended to increase whereas higher concentrations of HPA-12 counteracted this tendency and slightly reduced effects due to infections. In contrast to *C. trachomatis* infections, the reduction of bacteria-mediated cytotoxicity observed upon treatment with 40 µM HPA-12 was less prominent in *C. psittaci* infections (Figure 3.19, B).

In sum, HPA-12 does not affect host cell viability at concentrations that specifically interfere with chlamydial plaque formation but interferes with species-specific mechanisms of *Chlamydia*-dependent cytolysis. While *C. trachomatis*-dependent cytotoxicity is effectively reduced by 40 µM HPA-12, *C. psittaci*-induced cytolysis is marginally affected by HPA-12 treatment and is less efficiently reduced by using 40 µM of compound.

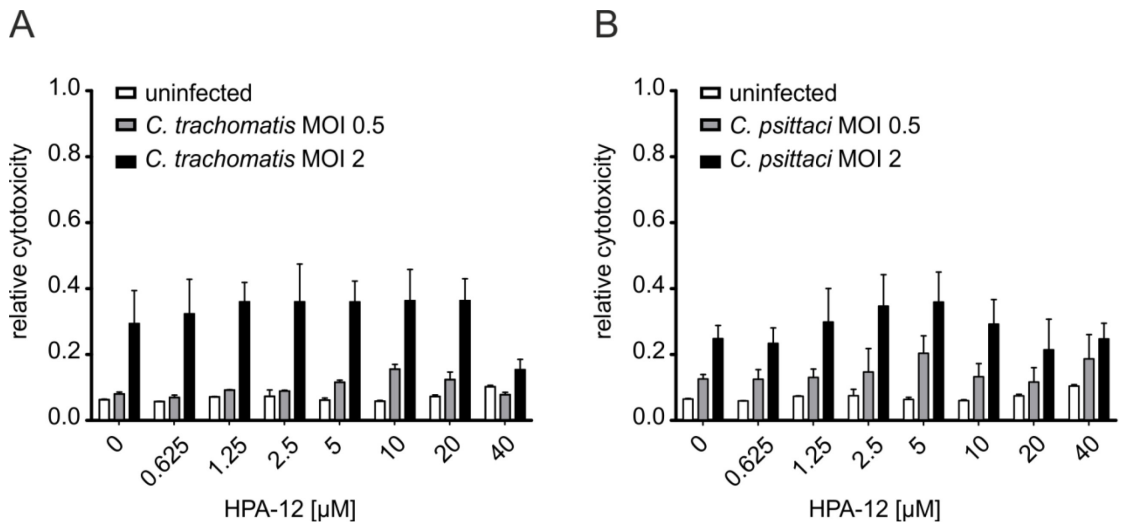

Figure 3.19 Cell viability is not impaired by HPA-12.
Diagram depicts relative cytotoxicity of HPA-12 as measured by LDH release on uninfected cells or cells infected with *C. trachomatis* or *C. psittaci* HeLa229 cells, uninfected, infected with *C. trachomatis* (A) or *C. psittaci* (B) were incubated with different concentrations of HPA-12 (µM) or left untreated (8 h *p.i.*). 48 h *p.i.* cell supernatants were used to measure LDH release. Values are corrected for background and normalized to positive control (chemically lysed cells). Data show mean ± SEM; n = 2

Effects of HPA-12 treatment during chlamydial development

To determine effects of HPA-12 on one chlamydial developmental cycle, I infected HeLa229 cells with each chlamydial species, treated cells with indicated amounts of HPA-12 at 8 h *p.i.* and analyzed samples at 48 h *p.i.* Chlamydial replication, expressed as relative genome copy number (GCN) was assessed by qPCR, generation of infectious *C. trachomatis* and *C. psittaci* progeny was determined by titration of infectious bacteria on new cells.

Comparing GCNs upon treatment with different concentrations of HPA-12 revealed that treatment with 10 µM HPA-12 did not affect *C. trachomatis* replication, independent of the initial bacterial load. However, when cells were treated with 20 µM HPA-12, bacterial replication in cells infected with MOI 0.5 was specifically reduced by 60% whereas chlamydial replication in cells initially infected with MOI 2 was unaltered. Considering infectious progeny formation, 10 µM HPA-12 reduced *C. trachomatis* progeny by 50% or 30% for infections with MOI 0.5 or MOI 2 respectively. This reduction of infectious progeny even dropped to 13% (MOI 0.5) or 20% (MOI 2) upon treatment with 20 µM HPA-12 (Figure 3.20, A).

Replication of *C. psittaci*, that was previously shown to be sensitive to HPA-12, was slightly promoted by treatment with 10 µM compound resulting in 1.5 fold more bacteria compared to untreated controls. This tendency was independent of the bacterial load. Opposed to this effect, treatment with 20 µM HPA-12 dramatically reduced replication rates by 30% for MOI 0.5 up to 70% for MOI 2. In addition to the reduced replication rates, a dose-dependent inhibition of *C. psittaci* progeny formation by HPA-12 was shown. Yet, 10 µM HPA-12 reduced infectious progeny by 40% (MOI 0.5) or 60% (MOI 2), doubling the inhibitory concentration reduced *C. psittaci* progeny by 97% (MOI 0.5) or 90% (MOI 2) (Figure 3.20, B).

In sum, HPA-12 treatment interferes with chlamydial development by affecting bacterial replication and infectious progeny formation in a species-specific manner. While HPA-12 induces marginal dose- and MOI-dependent variations of *C. trachomatis* replication, infectious progeny formation is in contrast highly sensitive to HPA-12 treatment in all conditions tested. The lower the infectious dose was, the higher the effects achieved by HPA-12 were. For *C. psittaci* infections, responses were dose-dependent to HPA-12 treatment. Here, bacterial replication tended to benefit from moderate HPA-12 treatment but already 20 µM HPA-12 alleviate these effects. In accordance to previous results, HPA-12 treatment reduces infectious progeny formation of *C. psittaci* in a dose-dependent manner.

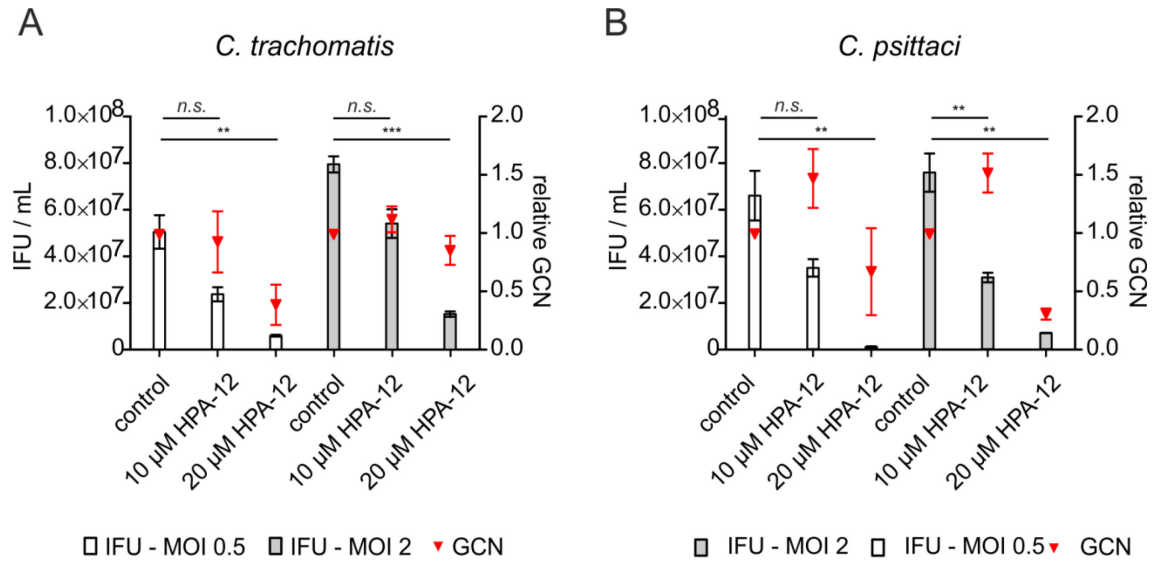

Figure 3.20 Treatment with HPA-12 impairs bacterial replication and reduces infectious progeny formation determined by a one-step reinfection assay.
Graphs showing relative genome copy numbers and quantification of infectious chlamydial progeny upon treatment with HPA-12. HeLa229 cells, infected with *C. trachomatis* (A) or *C. psittaci* (B) were treated with 10 µM or 20 µM HPA-12 or left untreated at 8 h *p.i.* After 48 h cells were harvested, lysed and further analyzed. Genome copy numbers were determined by qPCR and values were calculated relative to untreated control. Data represent mean ± SEM; n = 3. Infectious progeny formation was determined by a one-step reinfection assay. Cell lysates were titrated on fresh HeLa cells and infectious progeny, visualized by staining of chlamydial Hsp60, was counted 24 h *p.i.* Data show mean ± SEM; n = 3.

Morphologies of chlamydial developmental forms upon HPA-12 treatment

Chlamydial replication and differentiation are two possible processes that might be independently affected by the CERT inhibitor HPA-12. Discrepancies between bacterial replication, infectious progeny formation and infectivity might be explained by inefficient or delayed re-differentiation from RBs to EBs or by defective EBs with impaired virulence. To draw a distinction between (re)differentiation and infectivity I analyzed the distribution of bacterial developmental forms after 48 h *p.i.* with and without HPA-12 treatment using TEM. In line with previous experiments, HeLa229 cells were infected with *Chlamydia* spp., treated with 10 µM HPA-12 at 8 h *p.i.* and samples were fixed and processed for TEM at 48 h *p.i.*, the end of the bacterial developmental cycle.

Four morphological forms were described on an ultrastructural level: small, electron dense EBs, large marbled RBs, intermediate bodies (IBs) with a marbled structure and an electron dense core, as well as empty membrane ghosts. Quantification revealed no significant alterations of *C. trachomatis* morphology distribution upon HPA-12 treatment, although a tendency away from infectious EBs to residual non-infectious forms was observable. Even though *C. psittaci* infectivity was highly reduced by HPA-12 treatment, no shifts in bacterial morphologies from EBs to other forms were detected (Figure 3.21).

The ultrastructural results show that the (re)differentiation of neither *C. trachomatis* nor *C. psittaci* are significantly affected by HPA-12 treatment. Since compound treatment reduced infectivity of chlamydial pathogens, EBs observed by TEM and/or factors of bacterial virulence which determine infectivity might presumably be compromised by the inhibitor.

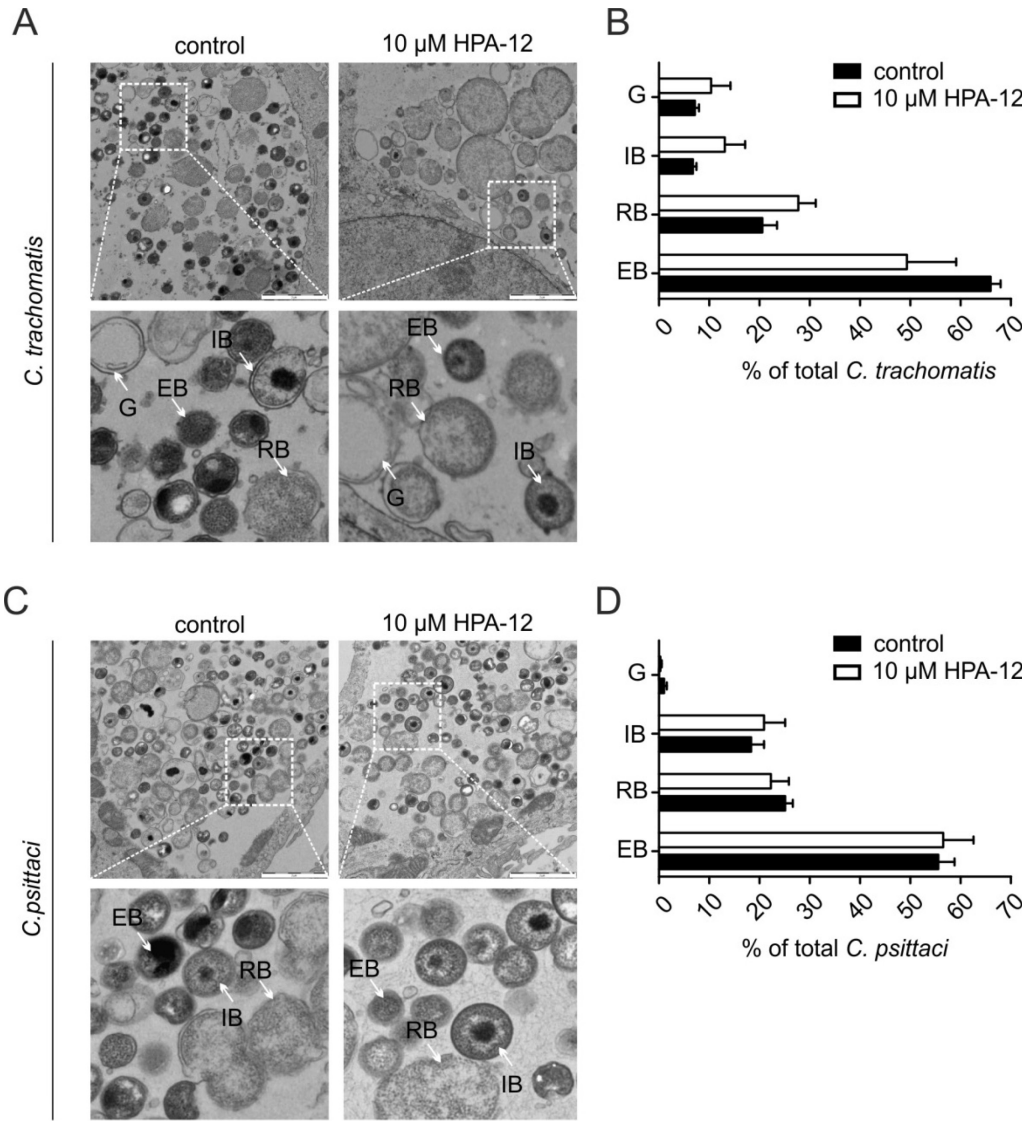

Figure 3.21 Distribution of bacterial morphologies is not significantly affected by HPA-12 treatment in both strains.
Electron micrographs showing different morphologies of *C. trachomatis* (A) or *C. psittaci* (C). HeLa229 cells were infected with *C. trachomatis* or *C. psittaci* (MOI 0.5) and incubated with or without 10 µM HPA-12 at 8 h *p.i.* Cells were fixed 48 h *p.i.* and processed for TEM. Scale bar, 2 µm. Quantification of distinct bacterial morphologies in cells treated with or without HPA-12 (B) + (D). Values were normalized to total bacteria and data show mean ± SEM, n = 3. EB = elementary body, RB = reticulate body, IB = intermediate body, G = ghost. *Electron microscopy was performed in the group of M. Laue, RKI, Berlin.*

Protein expression during HPA-12 treatment

Having shown that chemical inhibition of CERT targets distinct steps in *C. trachomatis* and *C. psittaci* development, we further asked if protein expression is altered due to HPA-12 treatment. For this, HeLa229 cells were infected with *C. trachomatis* or *C. psittaci* (MOI 0.5), treated with 10 µM HPA-12 at 8 h *p.i.* and samples were collected at indicated times. Using Western blot analysis, protein levels of cHsp60 were depicted, a conserved housekeeping protein, that is downregulated when bacteria enter a state of persistence (Gerard *et al.*, 2004). Additionally expression of selected inclusion proteins (IncA, IncB) was analyzed.

In correlation to the steady replication levels of *C. trachomatis* (Figure 3.22, A), both cHsp60 and IncA were equally expressed in untreated and HPA-12 treated cells. Throughout the mid- and late developmental cycle, protein expression remained stable (Figure 3.22, A).

In *C. psittaci* infections, a strong reduction in bacterial protein expression was induced by 10 µM HPA-12. At 24 h and 36 h *p.i.*, when bacteria usually are metabolically active and replicate, protein levels of cHsp60 and IncB were reduced by 30% and 70%, respectively. Finally at 48 h *p.i.* protein levels of untreated cells were almost equal to protein levels expressed in HPA-12 treated cells (Figure 3.22, B).

In summary, HPA-12 has no influence on *C. trachomatis* protein expression, but negatively interferes with *C. psittaci* protein expression at mid-infection time points.

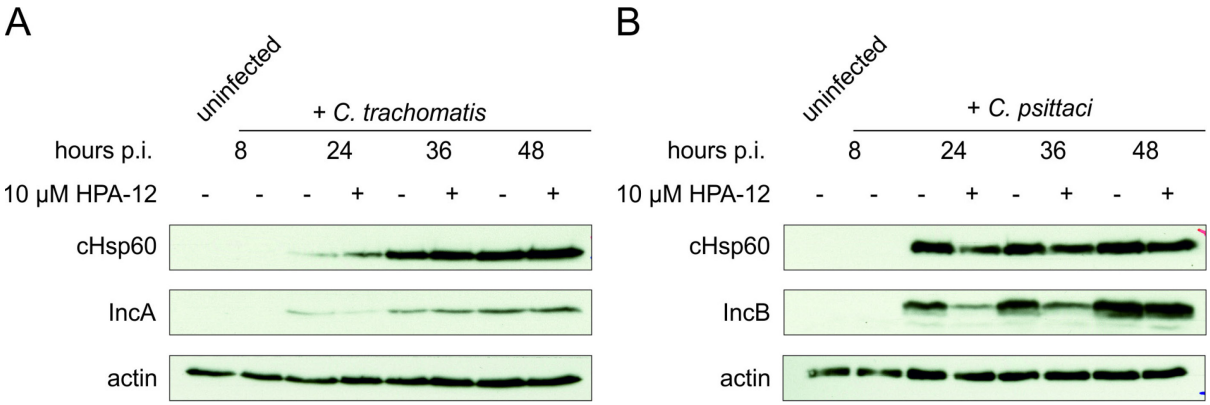

Figure 3.22 Moderate HPA-12 treatment changes protein expression of *C. psittaci* but has no effect on *C. trachomatis*.
Western Blot analysis of chlamydial proteins expressed upon treatment with HPA-12. HeLa229 cells were infected with *C. trachomatis* (A) or *C. psittaci* (B) (MOI 0.5) or left uninfected. Treatment with or without 10 µM HPA-12 started 8 h *p.i.* At indicated times, cells were harvested by direct lysis in hot SDS-sample buffer. Protein expression of selected proteins was analyzed by Western Blot analysis using antibodies directed against cHsp60, IncA (*C. trachomatis*), IncB (*C. psittaci*) or actin.

3.5 Quantitative analysis of chlamydial sphingolipid-composition

In this study the question of sphingolipid uptake to *Chlamydia* spp. was addressed by a quantitative mass spectrometry approach. For this purpose, I established and adapted a protocol for selective enrichment and purification of EBs from human *C. trachomatis* and zoonotic *C. psittaci* (Newhall *et al.*, 1986). In collaboration with lipid-chemists of the University of Potsdam, we were able to quantitatively determine a selection of sphingolipids as components of chlamydial EBs.

3.5.1 Selective enrichment and purification of chlamydial EBs

As we intended to gain a better understanding on the relationship of sphingolipid composition and infectivity, we introduced a protocol initially described by Newhall and colleagues for selective enrichment of chlamydial EBs (Newhall *et al.*, 1986). HeLa229 cells were infected with *C. trachomatis* or *C. psittaci* for 48 h. Afterwards cells were harvested, lysed and chlamydial EBs were partially purified by differential centrifugation followed by Percoll density gradient

centrifugation. Relevant samples were collected to validate EB enrichment by different methods. Bacterial content was determined by qPCR (genome copy number) and determination of infectious progeny. Beyond, the ratio between EBs and residual RBs was qualitatively determined by electron microscopy.

In Figure 3.23 the experimental workflow used in our study is depicted. To validate EB and RB content in Percoll fractions after centrifugation, we analyzed 100 µl aliquots by TEM. *C. trachomatis* EBs were selectively enriched in the bottom fraction and were, beside few RBs, the dominant developmental form in the second fraction. *C. psittaci* EBs also accumulated at the bottom of the Percoll gradient and formed dense clusters. In the second fraction a significant amount of RBs was found beside EBs (Figure 3.23, B). In higher fractions the amount of RBs highly increased whereas less EBs were found.

To allow a comparative sphingolipid analysis for *C. trachomatis* and *C. psittaci*, we decided to combine Percoll fractions 1 and 2 which are highly enriched in EBs.

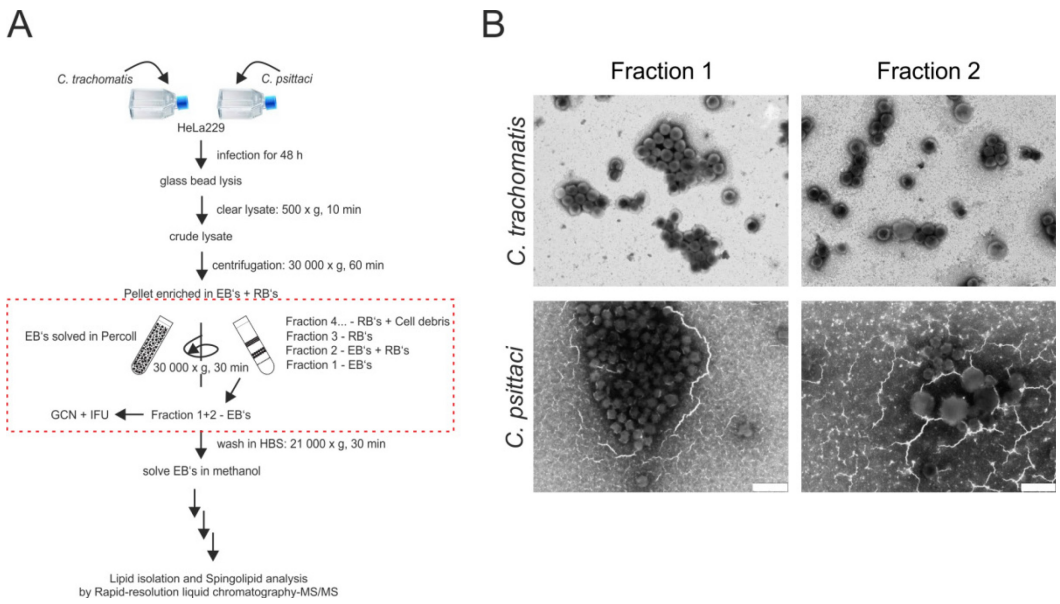

Figure 3.23 EBs of *C. trachomatis* and *C. psittaci* are highly enriched after Percoll density gradient centrifugation.
(A) Schematic representation of work-flow used to selectively enrich chlamydial EBs. (B) Electron micrographs showing fractions formed after Percoll density gradient centrifugation. HeLa229 cells infected with *C. trachomatis* or *C. psittaci* (MOI 2, 48 h) were scraped, mechanically lysed and EBs were enriched by a step-wise centrifugation procedure. Several fractions of a Percoll gradient were processed for and examined by electron microscopy. Scale bar, 1 µm.

3.5.2 Quantitative analysis of chlamydial sphingolipid composition

To define the sphingolipid composition of EBs from two different chlamydial species, lipids from selectively enriched EBs were extracted, extracts were mixed with relevant lipid standards and partial lipidomes were analyzed by rapid resolution liquid chromatography mass spectrometry. For both *C. trachomatis* and *C. psittaci*, total amounts of ceramides and sphingomyelins were determined and expressed relative to infectious progeny contained in the appropriate sample.

Mass spectrometric data revealed that in both chlamydial species a set of ceramides and sphingomyelins was incorporated. Surprisingly, infectious *C. psittaci* accumulated eight times more sphingolipids than *C. trachomatis* EBs, in particular ten times more ceramides and seven times more sphingomyelins (Figure 3.24, A). By comparing the ratios of sphingomyelin to ceramide, *C. psittaci* EBs had a lower affinity for ready-made sphingomyelin than *C. trachomatis* EBs (*C. psittaci* $_{SM:cer}$ 6:1 vs. *C. trachomatis* $_{SM:cer}$ 10:1).

We expanded our analysis of sphingomyelins and compared the composition of amide linked acyl chains varying from 16 to 24 carbons in length (Niemela *et al.*, 2006). Both chlamydial species showed preferences for C16-sphingomyelin and C24:1-sphingomyelin followed by C18-sphingomyelin and C22-sphingomyelin. However, distribution of acyl chains differed in a species-specific manner. The bias to C16-sphingomyelin was stronger in *C. trachomatis* EBs than in *C. psittaci* while in *C. psittaci* the proportion of C24:1-sphingomyelin was twice as high as in *C. trachomatis* (Figure 3.24, B).

In sum the measurements showed that ceramides as well as sphingomyelins are detectable components of chlamydial EBs. Quantification revealed that infectious *C. psittaci* bacteria accumulate 8 times more sphingolipids than *C. trachomatis*. For both bacterial species, sphingolipid content and distributions of sphingomyelins with different carbon chain lengths were defined by species-specific profiles.

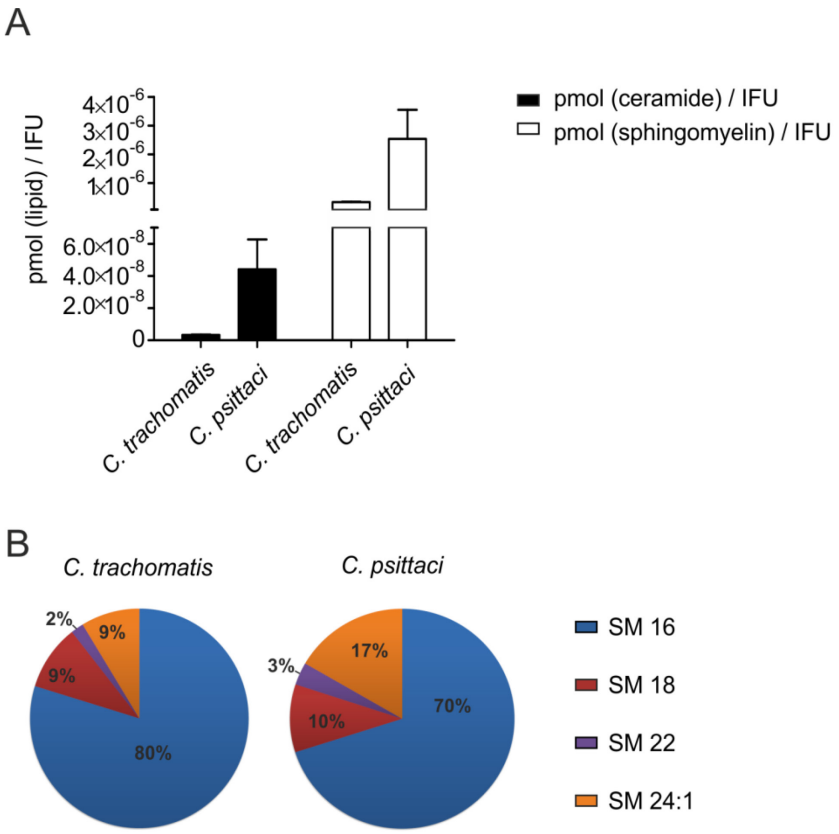

	[% ± SEM]			
	SM16	***SM18***	***SM22***	***SM24:1***
C. trachomatis L2	79.79 ± 0.68	9.66 ± 0.14	1.88 ± 0.26	8.67 ± 0.55
C. psittaci DC15	70.65 ± 1.18	10.59 ± 0.85	3.10 ± 0.47	15.67 ± 2.08

Figure 3.24 Infectious bacteria of *C. psittaci* accumulate 8 times more sphingolipids than infectious *C. trachomatis*.
(A) Representation of total amounts of ceramide and sphingomyelin normalized to amounts of infectious bacteria. HeLa229 cells infected with *C. trachomatis* or *C. psittaci* were incubated for 48 h and subsequently scraped and mechanically lysed. EBs were enriched by a step-wise centrifugation procedure. Lipids from pure EB fractions were extracted and analyzed by rapid resolution liquid chromatography MS/MS. Data were normalized to infectious units (IFU) and expressed as mean ± SEM; n = 3. (B) Pie charts showing proportional distribution of sphingomyelins (SM) with different carbon chain lengths. Corresponding values and errors are depicted in the table below (mean ± SEM; n = 3).

4 Discussion

Chlamydia spp. have an exceptional intracellular lifestyle that demands for complex interactions with the host cell (Bastidas *et al.*, 2013). To ensure intracellular replication and avoid eradication, *Chlamydia* spp. have evolved a rich repertoire of conserved and species-specific strategies that include mechanisms to efficiently acquire host nutrients and others to modify host signaling pathways and sustain host viability (Hackstadt *et al.*, 1996, Carabeo *et al.*, 2003, Beatty, 2006, Ying *et al.*, 2007). Some of these mechanisms might be conserved among species but, since many *Chlamydia* spp. have a narrow and defined host and tissue tropism, each species has adapted to host-specific demands (Dehoux *et al.*, 2011, Lutter *et al.*, 2012). The precise molecular mechanisms underlying chlamydial tissue tropisms and consequently might define species-specific disease outcomes are, although of great medical importance, just poorly understood.

A hallmark of *C. trachomatis* infections is the breakdown of the Golgi ribbon into inclusion-adjacent ministacks (Heuer *et al.*, 2009). While this process is essential for efficient sphingolipid uptake to inclusions little is known about ministack characteristics and the roles of host proteins involved in this process. The first part of the study showed that *C. trachomatis*-induced ministacks retain a *cis*- to *trans*-Golgi organization. While cisternal organization was not affected, dynamics of intra-cisternal enzymes were severely impaired in unlinked ministacks compared to intact ribbons. As a result, protein and lipid maturation or vesicle formation might be impeded.

The Golgi matrix protein golgin-84 was proposed as a key player of *C. trachomatis*-induced Golgi fragmentation. Here, microscopic analyses revealed that transiently expressed golgin-84 localizes to *C. trachomatis* inclusions. Proper recruitment of golgin-84, partially mediated by amino acids 1-148, enhanced *C. trachomatis* growth. Furthermore, in a subset of infected cells, N- and C-terminal parts of golgin-84 were separated, indicating a *C. trachomatis*-dependent processing of this protein.

The induction of Golgi fragmentation and interaction with Golgi related trafficking pathways are known mechanisms used by various human *Chlamydia* spp. In contrast, insights into host pathogen interactions of the avian and zoonotic pathogen *C. psittaci* are rare. The second part of this thesis addressed a number of conserved and species-specific mechanisms that include interactions with host trafficking pathways. *C. psittaci* induced the reorganization of Golgi structure but ministack phenotypes were distinct from *C. trachomatis*. *C. psittaci,* other than *C. trachomatis*, did not interact with any Golgi tethering factors and only attracted a reduced subset of Rab proteins. Interestingly, the interaction with CERT, mediator of non-vesicular ceramide transport was conserved among the different species.

The next part of the study therefore approached mechanisms behind this non-vesicular ceramide transport route and its implications for chlamydial infections. The chemical compound HPA-12 inhibits CERT and treatment of *Chlamydia*-infected cells specifically affected the progression of *C. psittaci* infections and, at higher concentrations, also impaired *C. trachomatis*. Interestingly,

HPA-12 affected different, species-specific aspects of chlamydial development. In *C. psittaci* infections, plaque formation, infectivity, replication and bacterial protein expression were affected and reduced by HPA-12 treatment, whereas differentiation and properties leading to cell lysis were almost unchanged. In *C. trachomatis* infected cells, HPA-12 treatment significantly reduced chlamydial infectivity. Other processes, however, were hardly altered and seemed to overcome applied inhibitor concentrations.

As *Chlamydia* spp. hijack different routes of vesicular and non-vesicular sphingolipid transport, the role of sphingolipid uptake for chlamydial development and infectivity, was further addressed by quantitative sphingolipid analyses. Data obtained by LC-MS revealed initial insights into the species-specific sphingolipid composition of chlamydial EBs. Although *C. psittaci* hijacked less or other host trafficking pathways than *C. trachomatis*, *C. psittaci* EBs accumulated eight times more sphingolipids than *C. trachomatis* EBs. Infective forms of the avian and zoonotic agent not only accumulated a higher amount of sphingolipids, but also species-specific differences in sphingolipid composition were observed. Prospective studies are now needed to elucidate the impact of CERT-dependent and -independent sphingolipid acquisition for this species-specific sphingolipid composition. Based on our results, the therapeutic potential of specific sphingolipids and their corresponding roles for chlamydial development, infectivity and host and tissue tropism should be investigated in future.

4.1 The role of golgin-84 in *C. trachomatis*-induced Golgi fragmentation

4.1.1 Functional characteristics of *C. trachomatis*-induced Golgi ministacks

The mammalian Golgi apparatus is organized in a complex ribbon structure and encloses specialized local compartments for protein and lipid maturation, sorting and secretion. During mitosis or apoptosis, times of high protein and lipid turnover, Golgi ribbons dissolve into Golgi ministacks (Hu *et al.*, 2005, Mukherjee *et al.*, 2007). The functionality of resulting ministacks is not completely understood but current data indicate that it strongly depends on underlying modes of ministack formation (Cole *et al.*, 1996, Cole *et al.*, 1996, Diao *et al.*, 2003, Puthenveedu *et al.*, 2006). In *C. trachomatis*-infected cells Golgi fragmentation results in Golgi ministacks that align around chlamydial inclusions and thereby support efficient sphingolipid transport to the bacteria (Heuer *et al.*, 2009, Rejman Lipinski *et al.*, 2009). On the other hand, *C. trachomatis*-induced disruption of ribbon continuity results in impaired glycoprotein processing (Heuer *et al.*, 2009). Here, in order to further characterize *C. trachomatis*-induced Golgi ministacks, localizations and dynamics of distinct Golgi glycosyltransferases were analyzed.

In intact Golgi ribbons of uninfected cells, glycosyltransferases located to distinct *cis*- and *trans*-Golgi cisternae. Even in infected cells ministacks retained their *cis*- to *trans*-organization, facing the inclusion with *cis*-sites (Figure 3.1). Although orientation of Golgi ministacks was not affected, enzyme dynamics were severely reduced, a consequence also observed upon

fragmentation induced by golgin-84 depletion or GM130 knockdown (Figure 3.1) (Puthenveedu *et al.*, 2006). Since the Golgi apparatus copes with a constant turnover of molecules, high dynamics are essential to equally distribute enzymes and organize distinct local functions. The impaired enzyme motility in inclusion-adjacent ministacks might henceforth affect efficient protein or lipid maturation (Puthenveedu *et al.*, 2006). Indeed, normal glycoprotein processing is impaired in *C. trachomatis*-infected cells (Heuer *et al.*, 2009).

This thesis for the first time provides experimental evidence for impaired Golgi enzyme dynamics in *C. trachomatis*-induced Golgi ministacks that potentially limit efficient protein and lipid maturation and correlate with defects in glycoprotein presentation. However, if and to what extend lipid processing and maturation are affected cannot be derived from these results and would need further investigations.

4.1.2 Golgin-84 in *C. trachomatis*-induced Golgi fragmentation

Golgi structure and vesicular transport are regulated by golgin coiled-coil tethering factors together with Rab proteins and other small GTPases (Barr & Short, 2003, Sinka *et al.*, 2008). The golgin tethering factor golgin-84 is of particular interest in the context of *C. trachomatis* infections. On the one hand, infection-induced Golgi fragmentation goes along with a putative proteolytic processing of golgin-84 (Heuer *et al.*, 2009). On the other hand, golgin-84-dependent Golgi fragmentation can be blocked by knockdown of Rab6A and Rab11A, indicating a functional interdependence of these proteins. As golgin-84 processing was not affected in knockdown cells, Golgi fragmentation and processing of golgin-84 might result from independent mechanisms (Rejman Lipinski *et al.*, 2009). Initial studies proposed that golgin-84 is processed by the chlamydial virulence factor CPAF (Christian *et al.*, 2011). Recent studies however challenged the biological background of golgin-84 processing in *C. trachomatis*-infected cells and demanded for additional methods to reconsider former conclusions (Chen *et al.*, 2012, Snavely *et al.*, 2014, Johnson *et al.*, 2015). In this study, the role and function of golgin-84 in *C. trachomatis* infected cells was addressed by different methods based on fluorescent microscopy in fixed and living cells.

Golgin-84 localizes to C. trachomatis-inclusions

Golgin-84 is a coiled-coil membrane protein that localizes to the *cis*-Golgi in uninfected cells (Diao *et al.*, 2003). The central coiled-coil domain mediates tethering events important for vesicle recognition and membrane fusion during cisternal maturation, processes that support Golgi structure (Malsam *et al.*, 2005, Santos *et al.*, 2015). In order to define the role of golgin-84 in *C. trachomatis*-infected cells, localization of full-length golgin-84 and functional mutants were microscopically analyzed. In *C. trachomatis* infected cells, golgin-84 was recruited to inclusions starting at 20 h *p.i.* and inclusions were positive for golgin-84 until at least 32 h *p.i.* (Figure 3.3, Figure 3.6). The nature of protein binding to the inclusions is not defined yet. In uninfected cells, golgin-84 localization is predominantly meditated by two intrinsic protein motifs, a C-terminal

transmembrane domain and a cytoplasmic coiled-coil domain (Bascom *et al.*, 1999). To clarify the necessity of the transmembrane domain for protein recruitment to *C. trachomatis* inclusions, a deletion mutant was generated and expressed in uninfected or infected cells. In uninfected cells, mutants lacking the transmembrane domain not only localized to the Golgi apparatus but were partially distributed throughout the cytosol, presumably as a soluble fraction. In infected cells, these mutants of golgin-84 were still or even more efficiently recruited to *C. trachomatis* inclusions, indicating that the cytoplasmic domain including the coiled-coil domain is the dominant factor for protein recruitment (Figure 3.3). As coiled-coil domains are predicted to form oligomers, I speculated that binding of golgin-84 could result from heterooligomers formed with inclusion adjacent proteins. Depending on the developmental cycle *C. trachomatis* expresses and secretes distinct subsets of proteins that define inclusion maturation and provide dynamic and time-dependent properties (Shaw *et al.*, 2002, Belland *et al.*, 2003, Nicholson *et al.*, 2003). Particularly Inc proteins bind to host cell factors and recruit proteins from different host organelles (Rzomp *et al.*, 2006, Agaisse & Derre, 2014, Mirrashidi *et al.*, 2015). One group of Inc proteins is characterized by SNARE-like coiled-coil domains, that most likely regulate protein-protein interactions (Delevoye *et al.*, 2008). It is therefore very likely that inclusion association of golgin-84 involves one or several chlamydial Inc proteins. Inclusion association might be additionally mediated by indirect binding of golgin-84 to active Rab1 or parts of the conserved oligomeric Golgi (COG) complex, factors that are also recruited to *C. trachomatis* compartments (Diao *et al.*, 2003, Rzomp *et al.*, 2003, Satoh *et al.*, 2003, Sohda *et al.*, 2010, Pokrovskaya *et al.*, 2012, Aeberhard *et al.*, 2015).

To investigate whether the N-terminal domain of golgin-84, which was previously proposed to be proteolytically cleaved during infections, is further involved in protein localization, N-terminal mutants were generated and analyzed as described. While Golgi localization was unaltered, N-terminally truncated golgin-84 was not recruited to inclusions although the mutant contained an intact coiled-coil domain (Figure 3.3). These results clearly show that protein recruitment of membrane bound golgin-84 to chlamydial inclusions depends on this N-terminal domain.

Double mutants of golgin-84 lacking both the transmembrane and the N-terminal domain were highly soluble and lost their affinity for Golgi localization in uninfected cells. In infected cells, these mutants were nevertheless recruited to inclusions, indicating that the interaction between coiled-coil domain and inclusion adjacent factors is sufficient to mediate localization of soluble golgin-84 mutants.

The finding that golgin-84 is recruited to *C. trachomatis* inclusions implies that the protein is of functional relevance for chlamydial development. Golgin-84, along with its role as Golgi membrane scaffold, is involved in retrograde Golgi trafficking and specifically tethers a subpopulation of COP I vesicles containing distinct enzymatic cargo (Malsam *et al.*, 2005). Its role in retrograde trafficking is further emphasized by the aforementioned interactions with active Rab1

and members of the COG complex. For *C. trachomatis* development, interactions with retrograde transport routes are of major importance and provide access to different pools of nutrients (Hackstadt *et al.*, 1995, Hackstadt *et al.*, 1996, Moore *et al.*, 2008, Aeberhard *et al.*, 2015). Since efficient recruitment of golgin-84 promoted infectious progeny formation whereas suppressed recruitment due to N-terminal truncation of the protein resulted in a reduction of progeny formation (Figure 3.5), I assume that golgin-84 positive compartments are acquired to provide specific molecular cargo and nutrients (Figure 4.1). At the mid-cycle of the infection, when replication rates are high and specific nutrients are required, the N-terminus of golgin-84 is recognized and the protein and adjacent compartments are approached (1). In proximity to the inclusion, golgin-84 can then bind to the coiled-coil domain of specific Inc proteins or inclusion associated Rab proteins. This coordinated binding of the N-terminal and coiled-coil domain to the inclusion might lead to vesicle uptake or nutrient release into the inclusion lumen, thereby supporting chlamydial development (2). To better understand the reason for this proposed acquisition of golgin-84-positive compartments, more knowledge about lipid and protein content of distinct COP I subpopulations would be needed. In the end, cleavage of golgin-84, as proposed previously, could possibly release no longer needed protein domains (3).

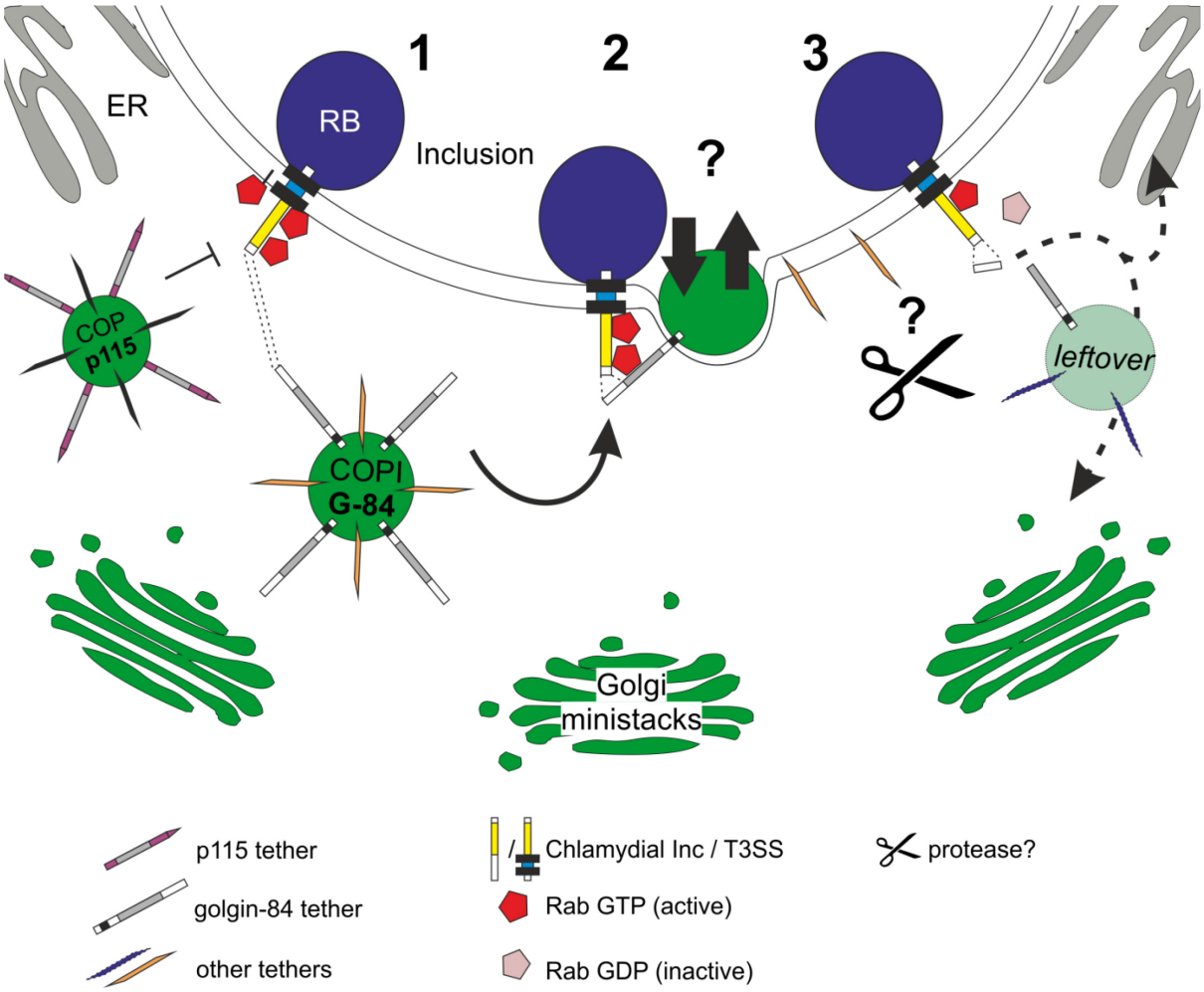

Figure 4.1 Model for the recruitment and processing of golgin-84 by *C. trachomatis*.
Schematic representation of selective recruitment of golgin-84-positive compartments and protein processing. Golgin-84 positive vesicles that traffic between Golgi apparatus and ER are specifically recognized and attracted by *C. trachomatis* RBs, potentially by interacting with a type three secreted Inc protein (1). Close proximity of vesicles with the inclusion allows the binding of active inclusion-associated Rab proteins to golgin-84 coiled-coil region. At this step, vesicle fusion or exchange of biomolecules between closely associated membrane compartments are conceivable (2). To release golgin-84 and associated membrane compartments, golgin-84 is proteolytically processed, keeping the N-terminus at the inclusion. To finally release the protein, Rab-coiled coil interactions must be resolved. Therefore Rab proteins must be inactivated by a chlamydial or host factor or by its intrinsic GTPase activity (3).

Due to the protein structure of golgin-84, particularly considering the coiled-coil domain, inclusion association might not only mediate vesicle acquisition but coud be furthermore useful to establish connections in between inclusions and might thereby contribute to homotypic fusion of multiple inclusions (Hackstadt *et al.*, 1999, Richards *et al.*, 2013).

Golgin-84 can be processed in a C. trachomatis-dependent manner

The hypothesis that golgin-84 processing occurs in vivo has recently been challenged (Chen *et al.*, 2012). To further uncover *C. trachomatis*-dependent processing of golgin-84 in living cells, live cell microscopy using a dually labeled golgin-84 probe was performed. These live-cell experiments revealed that N- and C-terminal signals were separated in a subset of infected cells meaning that cleavage of golgin-84 per se was possible (Figure 3.7). The proportion and efficiency of protein cleavage most likely depends on the ratio of endogenous processing protease and

transiently expressed fluorescent probe. In this case, as expression levels of enzyme and substrate may vary, the observation of golgin-84 processing might be underestimated.

With regard to the suggested model of golgin-84 recruitment to inclusions, the release of its C-terminus would require golgin-84 processing and subsequent inactivation of the putative Rab binding partner (Figure 4.1). This implies that proteases and Rab effector proteins of host or chlamydial origin would be involved in this process.

The chlamydial protease CPAF was suggested as the major chlamydial protease involved in this process but its endogenous proteolytic activity has recently come into question and needs to be reinvestigated (Christian *et al.*, 2011, Chen *et al.*, 2012, Snavely *et al.*, 2014, Johnson *et al.*, 2015). On the host side, calpain 2 and inflammatory caspases were proposed to catalyze golgin-84 processing upon *C. trachomatis* infection (Heuer *et al.*, 2009). Current bioinformatic data reinforce that golgin-84 contains a caspase-1 cleavage site at D272 (ExPASy – Peptide cutter – November 05 2015, http://web.expasy.org/peptide_cutter/). As caspase 1 is activated during *C. trachomatis* infections, it might be the crucial candidate that could regulate golgin-84 processing (Lu *et al.*, 2000, Cheng *et al.*, 2008, Abdul-Sater *et al.*, 2009).

Today, experimental evidence for the existence of inclusion-adjacent bacterial or host Rab effector proteins is missing. Similar to other intracellular pathogens like *L. pneumophila* or *S. flexneri*, that secrete their own GTPase activating proteins (GAP) or GTPase dissociation factors (GDF), *Chlamydia* spp. might modulate Rab activity (Ingmundson *et al.*, 2007, Dong *et al.*, 2012). Comprehensive bioinformatics considering current information of effector motifs would provide initial insight into candidate proteins (Bos *et al.*, 2007).

Annotated host Rab effectors were neither found in the inclusion proteome nor in the Inc-interactome, but indirect association cannot be completely excluded (Aeberhard *et al.*, 2015, Mirrashidi *et al.*, 2015).

Nonetheless, Rab proteins have an intrinsic slow GTPase activity that might be sufficient for Rab inactivation and subsequent release of golgin-84 fragments.

4.2 Golgi fragmentation is induced by human and zoonotic *Chlamydia* spp.

Infections with *Chlamydia* spp. are widespread throughout the animal kingdom. While research of the last decade has focused on the human species *C. trachomatis* and *C. pneumoniae*, the avian and zoonotic pathogen *C. psittaci* remained largely unexplored. Here, we extended previous studies and examined interactions of *C. psittaci* with the host Golgi apparatus and relevant Golgi associated trafficking pathways.

4.2.1 *Chlamydia*-spp. induce Golgi alterations in human epithelial cells

To establish an infection, the human pathogens *C. trachomatis* and *C. pneumoniae* rely on interactions with the host Golgi apparatus, to ensure efficient uptake of lipids, especially sphingolipids (Hackstadt *et al.*, 1995, Hackstadt *et al.*, 1996, Wolf & Hackstadt, 2001, Heuer *et al.*,

2009). One precondition for efficient sphingolipid uptake to *C. trachomatis* is the disruption of the Golgi ribbon, resulting in inclusion-adjacent Golgi ministacks (Heuer *et al.*, 2009, Rejman Lipinski *et al.*, 2009). The avian and zoonotic pathogen *C. psittaci* also acquires sphingolipids from the host, but pivotal molecular mechanisms are poorly described (Rockey *et al.*, 1996). Here, to examine the mechanisms underlying sphingolipid trafficking to the inclusion of *C. psittaci*, Golgi organization in infected human epithelial cells was analyzed.

Different serovars of *C. trachomatis,* including ocular and genital strains, induced Golgi fragmentation in human epithelial cells. Independent of the serovar, ministacks were recruited to bacteria and aligned around inclusions, indicating that sphingolipids might be easily acquired from inclusion-adjacent ministacks (Figure 3.8).

Different isolates of *C. psittaci* also induced severe rearrangements in Golgi structure in human epithelial cells. Interestingly, phenotypes of Golgi fragmentation were distinct from *C. trachomatis* and even more pronounced in *C. psittaci* infections (Figure 3.8). While Golgi ministacks aligned around *C. trachomatis* inclusions, smaller well-separated ministacks were distributed throughout the cytosol in *C. psittaci*-infected cells. Here, in contrast to the strictly human *C. trachomatis* strains, slight differences between *C. psittaci* isolates were observed. The strongest distribution of tiny ministacks was induced by the bovine isolate. In infections with ovine and human *C. psittaci* isolates, tiny separated stacks were distributed – but in proximity to the inclusions.

As Golgi fragmentation is induced by various *Chlamydia* spp. but appears with different phenotypes, it can be assumed that fragmentation per se is important but the mode of induction is species-specific. Ministacks in *C. trachomatis* infections phenotypically resembled ministacks observed in golgin-84 or GM130 knockdown cells (Figure 3.8) (Diao *et al.*, 2003, Puthenveedu *et al.*, 2006, Heuer *et al.*, 2009). Although transportation of vesicular cargo is hardly affected in any of these conditions, glycoprotein processing, in particular N-glycosylation, is significantly impaired. In contrast, ministack appearance in *C. psittaci*-infected cells, especially when infected with a high infectious dose, was phenocopied to p115 knockdown cells (Sohda *et al.*, 2005, Guo & Linstedt, 2013). In these cells, protein transport is significantly retarded and O-glycosylation but rather N-glycosylation is affected (Bachert & Linstedt, 2013, Guo & Linstedt, 2013). Since *C. trachomatis* and *C. psittaci* induce different phenotypes of Golgi ministacks, both pathogens might species-specifically modulate functions of the host glycosylation machinery and thereby provoke distinct glycosylation patterns. The differences in surface glycoprotein composition might influence cell membrane organization and further interfere with pathogen recognition or serve to modulate immune responses (Gutierrez-Martin *et al.*, 1997, Wolfert & Boons, 2013). On top, several cytoplasmic and nuclear proteins are regulated by O-glycosylation (Haltiwanger *et al.*, 1997, Comer & Hart, 2000). By affecting this distinct glycosylation machinery, *C. psittaci* might modulate host cell transcription and translation. Even if species-specific differences in glycoprotein modifications are possible, no experimental evidence is given yet.

For *C. trachomatis*, Golgi fragmentation is crucial for efficient sphingolipid acquisition. The close contact between ministacks and the inclusion reduces the distance for vesicular cargo and might thereby promote direct transport from ministacks to inclusions (Heuer *et al.*, 2009, Rejman Lipinski *et al.*, 2009). It needs to be further investigated if dispersed small ministacks induced by *C. psittaci* infections also determine sphingolipid acquisition. While dispersal might affect ministack characteristics it stretches the transportation route of Golgi vesicles and cargo towards inclusions, exacerbating fast transport. At the same time dispersal of ministacks creates gaps for other kinds of organellar contact that might supply different pools of nutrients (Matsumoto *et al.*, 1991).

4.2.2 *Chlamydia* spp.-induce Golgi alterations in chicken fibroblasts

Today, only few factors and mechanisms are known that determine host tropism and disease severity of chlamydial infections. Here, Golgi fragmentation was shown as one potential mechanism to interact with a human host thereby promoting chlamydial propagation. But is the mechanism of Golgi fragmentation also observed in an avian cell line, a natural host for *C. psittaci*? This thesis provided first experimental evidence that *C. psittaci* induces Golgi rearrangements in DF-1 chicken fibroblast but Golgi morphology and distribution of ministacks were distinct from human cells tested (Figure 3.8, Figure 3.9). Interestingly, *C. trachomatis* infections in theses cells, which are fostered in laboratory conditions but are unlikely to appear in nature, also induced Golgi alterations and even recruited ministacks to inclusions (Piraino, 1969). In sum, the alteration of Golgi structure and organization seemed to be a general process that human and avian *Chlamydia* spp. induce to efficiently establish their niche in different human and avian host cells.

4.2.3 *Chlamydia* spp. interact with Golgi-dependent trafficking pathways

Due to its central role in biomolecule processing and transport the Golgi apparatus is often targeted by intracellular bacteria that need to acquire nutrients or manipulate signaling of the host cell (Manire, 1966, Canton & Kima, 2012, Hilbi & Haas, 2012). I have shown that Golgi structure is affected by different *Chlamydia* spp. but phenotypic appearance of ministacks is species-specific. In the following different factors that usually maintain and regulate Golgi structure and functions were addressed in *C. trachomatis* and *C. psittaci* infections. To analyze if other proteins including selected golgin coiled-coil tethering factors, Rab GTPases and CERT contribute to chlamydial infections and might be involved in concomitant Golgi breakdown, protein localizations in both infection models were microscopically analyzed.

4.2.4 *Chlamydia* spp. interact with factors of Golgi-dependent vesicular transport

Interactions with golgins and other cargo receptors

The structure of the Golgi apparatus fundamentally relies on the homeostasis of proteins that define the Golgi matrix. Consequently, fluctuations in protein levels of golgins and several Rab

GTPases often result in disruption of the Golgi ribbon continuity and dispersal of Golgi ministacks (Diao *et al.*, 2003, Rejman Lipinski *et al.*, 2009, Munro, 2011). As shown previously, *C. trachomatis* provokes Golgi fragmentation that phenotypically resembles golgin-84 knockdown cells (Heuer *et al.*, 2009, Rejman Lipinski *et al.*, 2009). Recruitment of golgin-84 to *C. trachomatis* inclusions as described in section 3.1 might at least partially cause the imbalance in the Golgi matrix composition that leads to Golgi destabilization and infection-dependent fragmentation. Whether the acquisition of tethering factors might be generally associated with *Chlamydia*-dependent Golgi destabilization was addressed using localization studies in *C. trachomatis* and *C. psittaci* infections.

In contrast to *C. trachomatis, C. psittaci* did not recruit golgin-84 to inclusions implying that *C. psittaci*-induced Golgi fragmentation does not result from the directed reduction of golgin-84 in Golgi membranes. The zoonotic agent rather induced a species-specific distribution of Golgi elements that phenotypically resembled Golgi ministacks in p115 knockdown cells (Sohda *et al.*, 2005, Guo & Linstedt, 2013). The corresponding tethering factor p115 was however not found at *C. psittaci* inclusions meaning that Golgi dispersal is not either based on the relocation of p115 from the Golgi matrix to inclusions (Figure 3.10).

Similar to golgin-84 and p115, additional golgins that localize to *cis-, medial-* or *trans*-cisternae regulate Golgi structure and vesicle transport in anterograde or retrograde directions. These factors have multiple and distinct roles in maintaining Golgi structure, tethering vesicular cargo and in Golgi positioning, functions that not necessarily depend on one another (Diao *et al.*, 2003, Puthenveedu *et al.*, 2006, Marra *et al.*, 2007, Sohda *et al.*, 2010, Wong & Munro, 2014, Wei *et al.*, 2015). It was previously demonstrated that Golgi fragmentation due to downregulation of golgin-84, p115, GM130, Gpp130 and Giantin selectively promotes *C. trachomatis* development whereas no effects were seen for p230 (Heuer *et al.*, 2009, Rejman Lipinski *et al.*, 2009). To our surprise, except golgin-84, neither of the golgins showed a distinct rim-like localization to *C. trachomatis* inclusions (Figure 3.11). Also protein levels are not obviously changed upon infection. Thus, relocation of golgins to inclusions or other cellular destinations is a very unlikely determinant of infection-dependent Golgi fragmentation. The zoonotic agent *C. psittaci* neither showed obvious affinity to any of the potential tethering factors analyzed meaning that Golgi fragmentation as well has other, yet undefined reasons.

Since golgin-84 and p115 not only determine Golgi structure but also define two subtypes of COP I vesicles that shuttle cargo in the ER-Golgi interface, these proteins might be involved in selective metabolite delivery to human and zoonotic agents (Malsam *et al.*, 2005). The first indication for this hypothesis would be given by protein localization to inclusions. Other than *C. trachomatis*, that selectively recruited golgin-84, *C. psittaci* showed no affinity for this protein. The tethering factor p115 was neither recruited by *C. trachomatis* nor by *C. psittaci* and hence seemed to be redundant for vesicular transport to inclusions (Figure 3.10). The acquisition of

alternative factors for COP I tethering or retrograde cargo recognition might be dispensable, either due to redundant tethering capacities or due to untimeliness (Wong & Munro, 2014).

By recruiting golgin-84 and other components of retrograde trafficking *C. trachomatis* maintains the specific supply of essential nutrients (Figure 3.5) (Hackstadt *et al.*, 1995, Moore *et al.*, 2008, Aeberhard *et al.*, 2015). Whether *C. psittaci* likewise preferentially intercept retrograde transport routes is poorly described. Since neither golgin-84- nor p115-dependent retrograde transport was obviously targeted by *C. psittaci*, it is possible that other components of retrograde trafficking are used by this pathogen. This theory is supported by a study performed by Böcker and colleagues that showed that *C. psittaci* IncB interacts with Snapin, a regulator of late endocytic fusion as well as retrograde transport in neurons (Lu *et al.*, 2009, Cai *et al.*, 2010, Bocker *et al.*, 2014). As a consequence of IncB-Snapin interaction, *C. psittaci* inclusions become integrated into a network of retrograde transport and might acquire nutrients from distinct endosomal sources that are placed beyond Golgi-dependent pathways.

In addition to the interaction with retrograde pathways, anterograde trafficking routes might be targeted by *C. psittaci*. Focusing on anterograde transport at the ER-Golgi interface, the marker protein ERGIC-53, that participates in forward secretory trafficking and was proposed to promote nutrient transportation to *L. pneumophila,* was selected and its localization with respect to chlamydial infections was analyzed (Appenzeller *et al.*, 1999, Kagan & Roy, 2002). In cells infected with human or avian *Chlamydia* spp. neither localization nor distribution of ERGIC-53 were dramatically affected. However, loose ERGIC-53 positive vesicular structures were juxtaposed to inclusions. Despite this ambiguous localization pattern, ERGIC-53 was described as a component of *C. trachomatis* inclusions, and might promote nutrient supply as observed for *L. pneumophila* (Kagan & Roy, 2002, Aeberhard *et al.*, 2015). As the correlation of protein localization to inclusions and its function is not very clear for *C. trachomatis* infections, ERGIC-53, although not directly associated with *C. psittaci* inclusions, might have a specific function for bacterial development. To unveil this option, further experimental evidence would be needed.

Together, the localization studies show that human and zoonotic *Chlamydia* spp. recruit specific Golgi tethering factors or cargo receptors. *C. trachomatis* specifically interacts with golgin-84 while no other interactions with tethering factors are achieved. This species-specific interaction reveals another individual mechanism evolved in this strictly human agent to manipulate host processes. *C. psittaci* does neither obviously target ER-Golgi transportation routes, nor does it show affinity to any alternative tethering factor analyzed. The lack of specific interactions with Golgi tethering factors demonstrates that *C. psittaci*, that frequently switches hosts, is less adapted to humans. The lower degree of specification might cohere with a high autonomy towards human and other hosts and might provide unique features that enable *C. psittaci* to infect various hosts.

Interactions with Rab GTPases

Rab GTPases, together with golgins, regulate Golgi structure and are key mediators of vesicular trafficking pathways. Human *Chlamydia* spp. and also other intracellular pathogens manipulate specific Rab GTPases to modify cell trafficking for their own benefit (Rzomp *et al.*, 2003, Rzomp *et al.*, 2006, Seto *et al.*, 2011, Hoffmann *et al.*, 2014, Aeberhard *et al.*, 2015). In this study, I demonstrated that *C. psittaci* manipulates Golgi structure but does not obviously interact with golgins involved in this process. Alternatively, Rab GTPases that define Golgi structure and regulate Golgi trafficking pathways might be targeted by *C. psittaci* and were therefore analyzed with respect to their localizations in chlamydial infections.

C. trachomatis is highly adapted to its human host and interacts with a broad range of Rab-regulated pathways (Figure 3.12, Figure 3.13, Figure 3.14, Figure 3.15) (Rzomp *et al.*, 2003, Rejman Lipinski *et al.*, 2009, Capmany & Damiani, 2010, Aeberhard *et al.*, 2015). The interplay of golgin-84, Rab6A and Rab11A is furthermore essential for efficient sphingolipid uptake by this pathogen. Compared to *C. trachomatis*, *C. psittaci* did not recruit golgin-84 and only approached a reduced subset of Rab GTPases, with a clear preference for Rab proteins usually found on recycling endosomes (Table 3.1).

In this study, first indications were given that *C. psittaci* preferentially interacts with Rab8a, Rab11A and Rab35, proteins that regulate the recycling of endosomes (Figure 3.13). Interestingly, Rab4, a mediator of rapid recycling from early endosomes, was not recruited (Figure 3.14) (van der Sluijs *et al.*, 1992, McCaffrey *et al.*, 2001, Yudowski *et al.*, 2009). This selective interception of the so called slow recycling route implies that relevant functions placed at the hub of endo- and exocytosis could be used by *C. psittaci*.

Firstly, the hijack of recycling endosomes and containing cargoes could provide rich pools of nutrients. Rab8a for example is involved in the directed transport of LDL cholesterol from late endosomes to the plasma membrane (Kanerva *et al.*, 2013). By recruiting Rab8a *Chlamydia* spp. might reroute these pools of cholesterol to the inclusions. This mechanism might go along with the previously reported interception of Golgi-dependent cholesterol transport to *C. trachomatis* inclusions and thereby amplify cholesterol uptake by bacteria (Carabeo *et al.*, 2003). Analogous to this study and due to the observed recruitment of Rab8a, the role of cholesterol for *C. psittaci* infections would be a relevant question to address. Furthermore, *Chlamydia* spp. target Rab11A regulated sphingolipid transport mechanisms to get access to this essential nutrient. Upon knockdown of Rab11A *C. trachomatis*-induced Golgi fragmentation is blocked and efficient sphingolipid uptake by bacteria is severely impaired (Rejman Lipinski *et al.*, 2009). Though, it cannot be clearly distinguished if lipid transport from recycling endosomes or inclusion-adjacent Golgi elements, impeded in knockdown cells, is impaired. Since *C. psittaci* also recruited Rab11A it would be interesting to analyze effects of Rab11A deficiency on *C. psittaci* infections and related intracellular processes including infection-dependent Golgi fragmentation and sphingolipid

transport. The close proximity of Rab35 to inclusions of human and avian *Chlamydia* spp. also promotes the theory that recycling endosomes are targeted to acquire nutrients. Rab35 participates in exocytosis of multivesicular bodies by docking them to the plasma membrane prior to release (Hsu *et al.*, 2010). Accordingly, inclusion-associated Rab35 might dock these compartments to inclusion membranes and facilitate scavenging of this rich reservoir filled with various lipids including sphingolipids and cholesterol (Piper & Luzio, 2001).

Rab GTPases of the slow recycling route might be also targeted by *Chlamydia* spp. to modulate distinct host cell functions for their own benefit. The cargoes recycled via the slow route are among others MHC I complexes, β-integrins or syndecans a group of heparan sulfate proteoglycans (Powelka *et al.*, 2004, Zimmermann *et al.*, 2005, Barral *et al.*, 2008, Eyster *et al.*, 2009). Interrupting cargo recycling to the plasma membrane could reduce MHC I recycling, thus comprise a reduction of antigen presentation via MHC I complexes and thereby modulate subsequent immune responses and circumvent host cell death. The interception of MHC recycling is actually targeted by various intracellular pathogens that need to maintain their habitat. The intracellular pathogen *Mycobacterium tuberculosis* transcriptionally regulate MHC complexes while *Salmonella enterica* and *Helicobacter pylori* manipulate antigen loading or processing (Molinari *et al.*, 1998, Stenger *et al.*, 1998, Zhong *et al.*, 2000, Cheminay *et al.*, 2005). Though, for *C. trachomatis* unaltered expression and antigen presentation of MHC I complexes was recently reported and also *C. psittaci* antigens were efficiently presented via MHC I complexes at least on murine dendritic cells (Fiegl *et al.*, 2013, Kagebein *et al.*, 2014). The situation in epithelial cells that are not able to present exogenous antigens via the process of cross-presentation, might still be different (Neefjes & Sadaka, 2012). Nevertheless, the sum of current data indicate, that MHC I complex recycling is presumably not affected by *Chlamydia* spp. and is not concerned by chlamydial interactions with recycling endosomes.

Beyond MHC I recycling, the retention of recycling endosomes apposed to inclusions might still influence glycoprotein, in particular syndecan presentation at the cell surface. The infection-dependent modulation of cell surface syndecans could be a versatile strategy to impair sugar mediated recognition and binding of *Chlamydia* spp. to an already infected cell and thereby prevent a reinfection (Su *et al.*, 1996, Rasmussen-Lathrop *et al.*, 2000, Wuppermann *et al.*, 2001). The need for syndecans in *C. trachomatis* infections is however questionable because the pathogen expresses species-specific effectors that maintain host contact and interactions without the help of heparan sulfate proteoglycans (Clifton *et al.*, 2004, Stephens *et al.*, 2006, Fechtner *et al.*, 2013, Nans *et al.*, 2014). Unlike *C. trachomatis*, C. *psittaci* expresses other, presumably less host-specific, effector proteins. To compensate its relatively low degree of specialization it might therefore benefit from the interaction with syndecans to approach a human host. Heparan sulfate proteoglycans are further involved in cell migration. Hence, by interacting with glycan recycling, *Chlamydia* spp. might affect glycan presentation at the cell surface and might thereby impair host cell movement (Moon

et al., 2005). In cells infected with *C. trachomatis* severe defects in cell migration are observed and, as functional cell motility is an essential part of the process of wound healing, are related to chlamydial pathology and tissue scaring (Heymann *et al.*, 2013). Severe tissue lesions resulting from acute *C. psittaci* infections might hence be correlated to impaired cell migration that possibly results from modulations of recycling endosomes.

Beside Rab proteins specific for recycling endosomes, Rab3D, a novel mediator of secretory granule maturation and exocytosis, was associated with *C. trachomatis* and *C. psittaci* inclusions (Figure 3.15). Recruitment of the protein might promote inclusion contact to the plasma membrane and at late stages of the infection could contribute to bacterial egress by extrusions (Hybiske & Stephens, 2007, Kogel & Gerdes, 2010, Kogel *et al.*, 2013).

Together, *C. trachomatis* and *C. psittaci* are able to interact with a subset of specific Rab GTPases which might support efficient nutrient acquisition and moreover might serve to modulate superior host cell functions. The strictly human pathogen *C. trachomatis* recruits a variety of Rab proteins that regulate endosomal recycling and Golgi maturation, indicating that respective signaling and trafficking pathways are targeted and might be subverted. In contrast, *C. psittaci* recruited a reduced subset of Rab proteins, all shared with *C. trachomatis*. The findings that *C. psittaci* does not interact with golgin tethering factors and only interacts with few Rab GTPases promotes the idea that this pathogen keeps a high degree of autonomy and flexibility which allows interactions with different host species.

To further demonstrate species-specific preferences for golgin tethering factors and Rab protein interactions, additional validation experiments could be performed. Inclusion purification followed by proteomic analyses as recently performed for other chlamydial organisms would give a holistic view on species-specific interactions between bacteria and host cells (Aeberhard *et al.*, 2015, Herweg *et al.*, 2015). Also biochemical approaches like (co-)immunoprecipitations or yeast two-hybrid screens would help to define the Rab-*Chlamydia* interactomes. Furthermore, the emerging toolbox of genetic methods will in future allow manipulations of the yet poorly accessible chlamydial genomes and help to characterize putative bacterial factors (Wood *et al.*, 2014).

4.2.5 Interactions with non-vesicular ceramide transport

Since *C. trachomatis* and *C. psittaci* interact with distinct host factors, species-specific roles are possible. Beside vesicular trafficking pathways, *C. trachomatis* interacts with the non-vesicular ceramide transport to promote sphingolipid acquisition (Derre *et al.*, 2011, Agaisse & Derre, 2014). In this study I showed that CERT is also recruited to *C. psittaci* inclusions (Figure 3.16). To determine which bacterial and host factors might be involved in protein recruitment to chlamydial inclusions different mutants of CERT with compromised binding properties were analyzed in both infection models. In case of *C. trachomatis,* CERT binding is directly mediated by the bacterial protein IncD that interacts with CERT PH domain (Derre *et al.*, 2011, Agaisse & Derre, 2014).

Here, CERT mutants with an inactive PH domain (CERT G67E) did not localize to *C. trachomatis* inclusions confirming previous results (Figure 3.17). This mutation, interestingly, also affected CERT binding to *C. psittaci* inclusions suggesting a similar mode of CERT PH-Inc interaction. Since Inc proteins share little sequence similarity between species in general but comprise a subset of "core-Incs", I checked if *C. psittaci* contains homologues to *C. trachomatis* IncD (Dehoux *et al.*, 2011, Lutter *et al.*, 2012). Here, only proteins with little sequence similaritiy to IncD were identified meaning that other, yet unknown factors, must be responsible for CERT binding *C. psittaci* inclusions.

In uninfected cells, CERT PH domain binds to PI4P enriched in the *trans*-Golgi region. Moreover, Moorhead and colleagues suggested, that PI4P is present in *C. trachomatis* inclusions and might thereby partially mediate CERT binding (Moorhead *et al.*, 2010). Assuming that *C. psittaci* inclusions also contain PI4P, this mode of binding could be conserved and might be even more important than binding via species-specific Inc proteins. In addition, proteomic analysis of *C. trachomatis* inclusions revealed that VAPB, a binding partner of CERT is significantly enriched in the inclusion proteome (Aeberhard *et al.*, 2015). Whether VAPB is also associated with *C. psittaci* inclusions and facilitates CERT recruitment to the pathogen still needs to be determined. Future biochemical approaches, including CERT immunoprecipitations or even holistic proteomic and lipidomic analyses would be needed to characterize the nature of CERT binding to *C. psittaci* inclusions.

In sum, although the mode of CERT binding to inclusion is not completely defined, the result that CERT is recruited to different *Chlamydia* spp. implies that CERT-dependent ceramide transport plays a critical role for the development of chlamydial infections.

4.3 Consequences of CERT inhibition on infections with *Chlamydia* spp.

In eukaryotic cells, transport of ceramide from the ER to the Golgi apparatus is the precondition for the *de novo* synthesis of complex sphingolipids such as sphingomyelin, glycosphingolipids and ceramide-1-phosphate. The ceramide transfer protein CERT has a central role in this process and mediates transport of ceramide directly from the ER to Golgi apparatus along MCSs (Hanada *et al.*, 2003, Kawano *et al.*, 2006).

CERT exclusively mediates transport of ceramides and due to steric reasons, preferentially binds ceramides with acyl chains of C14:0 - C22:0. For ceramides with acyl chains of C24:1 transfer rates were reduced by 60%, and transport of C24:0 ceramides is actually negligible (Kumagai *et al.*, 2005, Kudo *et al.*, 2008). Although ceramide can be converted into various metabolites, CERT-dependent ceramide transport mostly drives sphingomyelin synthesis (Hanada *et al.*, 2003, Halter *et al.*, 2007). Consequently, glucosylceramide synthesis is primarily maintained by CERT-independent pathways which in case of CERT depletion also sustain a certain level of sphingomyelin synthesis (Hanada *et al.*, 2003). Today, insights into CERT-independent transport

which is ATP dependent and most likely mediated by COP II vesicles are rather poor (Fukasawa *et al.*, 1999, Hanada *et al.*, 2003, Giussani *et al.*, 2008).

Due to its central role in ceramide transport and sphingomyelin biogenesis, CERT is of particular interest for infections with *Chlamydia* spp. This and other studies have shown that CERT is recruited by different *Chlamydia* spp. and contributes to ER-inclusion MCSs (Figure 3.16, Figure 3.17) (Derre *et al.*, 2011, Elwell *et al.*, 2011). Associated with inclusions, CERT supports inclusion maturation and even determines infectivity of *C. trachomatis* and *C. muridarum*, processes which are severely affected upon CERT knockdown (Derre *et al.*, 2011, Elwell *et al.*, 2011). Here, to further examine the physiological relevance of CERT recruitment to *C. psittaci*, different aspects of CERT-inhibition were analyzed using the chemical compound HPA-12.

4.3.1 Inhibition of CERT by HPA-12

The pharmacological agent HPA-12 is a ceramide analogue that binds to CERT and thereby inhibits normal ceramide transport. Since the first description in 2001, HPA-12, its mode of action and in particular the way of CERT binding have been extensively studied (Yasuda *et al.*, 2001). The stereochemistry of the ceramide analogue as well as the length of the amide side chain, optimally containing 11 to 15 carbon atoms, define its inhibitory capacity (Nakamura *et al.*, 2003, Kudo *et al.*, 2008). Throughout this thesis, the isomer HPA-12 (1*R*,3*S*) was used which was synthesized by Christoph Arenz and colleagues using a recently optimized method and which showed the best CERT binding properties compared to other stereoisomers (Saied *et al.*, 2014, Santos *et al.*, 2015).

Due to the important role of CERT in non-vesicular ceramide transport and sphingolipid homeostasis, HPA-12 treatment might affect several host cell mechanisms and consequently act on *Chlamydia* spp. The framework of CERT and possible effects of HPA-12 treatment in *Chlamydia*-infected cells is illustrated in the following figure (Figure 4.2):

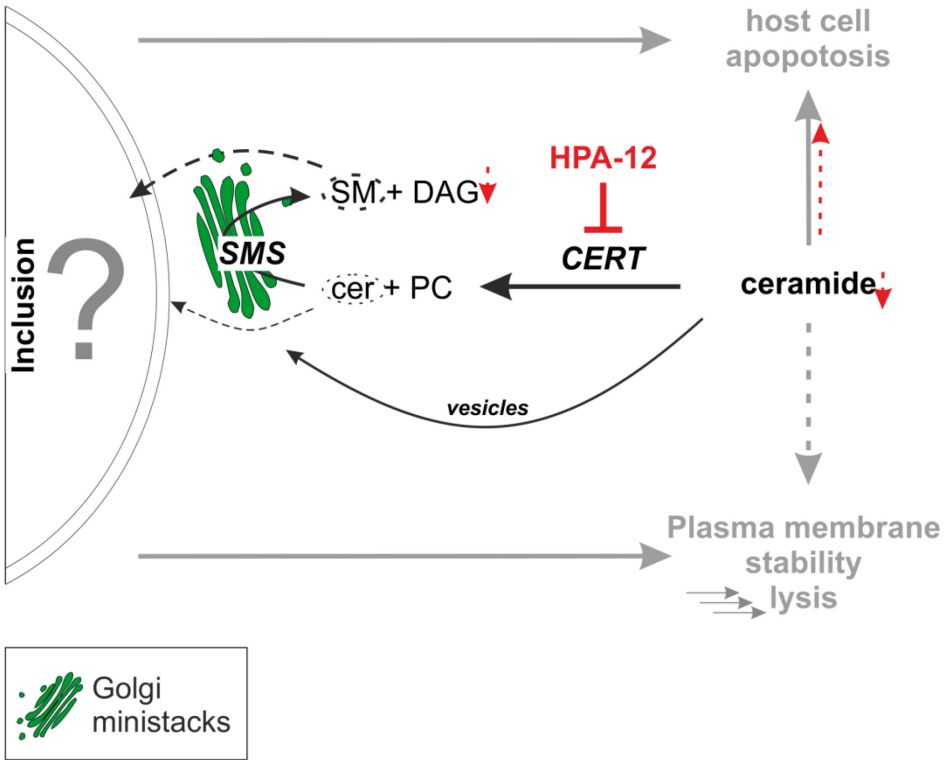

Figure 4.2 Framework of CERT and possible effects of HPA-12 treatment in cells infected with *Chlamydia* spp.
Schematic representation of HPA-12 mediated inhibition of CERT-dependent ceramide transport and putative consequences on *Chlamydia* spp. and the host cell. Black arrows depict sphingolipid routes, grey arrows depict host cell functions modulated upon infections or changed sphingolipid levels and red arrows depict known consequences of HPA-12 treatment on host cell functions.

First of all, HPA-12 inhibits CERT mediated transport of ceramide and might thereby affect the efficiency of ceramide recruitment to chlamydial inclusions. As a consequence, HPA-12 treatment would alter the efficient supply of sphingolipids which on the one hand might serve as building blocks for inclusion biogenesis and on the other hand might be directly transported to bacteria and participate in RB to EB condensation or shape EB membrane properties (Derre *et al.*, 2011, Elwell *et al.*, 2011). Binding properties of HPA-12 to CERT are well defined but secondary effects on *Chlamydia* spp. due to direct interactions with chlamydial proteins might further contribute to compound activity.

Considering the host cell site, HPA-12 treatment alters absolute levels of plasma membrane sphingomyelin and thereby could affect recognition and entry of *Chlamydia* spp. Towards the end of the infectious cycle, altered plasma membrane properties could furthermore influence the release of chlamydial particles by extrusions or facilitate cell lysis (Hackstadt *et al.*, 1996, Salaun *et al.*, 2004, Hybiske & Stephens, 2007, Raposo & Stoorvogel, 2013). Apart from that, HPA-12 mediated inhibition of CERT can induce apoptosis and might thereby antagonize with chlamydial mechanisms that inhibit apoptosis to protect their intracellular niche (Ying *et al.*, 2007, Charruyer *et al.*, 2008).

As *C. trachomatis* and *C. psittaci* recruited CERT to their inclusions, I investigated the impact of HPA-12 treatment on infections and specified different aspects considering pathogen biogenesis

and respective host cell functions (Derre *et al.*, 2011, Agaisse & Derre, 2014, Agaisse & Derre, 2015).

HPA-12 affects chlamydial plaque formation in a species-specific manner

First, to determine dose-dependent effects of HPA-12 treatment on chlamydial development a plaque assay allowing easy titration of the compound was performed. Surprisingly, although CERT was recruited to both *Chlamydia* spp., HPA-12 treatment hardly affected *C. trachomatis* plaque formation at concentrations up to 20 µM whereas already 10 µM of compound potently reduced *C. psittaci* plaque numbers (Figure 3.18). *C. trachomatis* is very well adapted to its human host and is able to employ a large repertoire of host mechanisms to interact with sphingolipid transport routes (section 1.4.2) (Hackstadt *et al.*, 1996, Rejman Lipinski *et al.*, 2009, Capmany & Damiani, 2010, Elwell *et al.*, 2011). To deal with different intracellular conditions, such as sphingolipid imbalances caused by HPA-12 treatment, *C. trachomatis* might switch between these mechanisms. Thus, to compensate CERT-inhibition the pathogen might alternatively target vesicular transport routes and could thereby efficiently overcome HPA-12 mediated fluctuations in non-vesicular ceramide transport and sphingomyelin levels. The observed reduction of *C. psittaci* plaque formation further implies that development of the zoonotic agent strongly depends on CERT activity. As *C. psittaci* was proposed to interact with fewer regulators of vesicular transport (sections 3.3, 4.2.4), CERT function in ceramide transport to inclusions might be predominant and if no alternative bacterial factors are involved, would be indispensable. Even if an alternative bacterial factor is involved in ceramide transport, it is not sufficient to substitute CERT function or might be blocked by HPA-12 itself.

HPA-12 is not cytotoxic but interferes with lytic properties of Chlamydia spp.

In the previous plaque assays, *C. trachomatis* did not respond to the tested dose-range of HPA-12 whereas treatment selectively affected *C. psittaci* plaque formation (Figure 3.18). Under the given experimental conditions, the integrity of host cell monolayers was not affected by HPA-12 treatment, indicating that during plaque assays, HPA-12 in principle induces no or only low levels of cytotoxicity. To further specify the cytotoxic potential of HPA-12 in uninfected cells as well as in cells infected with *C. trachomatis* or *C. psittaci*, LDH cytotoxicity assays were performed. Here, one optimal cycle of chlamydial development was considered meaning that cytotoxicity was assessed 48 h *p.i.*, independent of the inoculum.

In accordance with previous results, uninfected cells were not affected by treatment with up to 40 µM HPA-12 (Figure 3.19). Thus, the reduction of cellular sphingomyelin levels that result from CERT inhibition and potentially change plasma membrane properties, did not lead to cell lysis (Hanada *et al.*, 2003, Salaun *et al.*, 2004, Charruyer *et al.*, 2008, Raposo & Stoorvogel, 2013).

In untreated *Chlamydia*-infected cells, using MOI 0.5 or MOI 2 respectively, an MOI-dependent increase in cytotoxicity was observed (Figure 3.19). *Chlamydia* spp. induce cell lysis at the end of their developmental cycle. The cytotoxic or cytolytic potential of *Chlamydia* spp. is thereby

determined by the initial bacterial load and successful bacterial development that might be affected by inhibitory stimuli.

Treatment with HPA-12 did not alter *C. trachomatis*-induced cytolysis using concentrations up to 20 µM HPA-12. Treatment with 40 µM HPA-12 could however effectively reduce *C. trachomatis*-dependent cytolysis, for both infections with MOI 0.5 or MOI 2 (Figure 3.19). This finding suggests that HPA-12 might impair one or several aspects of *C. trachomatis* pathogenicity that in sum regulate bacteria-induced cytolysis.

C. psittaci infections, that also induced MOI-dependent cytolysis in untreated cells, showed a biphasic response to HPA-12 treatment. While treatment with up to 5 µM HPA-12 tended to amplify *C. psittaci*-related effects, HPA-12 concentrations above 10 µM counteracted this tendency and reduced cell lysis. As observed for *C. trachomatis,* 40 µM HPA-12 decreased *C. psittaci*-induced cell lysis but effects were less prominent (Figure 3.19). This biphasic dose-response indicates that low concentrations of HPA-12 support *C. psittaci*-induced processes that in sum promote cell lysis and bacterial egress. Though, when applied at higher concentrations HPA-12 might directly impair chlamydial development and thereby reduce *C. psittaci*-related effects (Figure 4.2). Which steps of bacterial and host cell functions are affected by HPA-12 and together determine *C. psittaci*-related cytolysis needs to be investigated further.

HPA-12 affects distinct steps of chlamydial replication and virulence

The exceptional biphasic developmental cycle of *Chlamydia* spp. is tightly regulated to generate infectious progeny (Belland *et al.*, 2003, Nicholson *et al.*, 2003). First, EBs have to differentiate into RBs to become metabolically active, replicate and optimize interactions with the host cell. To finish the cycle, RBs have to differentiate back into infectious EBs that are released and can start new rounds of infection. This thesis showed that HPA-12 impairs *C. trachomatis*-related cell lysis and potently inhibits *C. psittaci* infections (Figure 3.18, Figure 3.19). However, neither plaque assays nor cytotoxicity assays allowed to draw a distinction between effects on certain steps of the developmental cycle or on the host cell.

To specify effects on bacterial replication, progeny formed 48 h *p.i.* was quantified using qPCR. *C. trachomatis* replication in cells infected with an inoculum of MOI 2 was not altered by treatment with 10 µM or 20 µM HPA-12. Interestingly, when infections were started with a low infectious dose of MOI 0.5, treatment with 20 µM HPA-12 impaired *C. trachomatis* replication (Figure 3.20). This finding indicates that HPA-12 influences host cell mechanisms that can be overcome or counteracted by *C. trachomatis* depending on the MOI. Here, apoptosis is a possible host cell function that is affected by the chemical agent and is also targeted by *C. trachomatis* to ensure intracellular replication. HPA-12 mediated blocking of CERT-dependent ceramide transport leads to a local accumulation of ceramide which stimulates the induction of apoptosis (Charruyer *et al.*, 2008). Chlamydial development and replication on the contrary strongly depend on apoptosis inhibition (Ying *et al.*, 2007). Since the impact of *Chlamydia*-induced host modifications should

correlate with the bacterial load, apoptosis inhibition should be more effective in cells infected with a high MOI (Fan *et al.*, 1998). Consequently, cells infected with a high number of *C. trachomatis* would be more resistant to HPA-12 induced apoptosis.

Assuming that *C. trachomatis* counteracts HPA-12 induced apoptosis, *C. trachomatis*-induced Golgi rearrangements might be considered as a mechanistic link between apoptosis induction and inhibition. *C. trachomatis* induces Golgi fragmentation, recruits Golgi ministacks and establishes ER-inclusion contact sites and thereby locally concentrates all enzymes needed for sphingomyelin synthesis (Elwell *et al.*, 2011). This enzyme cluster might improve ceramide to sphingomyelin conversion in proximity to inclusions. Upon CERT inhibition by HPA-12, ceramide accumulates at the ER, the Golgi apparatus and in infected cells might also concentrate at ER-inclusion MCSs (Charruyer *et al.*, 2008, Derre *et al.*, 2011, Elwell *et al.*, 2011). Adjacent to the local enzyme cluster ceramide might be directly processed, avoiding accumulation. As a result, ceramide levels would stay below the level needed to stimulate apoptosis and infected cells would be more resistant to HPA-12 induced effects.

Considering the zoonotic agent *C. psittaci*, moderate treatment using 10 µM HPA-12 seemed to support bacterial replication independent of the infectious dose. Despite this observed improvement, treatment with 20 µM HPA-12 effectively diminished replication rates (Figure 3.20). Again, HPA-12 affects chlamydial development in a species-specific manner. Here, *C. psittaci* replication might benefit from one or several mechanisms HPA-12 interferes with. Firstly, similar to *C. trachomatis,* the balance between apoptosis induction by HPA-12 and inhibition by the pathogen might regulate bacterial replication. Moreover, beyond apoptosis, HPA-12-mediated CERT inhibition leads to mild changes in sphingomyelin levels and might thereby have an impact on membrane properties of the inclusion membrane or membranes of intracellular organelles such as endosomes or MVBs (Lingwood & Simons, 2010). Especially membrane curvatures and function strongly depend on sphingomyelin-rich domains. Upon HPA-12 treatment, sphingomyelin levels might be changed insofar as *C. psittaci* inclusion membranes, which under normal conditions are very irregular in shape and contain numerous invaginations, become reorganized (Spears & Storz, 1979). Reorganization might thereby optimize the host-pathogen interface, improve host-pathogen interactions such as uptake of endosomal cargo which finally promotes bacterial replication. As *C. trachomatis* inclusions, that usually form optimal spheres with a large optimized host-pathogen interface, would not obviously benefit from reorganizations, this mechanism might contribute to the species-specificity of HPA-12.

Furthermore, the boost in *C. psittaci* replication upon mild HPA-12 treatment could be correlated to CERT specificity for distinct ceramides. By blocking CERT with HPA-12, ceramides with chain lengths between C14 and C22, usually transported by this transporter, would rather reach the Golgi apparatus or the inclusion (Kumagai *et al.*, 2005, Kudo *et al.*, 2008). To avoid starvation, *C. psittaci* might henceforth switch to ceramides e.g. from the sphingomyelin salvage

pathway which would include ceramides with longer acyl chain lengths that provide more energy by β-oxidation. Alternatively, *C. psittaci* might directly benefit from ceramide that, upon HPA-12 treatment, accumulates at ER-inclusion MCSs by using it as a nutrient to fuel replication.

Beside replication, infectious progeny produced in one developmental cycle depends on chlamydial fitness and was determined after HPA-12 treatment. The performed reinfection assay revealed a strong reduction of *C. trachomatis* progeny formation upon HPA-12 treatment, independent of the MOI. Already 10 µM HPA-12 affected *C. trachomatis* progeny formation while 20 µM HPA-12 actually reduced infectious progeny even as potent as siRNA mediated knockdown of CERT (Figure 3.20) (Derre *et al.*, 2011). Interestingly, the strong reduction of infectious progeny implies that HPA-12 is far more efficient against *C. trachomatis* than, referring to previous results, expected. The antichlamydial effects observed here might most likely be ascribed to different experimental procedures. In all previous assays, both *Chlamydia* spp. and host cells were exposed to the same inhibitory pressure. In the present reinfection assay, *C. trachomatis* was extracted from treated cells and titrated onto untreated naïve cells for secondary infections. Determined progeny formation can therefore directly be related to fitness of the extracted pathogens. The observed HPA-12-dependent reduction in infections progeny henceforth leads to the conclusion that inhibitor treatment specifically impairs *C. trachomatis* development, differentiation or bacterial virulence factors that in sum determine the functionality of infectious progeny.

Likewise, progeny formation of *C. psittaci* was significantly reduced by HPA-12 treatment, meaning that *C. psittaci* differentiation or infectivity of formed EBs were affected (Figure 3.20).

Chlamydial RB-EB differentiation is not affected by HPA-12

The ceramide analogue HPA-12 effectively reduces infectivity of different *Chlamydia* spp., but as plaque formation, bacteria-induced cytolysis and replication were affected in a species-specific manner, the modes of HPA-12 action seem to be species-specific (Elwell *et al.*, 2011). In this work, 10 µM HPA-12 specifically reduced infectious progeny from *C. trachomatis* and *C. psittaci*. To distinguish between defects in RB-EB differentiation or reduced infectivity of formed EBs, electron micrographs were analyzed at 48 h *p.i.* In all conditions examined, EBs were the predominant developmental form, followed by RBs and at the moment converting IBs (Figure 3.21). As none of the strains showed significant changes in RB to EB differentiation upon HPA-12 treatment, loss of chlamydial infectivity must be related to other factors of virulence. To dissect species-specific modes of HPA-12 actions, virulence factor synthesis, secretion of effector proteins or EB stability could be further analyzed.

HPA-12 treatment specifically reduces protein expression of C. psittaci

Chlamydia spp. differentially respond to HPA-12 treatment supporting a species-specific mode of action for this compound. To complement previous experiments that considered host-pathogen interactions and chlamydial infectivity, protein synthesis of selected chlamydial markers was

further assessed by Western blot analysis. In the course of one developmental cycle, *C. trachomatis* continuously expressed Hsp60 and the T3SS effector IncA shown by a slight increase of protein levels over time (Figure 3.22) (Subtil *et al.*, 2001). HPA-12 treatment did not affect the expression of any of these proteins but defects in IncA membrane insertion that would consequently affect homotypic fusion of inclusions and impair inclusion biogenesis and host pathogen interactions cannot be excluded (Hackstadt *et al.*, 1999, Delevoye *et al.*, 2008).

In contrast, protein expression of *C. psittaci* was significantly affected under HPA-12 pressure. Interestingly, IncB expression was specifically reduced at 24 h and 36 h *p.i.*, times of RB replication and metabolic activity (Braukmann *et al.*, 2012). At 48 h, prior to chlamydial cell exit, levels of IncB were comparable to untreated conditions (Figure 3.22, B). By interacting with the host cell factor Snapin, that connects inclusions to the microtubule network, IncB occupies a central role in the acquisition host cell derived vesicular compounds (Bocker *et al.*, 2014). Here, the lack of this factor, especially during RB development, can consequently lead to the defects in infectivity.

In sum, inhibitor studies showed that CERT-dependent regulation of sphingolipid transport and sphingomyelin levels affects species-specific aspects of chlamydial development and infectivity. CERT activity for one is essential for *C. trachomatis* infections and potently reduces *C. trachomatis* infectivity at concentrations of 10 µM. The comprehensive analyses to determine the mode of inhibition that included plaque formation, bacteria-induced cytolysis, chlamydial replication, differentiation and protein synthesis revealed that despite the clear reduction of *C. trachomatis* infectivity neither of these other processes were significantly affected by CERT inhibition. Thus, although this strictly human pathogen can tolerate or even compensate various effects resulting from altered CERT activity, specific aspects of pathogenicity such as inclusion biogenesis, effector secretion or biogenesis of virulence factors seem to depend on CERT function. CERT activity was even more important for the development of the zoonotic agent *C. psittaci* and infections were effectively reduced using 10 µM HPA-12 ($IC_{50} \approx 10$ µM, Figure 3.18). For this pathogen, CERT activity not only determined infectivity but was also involved in all other processes analyzed, except RB-EB differentiation. Hence, CERT seems to be the major determinant that allows *C. psittaci* to interfere with sphingolipid transport, regulate ceramide levels and maintain intracellular development. Considering the introduced framework of CERT in Figure 4.2 the described modes of HPA-12 function on *Chlamydia* spp. are summarized in Figure 4.3. Finally, due to its antichlamydial activity in concentrations comparable to other antichlamydial compounds like chloramphenicol ($IC_{50} \approx 3$ µM) or 1-O-methyl-NBD-ceramide-C16 ($IC_{50} \approx 5$ µM), HPA-12 could in future become an interesting candidate for the development of novel sphingolipid-based therapies (Banhart *et al.*, 2014).

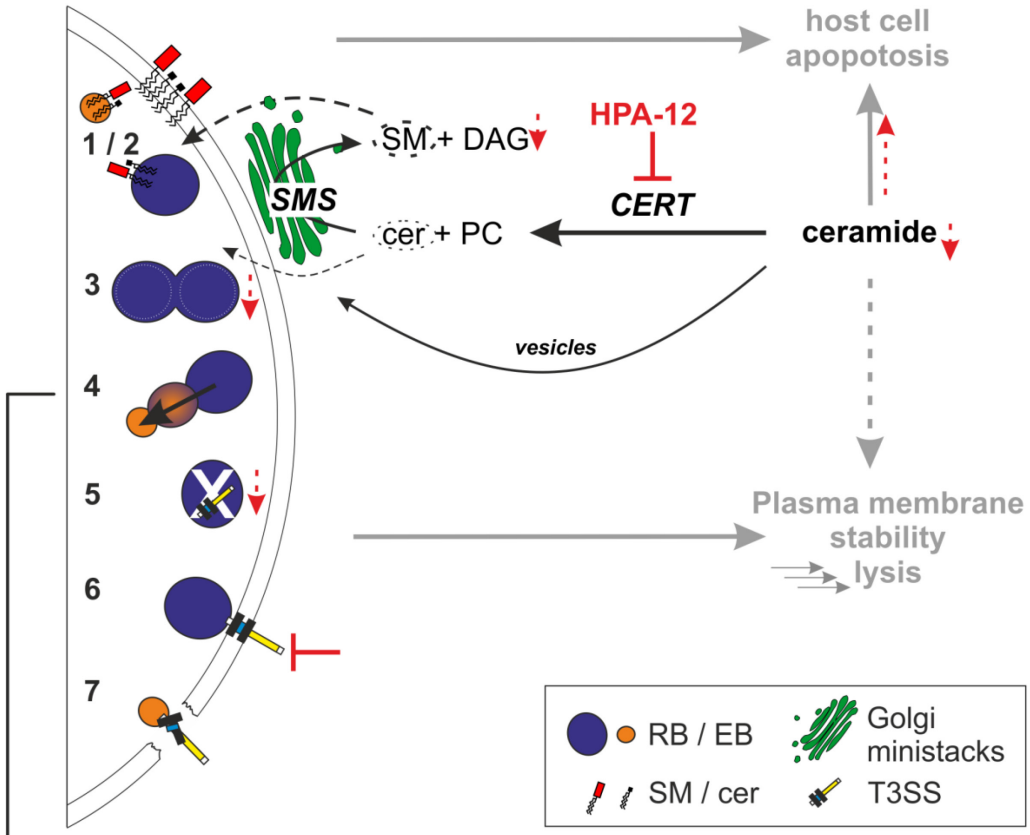

Effects of HPA-12 on:	Assay	*Ctr*	*Cpsi*
1) Inclusion biogenesis	-	**	**
2) lipid uptake	-	**	**
3) replication	GCN, Infectivity assay (indirect)	-/+	+
4) RB-EB differentiation	Morphology assay / TEM	-	-
5) protein expression	WB	-	+
6) effector secretion	WB (indirect)	?	+
7) T3SS biogenesis	WB (indirect), Infectivity assay (indirect)	*	*

\+ affected / reduced
\- not affected
** probably affected, published data
* eventually affected, indirectly shown
? not tested

Figure 4.3 Model for effects of HPA-12 treatment that affect infections with *Chlamydia* spp.
Schematic representation of HPA-12 mediated inhibition of CERT-dependent ceramide transport and its consequences on *Chlamydia* spp. and the host cell that together reduce chlamydial infectivity. Precise descriptions of species-specific consequences are found in the text. Black arrows depict sphingolipid routes, grey arrows depict consequences on the host cell and red arrows and lines depict known consequences of HPA-12 treatment. Possible consequences of HPA-12 treatment on *Chlamydia* spp. are described as No. 1-7 and are summarized in the depicted table.

4.4 Quantitative analysis of chlamydial sphingolipid-composition

Chlamydia spp. employ a variety of strategies to acquire essential lipids from the host cell. This and other studies have shown that infectivity of *Chlamydia* spp. depends on host cell sphingolipid synthesis and transport. Relative to their size, ceramides and sphingomyelins are transported via different routes which are hijacked by *Chlamydia* spp. to impel distinct steps of development. Some mechanisms of lipid acquisition are well conserved among different *Chlamydia* spp. though species-specific mechanisms become additionally necessary when host and tissue preferences evolve. Seminal studies by Hackstadt and colleagues obtained first insights into the particular meaning of sphingolipid transport and metabolism for *C. trachomatis* development (Hackstadt *et al.*, 1996, Scidmore *et al.*, 1996). Between then and now, the fluorescently labelled ceramide NBD-C_6-Ceramide was almost exclusively used to expand our knowledge about sphingolipid acquisition by *Chlamydia* spp. (Hackstadt *et al.*, 1996, Rockey *et al.*, 1996, Wolf & Hackstadt, 2001, Herweg *et al.*, 2015). Since a lot of ceramide properties are specified by its acyl chain lengths, novel approaches that consider endogenous ceramides should be used to validate, complement and extend these data (Koivusalo *et al.*, 2007, Shaner *et al.*, 2009, Grosch *et al.*, 2012). Today, technical advances give the opportunity to measure endogenous sphingolipid levels with sensitivities down to picomolar ranges. Here, in order to link sphingolipid properties to chlamydial infectivity, we used a customized approach of lipid chromatography-mass spectrometry and quantitatively determined ceramide and sphingomyelin composition of *C. trachomatis* and *C. psittaci*.

For this purpose, EBs were selectively enriched as described in section 3.5.1. In collaboration with Burkhard Kleuser and colleagues, lipids were extracted and sphingolipids were quantitatively determined by rapid resolution liquid chromatography MS/MS. The results gained by this methodology, for the first time provided comprehensive insights into the endogenous sphingolipid composition of *C. trachomatis* and *C. psittaci* EBs. For both *Chlamydia* spp. ceramides and sphingolipids carrying different physiologically important acyl chains were detectable (Figure 3.24). To our surprise, *C. psittaci* EBs enriched about eight times more sphingolipids than *C. trachomatis* EBs which implies that sphingolipids are of particular importance for the pathogen. As *C. psittaci* scavenged less or other sphingolipid transport routes than *C. trachomatis* the species-specific mode of sphingolipid acquisition seems to be very efficient. Autonomous sphingolipid synthesis by *C. psittaci* might also contribute to the relatively high amount of sphingolipids but has never been described for any other *Chlamydia* spp.

So far, although the fluorescently labelled sphingolipid ceramide NBD-C_6-Ceramide was transported to *C. psittaci* inclusions and also endogenous sphingolipids were detected in bacterial extracts, it was unclear whether sphingomyelin itself or its biosynthetic precursor ceramide are incorporated into bacteria (Figure 3.24) (Rockey *et al.*, 1996). By comparing the ratio of sphingomyelin to ceramide, I observed that *C. psittaci* EBs, compared to *C. trachomatis* EBs, have a higher affinity for ceramide, even though sphingomyelins predominate the absolute sphingolipid

composition (Figure 3.24). This result correlates with previous reports stating that *C. trachomatis* contains the metabolic product sphingomyelin rather than its precursor ceramide (Hackstadt *et al.*, 1995, Hackstadt *et al.*, 1996, Scidmore *et al.*, 1996). It also implies that ceramide plays an elevated role for *C. psittaci* EBs where it might promote membrane stability. Furthermore, when EB membranes enriched in ceramide make contact to host cells, ceramide levels would be locally elevated and might induce a set of host cell responses to support host-pathogen communication (Ogretmen & Hannun, 2004, Maceyka & Spiegel, 2014). However, since membranes of chlamydial EBs are surrounded by an additional layer of lipopolysaccharide, this layer would have to be removed to allow direct contact between EB membranes and the host cell (Nurminen *et al.*, 1985, Brade *et al.*, 1986). It is therefore more likely, that sphingolipids and especially ceramides are incorporated to improve EB membrane stability, a mechanism used by a number of capsulated viruses (Brugger *et al.*, 2000, Polozov *et al.*, 2008). This proposed higher degree of membrane stability would be convenient for the pathogen to exist and survive in its natural avian hosts that, due to body temperatures of around 40 °C, have other membrane requirements (Brugger *et al.*, 2000, Polozov *et al.*, 2008, Zungu *et al.*, 2013). Moreover, sphingolipid rich membrane domains might provide defined areas for the arrangement and organization of bacterial virulence factors like the T3SS. The observed differences in sphingolipid composition of *C. psittaci* and *C. trachomatis* EBs might therefore reflect the high variability of species-specific virulence factors and membrane proteins that accomplish distinct purposes during infection. Accordingly, distnct membrane proteins that mediate EB-EB contact or communication might be species-specifically enriched in *C. trachomatis* or *C. psittaci* membranes. These specific membrane properties might be correlated with the electron microscopic observations showing separated *C. trachomatis* EBs in contrast to grape-like accumulations of *C. psittaci* EBs (Figure 3.23).

The length of the acyl chain N-terminally attached to a sphingolipid might moreover provide information about lipid properties and transportation routes (Koivusalo *et al.*, 2007, Shaner *et al.*, 2009, Grosch *et al.*, 2012). Hence, if *Chlamydia* spp. contain distinct types of sphingolipids was addressed in the following. Comparisons of the fatty acid composition of sphingomyelins in *C. psittaci* and *C. trachomatis* EBs revealed species-specific sphingomyelin compositions where more sphingomyelins with long acyl chains were found in *C. psittaci* than in *C. trachomatis* (Figure 3.24). Species-specific sphingomyelin composition might on the one hand reflect differences in membrane composition, size and stability that characterize the human and the zoonotic pathogens. The accumulation of sphingomyelins with relatively long acyl chains would thereby improve membrane stability and for example allow existence in different cells or environments including aerosols. Species-specific accumulation of sphingomyelins on the other hand also reveal information about the sphingomyelin routes targeted by *Chlamydia* spp. Sphingomyelins with less than 22 carbon atoms are preferentially trafficked by CERT dependent transport, while longer acyl chains would be provided by vesicular or recycling routes (Kumagai *et*

al., 2005, Kudo *et al.*, 2008). Previous results indicated that *C. psittaci* strongly relies on CERT function and although ceramides with acyl chains from C14 to C22 are favored they are not exclusively found within EBs. The zoonotic pathogen actually tended to accumulate more sphingomyelins with longer acyl chains than *C. trachomatis* even though fewer interactions with vesicular sphigolipid transport routes have been proposed. To determine how respective trafficking routes contribute to the chlamydial sphingolipid composition, comparative studies using inhibitors, in particular HPA-12, could be performed in the future. Long chain sphingolipids, however, not necessarily originate from the host cell. Ceramides transported by CERT might be predominantly acquired by *Chlamydia* spp. and, inside the inclusion, might serve as precursors for *Chlamydia*-dependent processing, modification or extension. Also autonomous sphingolipid synthesis by *C. psittaci* or *C. trachomatis* could be considered. So far, relevant chlamydial enzymes such as fatty acid synthases, N-acyl transfereases or elongases have rarely been described and have for a long time thought to be nonexistent (Stephens *et al.*, 1998). Just recently, the genes for autonomous phospholipid synthesis in *C. trachomatis* have been identified (Yao *et al.*, 2014, Yao *et al.*, 2015). This knowledge might soon be extended to other *Chlamydia* spp. and lipid classes, which might open new perspectives in *Chlamydia*-related lipid research.

Using mass spectrometry to perform quantitative sphingolipid analyses has major sensitivity advantage towards other methods like thin layer chromatography, but also involves some limitations. Here, for all quantitative analyses internal lipid standards not present in endogenous membrane extracts were introduced in sample extracts. If these standard lipids are in contrast present in bacterial membranes is not known. Also the detection of shorter, longer or exotic sphingolipids would need the introduction of additional standards and controls. Due to the highly sensitivity of measurements contaminations of purified EBs with host cell components, that would affect data quality, cannot completely be excluded. In the applied protocol, sample puritiy, and separation of EBs and RBs was monitored by negative stain electron microscopy. Beside electron microscopy additional validation steps that consider host cell (membrane)-proteins could provide further information about possible contaminations. However, as inclusion membranes resemble host cell membranes and uptake of selected host proteins into the inclusion and to bacteria have been reported, it would still be hard to seize a distinction between host and chlamydial origins (Hatch, 1996, Hatch & McClarty, 1998, Capmany & Damiani, 2010, Dumoux *et al.*, 2012). Furthermore, expected protein amounts are very low and highly specific antibodies for protein detection by Western Blot analysis or ELISA would be needed that especially for *C. psittaci* are rarely available yet. To reduce or even exclude the background of EB-associated host cell sphingolipids an additional detergent washing steps, as proposed by Yao and colleagues, could be introduced in the workflow (Yao *et al.*, 2015). Nevertheless, since sphingolipids accumulate in detergent resistant membranes alternative biochemical or mechanical approaches to detach host cell membranes would have to be developed (Lingwood & Simons, 2010). Moreover, detergents would

lyse chlamydial EBs, reinfection assays and determination of infectivity would no longer be possible and as a consequence infectivity and sphingolipid content could not directly be associated.

In sum, our study provides for the first time insights into the species-specific sphingolipid composition of two pathogenic *Chlamydia* spp. Together with mechanistic studies of ceramide transportation and its effects on chlamydial infectivity these data emphasize the emerging role of sphingolipids as targets for antichlamydial interventions.

4.5 Conclusion and Outlook

This work could show that *C. trachomatis* infections induce Golgi fragmentation and thereby modify ministack functionality. Impaired *C. trachomatis*-dependent enzyme dynamics found in those ministacks are most likely the reason for previously reported defects in glycoprotein processing. In the course of infection golgin-84 is recruited to inclusions by a process that includes bindings to its N-terminal part and the coiled-coil domain. The recruitment of golgin-84, especially during times of bacterial replication, is important for *C. trachomatis* infections as recruitment might facilitate access to a specific pool of nutrient-rich compartments. Which host and bacterial binding partners of golgin-84 are involved and which content of golgin-84 positive compartments is indeed transferred to inclusions needs further investigations.

Golgi fragmentation is not only induced by *C. trachomatis* but is a hallmark of various chlamydial infections in human cells. Interestingly, phenotypes of Golgi rearrangements were distinct for highly adapted *C. trachomatis* and avian and zoonotic *C. psittaci*. The differences in *C. psittaci*-induced Golgi fragmentation were accompanied by a specific and reduced acquisition of host vesicular markers that primarily participate in retrograde transport. Yet, the interaction with non-vesicular transport of ceramide was particularly conserved in both *Chlamydia* spp.

CERT function, as demonstrated by inhibitor studies, is of particular importance for human and zoonotic *Chlamydia* spp. Here, although CERT was involved in species-specific aspects of chlamydial development, its inhibition ultimately reduced infectivity of both pathogens. Hence, the inhibitory compound HPA-12, which was used to block CERT, not only serves as a valuable tool to define species-specific mechanisms of intracellular pathogens but might be suitable candidate for an anti-pan-chlamydial drug.

Golgi fragmentation and CERT function are two key mechanisms that ensure sphingolipid acquisition by *Chlamydia* spp. Here, quantitative sphingolipid analyses for the first time revealed that *C. trachomatis* and *C. psittaci* EBs contain endogenous sphingolipids. The species-specific sphingolipid compositions clearly differed in quantity and the distribution of sphingolipid classes. These distinct lipid compositions might partially reflect the characteristics that human and zoonotic pathogens need to establish infections in their respective hosts. Which pathways and compartments provide appropriate lipid components and which modifications would affect EB lipid compositions is currently unknown. Future approaches that combine inhibitor studies with quantitative sphingolipids would therefore provide valuable information about the molecular mechanisms behind human and zoonotic chlamydial infections.

In sum this study makes a substantial contribution towards our understanding of species-specific mechanisms that enable *Chlamydia* spp. to establish infections in a human host. It furthermore provides important data that pronounces the emerging role of sphingolipids as targets for antichlamydial interventions.

5 Bibliography

Abdul-Sater AA, Koo E, Hacker G & Ojcius DM (2009) Inflammasome-dependent caspase-1 activation in cervical epithelial cells stimulates growth of the intracellular pathogen Chlamydia trachomatis. *J Biol Chem* **284**: 26789-26796.

Aeberhard L, Banhart S, Fischer M, Jehmlich N, Rose L, Koch S, Laue M, Renard BY, Schmidt F & Heuer D (2015) The Proteome of the Isolated Chlamydia trachomatis Containing Vacuole Reveals a Complex Trafficking Platform Enriched for Retromer Components. *PLoS Pathog* **11**: e1004883.

Agaisse H & Derre I (2014) Expression of the effector protein IncD in Chlamydia trachomatis mediates recruitment of the lipid transfer protein CERT and the endoplasmic reticulum-resident protein VAPB to the inclusion membrane. *Infect Immun* **82**: 2037-2047.

Agaisse H & Derre I (2015) STIM1 Is a Novel Component of ER-Chlamydia trachomatis Inclusion Membrane Contact Sites. *PLoS One* **10**: e0125671.

Allaire PD, Seyed Sadr M, Chaineau M, Seyed Sadr E, Konefal S, Fotouhi M, Maret D, Ritter B, Del Maestro RF & McPherson PS (2013) Interplay between Rab35 and Arf6 controls cargo recycling to coordinate cell adhesion and migration. *J Cell Sci* **126**: 722-731.

Andersen AA & Vanrompay D (2000) Avian chlamydiosis. *Rev Sci Tech* **19**: 396-404.

Appenzeller C, Andersson H, Kappeler F & Hauri HP (1999) The lectin ERGIC-53 is a cargo transport receptor for glycoproteins. *Nat Cell Biol* **1**: 330-334.

Bachert C & Linstedt AD (2013) A sensor of protein O-glycosylation based on sequential processing in the Golgi apparatus. *Traffic* **14**: 47-56.

Banhart S, Saied EM, Martini A, Koch S, Aeberhard L, Madela K, Arenz C & Heuer D (2014) Improved plaque assay identifies a novel anti-Chlamydia ceramide derivative with altered intracellular localization. *Antimicrob Agents Chemother* **58**: 5537-5546.

Bannantine JP, Griffiths RS, Viratyosin W, Brown WJ & Rockey DD (2000) A secondary structure motif predictive of protein localization to the chlamydial inclusion membrane. *Cell Microbiol* **2**: 35-47.

Barr FA & Short B (2003) Golgins in the structure and dynamics of the Golgi apparatus. *Curr Opin Cell Biol* **15**: 405-413.

Barral DC, Cavallari M, McCormick PJ, Garg S, Magee AI, Bonifacino JS, De Libero G & Brenner MB (2008) CD1a and MHC class I follow a similar endocytic recycling pathway. *Traffic* **9**: 1446-1457.

Barry CE, 3rd, Brickman TJ & Hackstadt T (1993) Hc1-mediated effects on DNA structure: a potential regulator of chlamydial development. *Mol Microbiol* **9**: 273-283.

Bascom RA, Srinivasan S & Nussbaum RL (1999) Identification and characterization of golgin-84, a novel Golgi integral membrane protein with a cytoplasmic coiled-coil domain. *J Biol Chem* **274**: 2953-2962.

Bastidas RJ, Elwell CA, Engel JN & Valdivia RH (2013) Chlamydial intracellular survival strategies. *Cold Spring Harb Perspect Med* **3**: a010256.

Baumann NA, Sullivan DP, Ohvo-Rekila H, Simonot C, Pottekat A, Klaassen Z, Beh CT & Menon AK (2005) Transport of newly synthesized sterol to the sterol-enriched plasma membrane occurs via nonvesicular equilibration. *Biochemistry* **44**: 5816-5826.

Beatty WL (2006) Trafficking from CD63-positive late endocytic multivesicular bodies is essential for intracellular development of Chlamydia trachomatis. *J Cell Sci* **119**: 350-359.

Belland RJ, Zhong G, Crane DD, Hogan D, Sturdevant D, Sharma J, Beatty WL & Caldwell HD (2003) Genomic transcriptional profiling of the developmental cycle of Chlamydia trachomatis. *Proc Natl Acad Sci U S A* **100**: 8478-8483.

Ben-Tekaya H, Miura K, Pepperkok R & Hauri HP (2005) Live imaging of bidirectional traffic from the ERGIC. *J Cell Sci* **118**: 357-367.

Berridge MJ (2002) The endoplasmic reticulum: a multifunctional signaling organelle. *Cell Calcium* **32**: 235-249.

Blasi F, Tarsia P & Aliberti S (2009) Chlamydophila pneumoniae. *Clin Microbiol Infect* **15**: 29-35.

Bocker S, Heurich A, Franke C, Monajembashi S, Sachse K, Saluz HP & Hanel F (2014) Chlamydia psittaci inclusion membrane protein IncB associates with host protein Snapin. *Int J Med Microbiol* **304**: 542-553.
Bos JL, Rehmann H & Wittinghofer A (2007) GEFs and GAPs: critical elements in the control of small G proteins. *Cell* **129**: 865-877.
Braakman I & Bulleid NJ (2011) Protein folding and modification in the mammalian endoplasmic reticulum. *Annu Rev Biochem* **80**: 71-99.
Brade L, Schramek S, Schade U & Brade H (1986) Chemical, biological, and immunochemical properties of the Chlamydia psittaci lipopolysaccharide. *Infect Immun* **54**: 568-574.
Brandizzi F & Barlowe C (2013) Organization of the ER-Golgi interface for membrane traffic control. *Nat Rev Mol Cell Biol* **14**: 382-392.
Braukmann M, Sachse K, Jacobsen ID, Westermann M, Menge C, Saluz HP & Berndt A (2012) Distinct intensity of host-pathogen interactions in Chlamydia psittaci- and Chlamydia abortus-infected chicken embryos. *Infect Immun* **80**: 2976-2988.
Brugger B, Sandhoff R, Wegehingel S, Gorgas K, Malsam J, Helms JB, Lehmann WD, Nickel W & Wieland FT (2000) Evidence for segregation of sphingomyelin and cholesterol during formation of COPI-coated vesicles. *J Cell Biol* **151**: 507-518.
Bush RM & Everett KD (2001) Molecular evolution of the Chlamydiaceae. *Int J Syst Evol Microbiol* **51**: 203-220.
BZGA (2014) Wissen der Allgemeinbevölkerung zu sexuell übertragbaren Infektionen (STI). *BZGA, Bundeszentrale für gesundheitliche Aufklärung*.
Cai Q, Lu L, Tian JH, Zhu YB, Qiao H & Sheng ZH (2010) Snapin-regulated late endosomal transport is critical for efficient autophagy-lysosomal function in neurons. *Neuron* **68**: 73-86.
Canton J & Kima PE (2012) Interactions of pathogen-containing compartments with the secretory pathway. *Cell Microbiol* **14**: 1676-1686.
Capmany A & Damiani MT (2010) Chlamydia trachomatis intercepts Golgi-derived sphingolipids through a Rab14-mediated transport required for bacterial development and replication. *PLoS One* **5**: e14084.
Carabeo RA, Mead DJ & Hackstadt T (2003) Golgi-dependent transport of cholesterol to the Chlamydia trachomatis inclusion. *Proc Natl Acad Sci U S A* **100**: 6771-6776.
Carabeo RA, Dooley CA, Grieshaber SS & Hackstadt T (2007) Rac interacts with Abi-1 and WAVE2 to promote an Arp2/3-dependent actin recruitment during chlamydial invasion. *Cell Microbiol* **9**: 2278-2288.
Carter HE, Haines WJ & et al. (1947) Biochemistry of the sphingolipides; preparation of sphingolipides from beef brain and spinal cord. *J Biol Chem* **169**: 77-82.
CDC (2009) Biosafety in Microbiological and Biomedical Laboratories. *CDC, Centers for Disease Control and Prevention* **5**.
Charruyer A, Bell SM, Kawano M, Douangpanya S, Yen TY, Macher BA, Kumagai K, Hanada K, Holleran WM & Uchida Y (2008) Decreased ceramide transport protein (CERT) function alters sphingomyelin production following UVB irradiation. *J Biol Chem* **283**: 16682-16692.
Cheminay C, Mohlenbrink A & Hensel M (2005) Intracellular Salmonella inhibit antigen presentation by dendritic cells. *J Immunol* **174**: 2892-2899.
Chen AL, Johnson KA, Lee JK, Sutterlin C & Tan M (2012) CPAF: a Chlamydial protease in search of an authentic substrate. *PLoS Pathog* **8**: e1002842.
Cheng W, Shivshankar P, Li Z, Chen L, Yeh IT & Zhong G (2008) Caspase-1 contributes to Chlamydia trachomatis-induced upper urogenital tract inflammatory pathologies without affecting the course of infection. *Infect Immun* **76**: 515-522.
Christian JG, Heymann J, Paschen SA, Vier J, Schauenburg L, Rupp J, Meyer TF, Hacker G & Heuer D (2011) Targeting of a chlamydial protease impedes intracellular bacterial growth. *PLoS Pathog* **7**: e1002283.
Clifton DR, Fields KA, Grieshaber SS, Dooley CA, Fischer ER, Mead DJ, Carabeo RA & Hackstadt T (2004) A chlamydial type III translocated protein is tyrosine-phosphorylated at the site of entry and associated with recruitment of actin. *Proc Natl Acad Sci U S A* **101**: 10166-10171.
Colanzi A & Corda D (2007) Mitosis controls the Golgi and the Golgi controls mitosis. *Curr Opin Cell Biol* **19**: 386-393.

Cole NB, Sciaky N, Marotta A, Song J & Lippincott-Schwartz J (1996) Golgi dispersal during microtubule disruption: regeneration of Golgi stacks at peripheral endoplasmic reticulum exit sites. *Mol Biol Cell* **7**: 631-650.
Cole NB, Smith CL, Sciaky N, Terasaki M, Edidin M & Lippincott-Schwartz J (1996) Diffusional mobility of Golgi proteins in membranes of living cells. *Science* **273**: 797-801.
Collingro A, Tischler P, Weinmaier T*, et al.* (2011) Unity in variety--the pan-genome of the Chlamydiae. *Mol Biol Evol* **28**: 3253-3270.
Comer FI & Hart GW (2000) O-Glycosylation of nuclear and cytosolic proteins. Dynamic interplay between O-GlcNAc and O-phosphate. *J Biol Chem* **275**: 29179-29182.
Cortes C, Rzomp KA, Tvinnereim A, Scidmore MA & Wizel B (2007) Chlamydia pneumoniae inclusion membrane protein Cpn0585 interacts with multiple Rab GTPases. *Infect Immun* **75**: 5586-5596.
De Matteis MA & Luini A (2008) Exiting the Golgi complex. *Nat Rev Mol Cell Biol* **9**: 273-284.
Dehoux P, Flores R, Dauga C, Zhong G & Subtil A (2011) Multi-genome identification and characterization of chlamydiae-specific type III secretion substrates: the Inc proteins. *BMC Genomics* **12**: 109.
Delevoye C, Nilges M, Dehoux P, Paumet F, Perrinet S, Dautry-Varsat A & Subtil A (2008) SNARE protein mimicry by an intracellular bacterium. *PLoS Pathog* **4**: e1000022.
Derre I, Swiss R & Agaisse H (2011) The lipid transfer protein CERT interacts with the Chlamydia inclusion protein IncD and participates to ER-Chlamydia inclusion membrane contact sites. *PLoS Pathog* **7**: e1002092.
Derre I, Pypaert M, Dautry-Varsat A & Agaisse H (2007) RNAi screen in Drosophila cells reveals the involvement of the Tom complex in Chlamydia infection. *PLoS Pathog* **3**: 1446-1458.
Diao A, Rahman D, Pappin DJ, Lucocq J & Lowe M (2003) The coiled-coil membrane protein golgin-84 is a novel rab effector required for Golgi ribbon formation. *J Cell Biol* **160**: 201-212.
Dong N, Zhu Y, Lu Q, Hu L, Zheng Y & Shao F (2012) Structurally distinct bacterial TBC-like GAPs link Arf GTPase to Rab1 inactivation to counteract host defenses. *Cell* **150**: 1029-1041.
Dumke R, Schnee C, Pletz MW, Rupp J, Jacobs E, Sachse K, Rohde G & Capnetz Study G (2015) Mycoplasma pneumoniae and Chlamydia spp. infection in community-acquired pneumonia, Germany, 2011-2012. *Emerg Infect Dis* **21**: 426-434.
Dumoux M, Clare DK, Saibil HR & Hayward RD (2012) Chlamydiae assemble a pathogen synapse to hijack the host endoplasmic reticulum. *Traffic* **13**: 1612-1627.
Ellgaard L & Helenius A (2003) Quality control in the endoplasmic reticulum. *Nat Rev Mol Cell Biol* **4**: 181-191.
Elwell CA, Jiang S, Kim JH, Lee A, Wittmann T, Hanada K, Melancon P & Engel JN (2011) Chlamydia trachomatis co-opts GBF1 and CERT to acquire host sphingomyelin for distinct roles during intracellular development. *PLoS Pathog* **7**: e1002198.
Everett KD, Bush RM & Andersen AA (1999) Emended description of the order Chlamydiales, proposal of Parachlamydiaceae fam. nov. and Simkaniaceae fam. nov., each containing one monotypic genus, revised taxonomy of the family Chlamydiaceae, including a new genus and five new species, and standards for the identification of organisms. *Int J Syst Bacteriol* **49 Pt 2**: 415-440.
Eyster CA, Higginson JD, Huebner R, Porat-Shliom N, Weigert R, Wu WW, Shen RF & Donaldson JG (2009) Discovery of new cargo proteins that enter cells through clathrin-independent endocytosis. *Traffic* **10**: 590-599.
Fan T, Lu H, Hu H, Shi L, McClarty GA, Nance DM, Greenberg AH & Zhong G (1998) Inhibition of apoptosis in chlamydia-infected cells: blockade of mitochondrial cytochrome c release and caspase activation. *J Exp Med* **187**: 487-496.
Fayyaz S, Henkel J, Japtok L, Kramer S, Damm G, Seehofer D, Puschel GP & Kleuser B (2014) Involvement of sphingosine 1-phosphate in palmitate-induced insulin resistance of hepatocytes via the S1P2 receptor subtype. *Diabetologia* **57**: 373-382.
Fechtner T, Stallmann S, Moelleken K, Meyer KL & Hegemann JH (2013) Characterization of the interaction between the chlamydial adhesin OmcB and the human host cell. *J Bacteriol* **195**: 5323-5333.

Fiegl D, Kagebein D, Liebler-Tenorio EM, Weisser T, Sens M, Gutjahr M & Knittler MR (2013) Amphisomal route of MHC class I cross-presentation in bacteria-infected dendritic cells. *J Immunol* **190**: 2791-2806.
Fisher DJ, Fernandez RE & Maurelli AT (2013) Chlamydia trachomatis transports NAD via the Npt1 ATP/ADP translocase. *J Bacteriol* **195**: 3381-3386.
Franch-Marro X, Wendler F, Guidato S, Griffith J, Baena-Lopez A, Itasaki N, Maurice MM & Vincent JP (2008) Wingless secretion requires endosome-to-Golgi retrieval of Wntless/Evi/Sprinter by the retromer complex. *Nat Cell Biol* **10**: 170-177.
Fugmann T, Hausser A, Schoffler P, Schmid S, Pfizenmaier K & Olayioye MA (2007) Regulation of secretory transport by protein kinase D-mediated phosphorylation of the ceramide transfer protein. *J Cell Biol* **178**: 15-22.
Fukasawa M, Nishijima M & Hanada K (1999) Genetic evidence for ATP-dependent endoplasmic reticulum-to-Golgi apparatus trafficking of ceramide for sphingomyelin synthesis in Chinese hamster ovary cells. *J Cell Biol* **144**: 673-685.
Gaede W, Reckling KF, Dresenkamp B, Kenklies S, Schubert E, Noack U, Irmscher HM, Ludwig C, Hotzel H & Sachse K (2008) Chlamydophila psittaci infections in humans during an outbreak of psittacosis from poultry in Germany. *Zoonoses Public Health* **55**: 184-188.
Gerard HC, Whittum-Hudson JA, Schumacher HR & Hudson AP (2004) Differential expression of three Chlamydia trachomatis hsp60-encoding genes in active vs. persistent infections. *Microb Pathog* **36**: 35-39.
Gieffers J, Rupp J, Gebert A, Solbach W & Klinger M (2004) First-choice antibiotics at subinhibitory concentrations induce persistence of Chlamydia pneumoniae. *Antimicrob Agents Chemother* **48**: 1402-1405.
Giles DK & Wyrick PB (2008) Trafficking of chlamydial antigens to the endoplasmic reticulum of infected epithelial cells. *Microbes Infect* **10**: 1494-1503.
Giussani P, Colleoni T, Brioschi L, Bassi R, Hanada K, Tettamanti G, Riboni L & Viani P (2008) Ceramide traffic in C6 glioma cells: evidence for CERT-dependent and independent transport from ER to the Golgi apparatus. *Biochim Biophys Acta* **1781**: 40-51.
Grant BD & Donaldson JG (2009) Pathways and mechanisms of endocytic recycling. *Nat Rev Mol Cell Biol* **10**: 597-608.
Grayston JT (2000) Background and current knowledge of Chlamydia pneumoniae and atherosclerosis. *J Infect Dis* **181 Suppl 3**: S402-410.
Grayston JT, Belland RJ, Byrne GI, Kuo CC, Schachter J, Stamm WE & Zhong G (2015) Infection with Chlamydia pneumoniae as a cause of coronary heart disease: the hypothesis is still untested. *Pathog Dis* **73**: 1-9.
Grieshaber SS, Grieshaber NA & Hackstadt T (2003) Chlamydia trachomatis uses host cell dynein to traffic to the microtubule-organizing center in a p50 dynamitin-independent process. *J Cell Sci* **116**: 3793-3802.
Griffiths E, Ventresca MS & Gupta RS (2006) BLAST screening of chlamydial genomes to identify signature proteins that are unique for the Chlamydiales, Chlamydiaceae, Chlamydophila and Chlamydia groups of species. *BMC Genomics* **7**: 14.
Grigoriev I, Splinter D, Keijzer N*, et al.* (2007) Rab6 regulates transport and targeting of exocytotic carriers. *Dev Cell* **13**: 305-314.
Grosch S, Schiffmann S & Geisslinger G (2012) Chain length-specific properties of ceramides. *Prog Lipid Res* **51**: 50-62.
Guizetti J, Schermelleh L, Mantler J, Maar S, Poser I, Leonhardt H, Muller-Reichert T & Gerlich DW (2011) Cortical constriction during abscission involves helices of ESCRT-III-dependent filaments. *Science* **331**: 1616-1620.
Guo Y & Linstedt AD (2013) Binding of the vesicle docking protein p115 to the GTPase Rab1b regulates membrane recruitment of the COPI vesicle coat. *Cell Logist* **3**: e27687.
Gupta RS & Griffiths E (2006) Chlamydiae-specific proteins and indels: novel tools for studies. *Trends Microbiol* **14**: 527-535.
Gutierrez-Martin CB, Ojcius DM, Hsia R, Hellio R, Bavoil PM & Dautry-Varsat A (1997) Heparin-mediated inhibition of Chlamydia psittaci adherence to HeLa cells. *Microb Pathog* **22**: 47-57.

Hackstadt T, Scidmore MA & Rockey DD (1995) Lipid metabolism in Chlamydia trachomatis-infected cells: directed trafficking of Golgi-derived sphingolipids to the chlamydial inclusion. *Proc Natl Acad Sci U S A* **92**: 4877-4881.
Hackstadt T, Rockey DD, Heinzen RA & Scidmore MA (1996) Chlamydia trachomatis interrupts an exocytic pathway to acquire endogenously synthesized sphingomyelin in transit from the Golgi apparatus to the plasma membrane. *EMBO J* **15**: 964-977.
Hackstadt T, Scidmore-Carlson MA, Shaw EI & Fischer ER (1999) The Chlamydia trachomatis IncA protein is required for homotypic vesicle fusion. *Cell Microbiol* **1**: 119-130.
Halter D, Neumann S, van Dijk SM, Wolthoorn J, de Maziere AM, Vieira OV, Mattjus P, Klumperman J, van Meer G & Sprong H (2007) Pre- and post-Golgi translocation of glucosylceramide in glycosphingolipid synthesis. *J Cell Biol* **179**: 101-115.
Haltiwanger RS, Busby S, Grove K, Li S, Mason D, Medina L, Moloney D, Philipsberg G & Scartozzi R (1997) O-glycosylation of nuclear and cytoplasmic proteins: regulation analogous to phosphorylation? *Biochem Biophys Res Commun* **231**: 237-242.
Hanada K (2005) Sphingolipids in infectious diseases. *Jpn J Infect Dis* **58**: 131-148.
Hanada K, Kumagai K, Yasuda S, Miura Y, Kawano M, Fukasawa M & Nishijima M (2003) Molecular machinery for non-vesicular trafficking of ceramide. *Nature* **426**: 803-809.
Hannun YA & Obeid LM (2008) Principles of bioactive lipid signalling: lessons from sphingolipids. *Nat Rev Mol Cell Biol* **9**: 139-150.
Hartley JC, Stevenson S, Robinson AJ, Littlewood JD, Carder C, Cartledge J, Clark C & Ridgway GL (2001) Conjunctivitis due to Chlamydophila felis (Chlamydia psittaci feline pneumonitis agent) acquired from a cat: case report with molecular characterization of isolates from the patient and cat. *J Infect* **43**: 7-11.
Hatch GM & McClarty G (1998) Phospholipid composition of purified Chlamydia trachomatis mimics that of the eucaryotic host cell. *Infect Immun* **66**: 3727-3735.
Hatch TP (1996) Disulfide cross-linked envelope proteins: the functional equivalent of peptidoglycan in chlamydiae? *J Bacteriol* **178**: 1-5.
Hatch TP, Miceli M & Sublett JE (1986) Synthesis of disulfide-bonded outer membrane proteins during the developmental cycle of Chlamydia psittaci and Chlamydia trachomatis. *J Bacteriol* **165**: 379-385.
Helle SC, Kanfer G, Kolar K, Lang A, Michel AH & Kornmann B (2013) Organization and function of membrane contact sites. *Biochim Biophys Acta* **1833**: 2526-2541.
Herweg JA, Pons V, Becher D, Hecker M, Krohne G, Barbier J, Berger H, Rudel T & Mehlitz A (2015) Proteomic analysis of the Simkania-containing vacuole: the central role of retrograde transport. *Mol Microbiol*.
Heuer D, Rejman Lipinski A, Machuy N, Karlas A, Wehrens A, Siedler F, Brinkmann V & Meyer TF (2009) Chlamydia causes fragmentation of the Golgi compartment to ensure reproduction. *Nature* **457**: 731-735.
Heymann J, Rejman Lipinski A, Bauer B, Meyer TF & Heuer D (2013) Chlamydia trachomatis infection prevents front-rear polarity of migrating HeLa cells. *Cell Microbiol* **15**: 1059-1069.
Hilbi H & Haas A (2012) Secretive bacterial pathogens and the secretory pathway. *Traffic* **13**: 1187-1197.
Hoffmann C, Finsel I, Otto A, Pfaffinger G, Rothmeier E, Hecker M, Becher D & Hilbi H (2014) Functional analysis of novel Rab GTPases identified in the proteome of purified Legionella-containing vacuoles from macrophages. *Cell Microbiol* **16**: 1034-1052.
Horn M, Collingro A, Schmitz-Esser S*, et al.* (2004) Illuminating the evolutionary history of chlamydiae. *Science* **304**: 728-730.
Hsu C, Morohashi Y, Yoshimura S*, et al.* (2010) Regulation of exosome secretion by Rab35 and its GTPase-activating proteins TBC1D10A-C. *J Cell Biol* **189**: 223-232.
Hu W, Xu R, Zhang G, Jin J, Szulc ZM, Bielawski J, Hannun YA, Obeid LM & Mao C (2005) Golgi fragmentation is associated with ceramide-induced cellular effects. *Mol Biol Cell* **16**: 1555-1567.
Huitema K, van den Dikkenberg J, Brouwers JF & Holthuis JC (2004) Identification of a family of animal sphingomyelin synthases. *EMBO J* **23**: 33-44.
Hwang C, Sinskey AJ & Lodish HF (1992) Oxidized redox state of glutathione in the endoplasmic reticulum. *Science* **257**: 1496-1502.

Hybiske K & Stephens RS (2007) Mechanisms of Chlamydia trachomatis entry into nonphagocytic cells. *Infect Immun* **75**: 3925-3934.
Hybiske K & Stephens RS (2007) Mechanisms of host cell exit by the intracellular bacterium Chlamydia. *Proc Natl Acad Sci U S A* **104**: 11430-11435.
Ingmundson A, Delprato A, Lambright DG & Roy CR (2007) Legionella pneumophila proteins that regulate Rab1 membrane cycling. *Nature* **450**: 365-369.
Jewett TJ, Fischer ER, Mead DJ & Hackstadt T (2006) Chlamydial TARP is a bacterial nucleator of actin. *Proc Natl Acad Sci U S A* **103**: 15599-15604.
Johnson KA, Lee JK, Chen AL, Tan M & Sutterlin C (2015) Induction and inhibition of CPAF activity during analysis of Chlamydia-infected cells. *Pathog Dis* **73**: 1-8.
Kagan JC & Roy CR (2002) Legionella phagosomes intercept vesicular traffic from endoplasmic reticulum exit sites. *Nat Cell Biol* **4**: 945-954.
Kagebein D, Gutjahr M, Grosse C, Vogel AB, Rodel J & Knittler MR (2014) Chlamydia trachomatis-infected epithelial cells and fibroblasts retain the ability to express surface-presented major histocompatibility complex class I molecules. *Infect Immun* **82**: 993-1006.
Kalman S, Mitchell W, Marathe R, Lammel C, Fan J, Hyman RW, Olinger L, Grimwood J, Davis RW & Stephens RS (1999) Comparative genomes of Chlamydia pneumoniae and C. trachomatis. *Nat Genet* **21**: 385-389.
Kanerva K, Uronen RL, Blom T, Li S, Bittman R, Lappalainen P, Peranen J, Raposo G & Ikonen E (2013) LDL cholesterol recycles to the plasma membrane via a Rab8a-Myosin5b-actin-dependent membrane transport route. *Dev Cell* **27**: 249-262.
Kawano M, Kumagai K, Nishijima M & Hanada K (2006) Efficient trafficking of ceramide from the endoplasmic reticulum to the Golgi apparatus requires a VAMP-associated protein-interacting FFAT motif of CERT. *J Biol Chem* **281**: 30279-30288.
Kim PS & Arvan P (1995) Calnexin and BiP act as sequential molecular chaperones during thyroglobulin folding in the endoplasmic reticulum. *J Cell Biol* **128**: 29-38.
Klumperman J (2011) Architecture of the mammalian Golgi. *Cold Spring Harb Perspect Biol* **3**.
Knittler MR & Sachse K (2015) Chlamydia psittaci: update on an underestimated zoonotic agent. *Pathog Dis* **73**: 1-15.
Knittler MR, Berndt A, Bocker S*, et al.* (2014) Chlamydia psittaci: new insights into genomic diversity, clinical pathology, host-pathogen interaction and anti-bacterial immunity. *Int J Med Microbiol* **304**: 877-893.
Knop M, Aareskjold E, Bode G & Gerke V (2004) Rab3D and annexin A2 play a role in regulated secretion of vWF, but not tPA, from endothelial cells. *EMBO J* **23**: 2982-2992.
Kogel T & Gerdes HH (2010) Roles of myosin Va and Rab3D in membrane remodeling of immature secretory granules. *Cell Mol Neurobiol* **30**: 1303-1308.
Kogel T, Rudolf R, Hodneland E, Copier J, Regazzi R, Tooze SA & Gerdes HH (2013) Rab3D is critical for secretory granule maturation in PC12 cells. *PLoS One* **8**: e57321.
Koivusalo M, Jansen M, Somerharju P & Ikonen E (2007) Endocytic trafficking of sphingomyelin depends on its acyl chain length. *Mol Biol Cell* **18**: 5113-5123.
Kudo N, Kumagai K, Matsubara R, Kobayashi S, Hanada K, Wakatsuki S & Kato R (2010) Crystal structures of the CERT START domain with inhibitors provide insights into the mechanism of ceramide transfer. *J Mol Biol* **396**: 245-251.
Kudo N, Kumagai K, Tomishige N, Yamaji T, Wakatsuki S, Nishijima M, Hanada K & Kato R (2008) Structural basis for specific lipid recognition by CERT responsible for nonvesicular trafficking of ceramide. *Proc Natl Acad Sci U S A* **105**: 488-493.
Kumagai K, Yasuda S, Okemoto K, Nishijima M, Kobayashi S & Hanada K (2005) CERT mediates intermembrane transfer of various molecular species of ceramides. *J Biol Chem* **280**: 6488-6495.
Kumar Y, Cocchiaro J & Valdivia RH (2006) The obligate intracellular pathogen Chlamydia trachomatis targets host lipid droplets. *Curr Biol* **16**: 1646-1651.
Lavieu G, Zheng H & Rothman JE (2013) Stapled Golgi cisternae remain in place as cargo passes through the stack. *Elife* **2**: e00558.
Levine T (2004) Short-range intracellular trafficking of small molecules across endoplasmic reticulum junctions. *Trends Cell Biol* **14**: 483-490.

Levine T & Loewen C (2006) Inter-organelle membrane contact sites: through a glass, darkly. *Curr Opin Cell Biol* **18**: 371-378.
Liechti GW, Kuru E, Hall E, Kalinda A, Brun YV, VanNieuwenhze M & Maurelli AT (2014) A new metabolic cell-wall labelling method reveals peptidoglycan in Chlamydia trachomatis. *Nature* **506**: 507-510.
Lienard J, Croxatto A, Aeby S, Jaton K, Posfay-Barbe K, Gervaix A & Greub G (2011) Development of a new chlamydiales-specific real-time PCR and its application to respiratory clinical samples. *J Clin Microbiol* **49**: 2637-2642.
Lingwood D & Simons K (2010) Lipid rafts as a membrane-organizing principle. *Science* **327**: 46-50.
Liou J, Fivaz M, Inoue T & Meyer T (2007) Live-cell imaging reveals sequential oligomerization and local plasma membrane targeting of stromal interaction molecule 1 after Ca2+ store depletion. *Proc Natl Acad Sci U S A* **104**: 9301-9306.
Longbottom D & Coulter LJ (2003) Animal chlamydioses and zoonotic implications. *J Comp Pathol* **128**: 217-244.
Lu H, Shen C & Brunham RC (2000) Chlamydia trachomatis infection of epithelial cells induces the activation of caspase-1 and release of mature IL-18. *J Immunol* **165**: 1463-1469.
Lu L, Cai Q, Tian JH & Sheng ZH (2009) Snapin associates with late endocytic compartments and interacts with late endosomal SNAREs. *Biosci Rep* **29**: 261-269.
Lutter EI, Martens C & Hackstadt T (2012) Evolution and conservation of predicted inclusion membrane proteins in chlamydiae. *Comp Funct Genomics* **2012**: 362104.
Maceyka M & Spiegel S (2014) Sphingolipid metabolites in inflammatory disease. *Nature* **510**: 58-67.
Malsam J, Satoh A, Pelletier L & Warren G (2005) Golgin tethers define subpopulations of COPI vesicles. *Science* **307**: 1095-1098.
Manire GP (1966) Structure of purified cell walls of dense forms of meningopneumonitis organisms. *J Bacteriol* **91**: 409-413.
Marra P, Salvatore L, Mironov A, Jr., Di Campli A, Di Tullio G, Trucco A, Beznoussenko G, Mironov A & De Matteis MA (2007) The biogenesis of the Golgi ribbon: the roles of membrane input from the ER and of GM130. *Mol Biol Cell* **18**: 1595-1608.
Martinez O, Antony C, Pehau-Arnaudet G, Berger EG, Salamero J & Goud B (1997) GTP-bound forms of rab6 induce the redistribution of Golgi proteins into the endoplasmic reticulum. *Proc Natl Acad Sci U S A* **94**: 1828-1833.
Matsumoto A & Manire GP (1970) Electron Microscopic Observations on the Fine Structure of Cell Walls of Chlamydia psittaci. *J Bacteriol* **104**: 1332-1337.
Matsumoto A, Bessho H, Uehira K & Suda T (1991) Morphological studies of the association of mitochondria with chlamydial inclusions and the fusion of chlamydial inclusions. *J Electron Microsc (Tokyo)* **40**: 356-363.
McCaffrey MW, Bielli A, Cantalupo G, Mora S, Roberti V, Santillo M, Drummond F & Bucci C (2001) Rab4 affects both recycling and degradative endosomal trafficking. *FEBS Lett* **495**: 21-30.
Mirrashidi KM, Elwell CA, Verschueren E*, et al.* (2015) Global Mapping of the Inc-Human Interactome Reveals that Retromer Restricts Chlamydia Infection. *Cell Host Microbe* **18**: 109-121.
Miserey-Lenkei S, Waharte F, Boulet A*, et al.* (2007) Rab6-interacting protein 1 links Rab6 and Rab11 function. *Traffic* **8**: 1385-1403.
Molinari M, Salio M, Galli C, Norais N, Rappuoli R, Lanzavecchia A & Montecucco C (1998) Selective inhibition of Ii-dependent antigen presentation by Helicobacter pylori toxin VacA. *J Exp Med* **187**: 135-140.
Monier S, Jollivet F, Janoueix-Lerosey I, Johannes L & Goud B (2002) Characterization of novel Rab6-interacting proteins involved in endosome-to-TGN transport. *Traffic* **3**: 289-297.
Moon JJ, Matsumoto M, Patel S, Lee L, Guan JL & Li S (2005) Role of cell surface heparan sulfate proteoglycans in endothelial cell migration and mechanotransduction. *J Cell Physiol* **203**: 166-176.
Moore ER, Fischer ER, Mead DJ & Hackstadt T (2008) The chlamydial inclusion preferentially intercepts basolaterally directed sphingomyelin-containing exocytic vacuoles. *Traffic* **9**: 2130-2140.

Moorhead AM, Jung JY, Smirnov A, Kaufer S & Scidmore MA (2010) Multiple host proteins that function in phosphatidylinositol-4-phosphate metabolism are recruited to the chlamydial inclusion. *Infect Immun* **78**: 1990-2007.
Moulder JW (1966) The relation of the psittacosis group (Chlamydiae) to bacteria and viruses. *Annu Rev Microbiol* **20**: 107-130.
Mounier J, Boncompain G, Senerovic L, Lagache T, Chretien F, Perez F, Kolbe M, Olivo-Marin JC, Sansonetti PJ & Sauvonnet N (2012) Shigella effector IpaB-induced cholesterol relocation disrupts the Golgi complex and recycling network to inhibit host cell secretion. *Cell Host Microbe* **12**: 381-389.
Mukherjee S, Chiu R, Leung SM & Shields D (2007) Fragmentation of the Golgi apparatus: an early apoptotic event independent of the cytoskeleton. *Traffic* **8**: 369-378.
Munro S (2011) The golgin coiled-coil proteins of the Golgi apparatus. *Cold Spring Harb Perspect Biol* **3**.
Myers GS, Mathews SA, Eppinger M*, et al.* (2009) Evidence that human Chlamydia pneumoniae was zoonotically acquired. *J Bacteriol* **191**: 7225-7233.
Naik E & Dixit VM (2011) Mitochondrial reactive oxygen species drive proinflammatory cytokine production. *J Exp Med* **208**: 417-420.
Nakamura Y, Matsubara R, Kitagawa H, Kobayashi S, Kumagai K, Yasuda S & Hanada K (2003) Stereoselective synthesis and structure-activity relationship of novel ceramide trafficking inhibitors. (1R,3R)-N-(3-hydroxy-1-hydroxymethyl-3-phenylpropyl)dodecanamide and its analogues. *J Med Chem* **46**: 3688-3695.
Nans A, Saibil HR & Hayward RD (2014) Pathogen-host reorganization during Chlamydia invasion revealed by cryo-electron tomography. *Cell Microbiol* **16**: 1457-1472.
Neefjes J & Sadaka C (2012) Into the intracellular logistics of cross-presentation. *Front Immunol* **3**: 31.
Newhall WJt, Terho P, Wilde CE, 3rd, Batteiger BE & Jones RB (1986) Serovar determination of Chlamydia trachomatis isolates by using type-specific monoclonal antibodies. *J Clin Microbiol* **23**: 333-338.
Nicholson TL, Olinger L, Chong K, Schoolnik G & Stephens RS (2003) Global stage-specific gene regulation during the developmental cycle of Chlamydia trachomatis. *J Bacteriol* **185**: 3179-3189.
Niemela PS, Hyvonen MT & Vattulainen I (2006) Influence of chain length and unsaturation on sphingomyelin bilayers. *Biophys J* **90**: 851-863.
Nurminen M, Rietschel ET & Brade H (1985) Chemical characterization of Chlamydia trachomatis lipopolysaccharide. *Infect Immun* **48**: 573-575.
Ogretmen B & Hannun YA (2004) Biologically active sphingolipids in cancer pathogenesis and treatment. *Nat Rev Cancer* **4**: 604-616.
Ouellette SP, Dorsey FC, Moshiach S, Cleveland JL & Carabeo RA (2011) Chlamydia species-dependent differences in the growth requirement for lysosomes. *PLoS One* **6**: e16783.
Page LA (1966) Interspecies transfer of psittacosis-LGV-trachoma agents: pathogenicity of two avian and two mammalian strains for eight species of birds and mammals. *Am J Vet Res* **27**: 397-407.
Palfy M, Remenyi A & Korcsmaros T (2012) Endosomal crosstalk: meeting points for signaling pathways. *Trends Cell Biol* **22**: 447-456.
Pellinen T, Arjonen A, Vuoriluoto K, Kallio K, Fransen JA & Ivaska J (2006) Small GTPase Rab21 regulates cell adhesion and controls endosomal traffic of beta1-integrins. *J Cell Biol* **173**: 767-780.
Pellinen T, Tuomi S, Arjonen A*, et al.* (2008) Integrin trafficking regulated by Rab21 is necessary for cytokinesis. *Dev Cell* **15**: 371-385.
Pewzner-Jung Y, Tavakoli Tabazavareh S, Grassme H*, et al.* (2014) Sphingoid long chain bases prevent lung infection by Pseudomonas aeruginosa. *EMBO Mol Med* **6**: 1205-1214.
Pfeffer SR (2009) Multiple routes of protein transport from endosomes to the trans Golgi network. *FEBS Lett* **583**: 3811-3816.
Pilhofer M, Aistleitner K, Ladinsky MS, Konig L, Horn M & Jensen GJ (2014) Architecture and host interface of environmental chlamydiae revealed by electron cryotomography. *Environ Microbiol* **16**: 417-429.

Piper RC & Luzio JP (2001) Late endosomes: sorting and partitioning in multivesicular bodies. *Traffic* **2**: 612-621.
Piraino F (1969) Plaque formation in chick embryo fibroblast cells by Chlamydia isolated from avian and mammalian sources. *J Bacteriol* **98**: 475-480.
Pokrovskaya ID, Szwedo JW, Goodwin A, Lupashina TV, Nagarajan UM & Lupashin VV (2012) Chlamydia trachomatis hijacks intra-Golgi COG complex-dependent vesicle trafficking pathway. *Cell Microbiol* **14**: 656-668.
Polozov IV, Bezrukov L, Gawrisch K & Zimmerberg J (2008) Progressive ordering with decreasing temperature of the phospholipids of influenza virus. *Nat Chem Biol* **4**: 248-255.
Powelka AM, Sun J, Li J, Gao M, Shaw LM, Sonnenberg A & Hsu VW (2004) Stimulation-dependent recycling of integrin beta1 regulated by ARF6 and Rab11. *Traffic* **5**: 20-36.
Puthenveedu MA, Bachert C, Puri S, Lanni F & Linstedt AD (2006) GM130 and GRASP65-dependent lateral cisternal fusion allows uniform Golgi-enzyme distribution. *Nat Cell Biol* **8**: 238-248.
Raposo G & Stoorvogel W (2013) Extracellular vesicles: exosomes, microvesicles, and friends. *J Cell Biol* **200**: 373-383.
Rasmussen-Lathrop SJ, Koshiyama K, Phillips N & Stephens RS (2000) Chlamydia-dependent biosynthesis of a heparan sulphate-like compound in eukaryotic cells. *Cell Microbiol* **2**: 137-144.
Raulston JE (1997) Response of Chlamydia trachomatis serovar E to iron restriction in vitro and evidence for iron-regulated chlamydial proteins. *Infect Immun* **65**: 4539-4547.
Rejman Lipinski A, Heymann J, Meissner C, Karlas A, Brinkmann V, Meyer TF & Heuer D (2009) Rab6 and Rab11 regulate Chlamydia trachomatis development and golgin-84-dependent Golgi fragmentation. *PLoS Pathog* **5**: e1000615.
Richards TS, Knowlton AE & Grieshaber SS (2013) Chlamydia trachomatis homotypic inclusion fusion is promoted by host microtubule trafficking. *BMC Microbiol* **13**: 185.
Rockey DD, Fischer ER & Hackstadt T (1996) Temporal analysis of the developing Chlamydia psittaci inclusion by use of fluorescence and electron microscopy. *Infect Immun* **64**: 4269-4278.
Roy CR, Salcedo SP & Gorvel JP (2006) Pathogen-endoplasmic-reticulum interactions: in through the out door. *Nat Rev Immunol* **6**: 136-147.
Ruwisch L, Schafer-Korting M & Kleuser B (2001) An improved high-performance liquid chromatographic method for the determination of sphingosine-1-phosphate in complex biological materials. *Naunyn Schmiedebergs Arch Pharmacol* **363**: 358-363.
Rzomp KA, Moorhead AR & Scidmore MA (2006) The GTPase Rab4 interacts with Chlamydia trachomatis inclusion membrane protein CT229. *Infect Immun* **74**: 5362-5373.
Rzomp KA, Scholtes LD, Briggs BJ, Whittaker GR & Scidmore MA (2003) Rab GTPases are recruited to chlamydial inclusions in both a species-dependent and species-independent manner. *Infect Immun* **71**: 5855-5870.
Sachse K, Bavoil PM, Kaltenboeck B, Stephens RS, Kuo CC, Rossello-Mora R & Horn M (2015) Emendation of the family Chlamydiaceae: proposal of a single genus, Chlamydia, to include all currently recognized species. *Syst Appl Microbiol* **38**: 99-103.
Saied EM, Diederich S & Arenz C (2014) Facile synthesis of the CERT inhibitor HPA-12 and some novel derivatives. *Chem Asian J* **9**: 2092-2094.
Salaun C, James DJ & Chamberlain LH (2004) Lipid rafts and the regulation of exocytosis. *Traffic* **5**: 255-264.
Santos C, Fleury L, Rodriguez F, Markus J, Berkes D, Daich A, Ausseil F, Baudoin-Dehoux C, Ballereau S & Genisson Y (2015) The CERT antagonist HPA-12: first practical synthesis and individual binding evaluation of the four stereoisomers. *Bioorg Med Chem* **23**: 2004-2009.
Satoh A, Wang Y, Malsam J, Beard MB & Warren G (2003) Golgin-84 is a rab1 binding partner involved in Golgi structure. *Traffic* **4**: 153-161.
Schachter J, Stephens RS, Timms P*, et al.* (2001) Radical changes to chlamydial taxonomy are not necessary just yet. *Int J Syst Evol Microbiol* **51**: 249; author reply 251-243.
Schofl G, Voigt A, Litsche K, Sachse K & Saluz HP (2011) Complete genome sequences of four mammalian isolates of Chlamydophila psittaci. *J Bacteriol* **193**: 4258.
Scidmore MA, Fischer ER & Hackstadt T (1996) Sphingolipids and glycoproteins are differentially trafficked to the Chlamydia trachomatis inclusion. *J Cell Biol* **134**: 363-374.

Scidmore MA, Fischer ER & Hackstadt T (2003) Restricted fusion of Chlamydia trachomatis vesicles with endocytic compartments during the initial stages of infection. *Infect Immun* **71**: 973-984.
Seemann J, Jokitalo E, Pypaert M & Warren G (2000) Matrix proteins can generate the higher order architecture of the Golgi apparatus. *Nature* **407**: 1022-1026.
Seto S, Tsujimura K & Koide Y (2011) Rab GTPases regulating phagosome maturation are differentially recruited to mycobacterial phagosomes. *Traffic* **12**: 407-420.
Shaner RL, Allegood JC, Park H, Wang E, Kelly S, Haynes CA, Sullards MC & Merrill AH, Jr. (2009) Quantitative analysis of sphingolipids for lipidomics using triple quadrupole and quadrupole linear ion trap mass spectrometers. *J Lipid Res* **50**: 1692-1707.
Shaw AC, Vandahl BB, Larsen MR, Roepstorff P, Gevaert K, Vandekerckhove J, Christiansen G & Birkelund S (2002) Characterization of a secreted Chlamydia protease. *Cell Microbiol* **4**: 411-424.
Shima K, Klinger M, Schutze S, Kaufhold I, Solbach W, Reiling N & Rupp J (2015) The role of endoplasmic reticulum-related BiP/GRP78 in interferon gamma-induced persistent Chlamydia pneumoniae infection. *Cell Microbiol* **17**: 923-934.
Short B, Haas A & Barr FA (2005) Golgins and GTPases, giving identity and structure to the Golgi apparatus. *Biochim Biophys Acta* **1744**: 383-395.
Simpson JC, Griffiths G, Wessling-Resnick M, Fransen JA, Bennett H & Jones AT (2004) A role for the small GTPase Rab21 in the early endocytic pathway. *J Cell Sci* **117**: 6297-6311.
Sinka R, Gillingham AK, Kondylis V & Munro S (2008) Golgi coiled-coil proteins contain multiple binding sites for Rab family G proteins. *J Cell Biol* **183**: 607-615.
Snavely EA, Kokes M, Dunn JD, Saka HA, Nguyen BD, Bastidas RJ, McCafferty DG & Valdivia RH (2014) Reassessing the role of the secreted protease CPAF in Chlamydia trachomatis infection through genetic approaches. *Pathog Dis* **71**: 336-351.
Sohda M, Misumi Y, Yamamoto A, Nakamura N, Ogata S, Sakisaka S, Hirose S, Ikehara Y & Oda K (2010) Interaction of Golgin-84 with the COG complex mediates the intra-Golgi retrograde transport. *Traffic* **11**: 1552-1566.
Sohda M, Misumi Y, Yoshimura S, Nakamura N, Fusano T, Sakisaka S, Ogata S, Fujimoto J, Kiyokawa N & Ikehara Y (2005) Depletion of vesicle-tethering factor p115 causes mini-stacked Golgi fragments with delayed protein transport. *Biochem Biophys Res Commun* **338**: 1268-1274.
Sonnichsen B, De Renzis S, Nielsen E, Rietdorf J & Zerial M (2000) Distinct membrane domains on endosomes in the recycling pathway visualized by multicolor imaging of Rab4, Rab5, and Rab11. *J Cell Biol* **149**: 901-914.
Spears P & Storz J (1979) Biotyping of Chlamydia psittaci based on inclusion morphology and response to diethylaminoethyl-dextran and cycloheximide. *Infect Immun* **24**: 224-232.
Stenger S, Niazi KR & Modlin RL (1998) Down-regulation of CD1 on antigen-presenting cells by infection with Mycobacterium tuberculosis. *J Immunol* **161**: 3582-3588.
Stephens RS, Poteralski JM & Olinger L (2006) Interaction of Chlamydia trachomatis with mammalian cells is independent of host cell surface heparan sulfate glycosaminoglycans. *Infect Immun* **74**: 1795-1799.
Stephens RS, Myers G, Eppinger M & Bavoil PM (2009) Divergence without difference: phylogenetics and taxonomy of Chlamydia resolved. *FEMS Immunol Med Microbiol* **55**: 115-119.
Stephens RS, Kalman S, Lammel C*, et al.* (1998) Genome sequence of an obligate intracellular pathogen of humans: Chlamydia trachomatis. *Science* **282**: 754-759.
Su H, Raymond L, Rockey DD, Fischer E, Hackstadt T & Caldwell HD (1996) A recombinant Chlamydia trachomatis major outer membrane protein binds to heparan sulfate receptors on epithelial cells. *Proc Natl Acad Sci U S A* **93**: 11143-11148.
Su H, McClarty G, Dong F, Hatch GM, Pan ZK & Zhong G (2004) Activation of Raf/MEK/ERK/cPLA2 signaling pathway is essential for chlamydial acquisition of host glycerophospholipids. *J Biol Chem* **279**: 9409-9416.
Subtil A, Parsot C & Dautry-Varsat A (2001) Secretion of predicted Inc proteins of Chlamydia pneumoniae by a heterologous type III machinery. *Mol Microbiol* **39**: 792-800.
Tafesse FG, Huitema K, Hermansson M, van der Poel S, van den Dikkenberg J, Uphoff A, Somerharju P & Holthuis JC (2007) Both sphingomyelin synthases SMS1 and SMS2 are required for sphingomyelin homeostasis and growth in human HeLa cells. *J Biol Chem* **282**: 17537-17547.

Tamura A, Matsumoto A & Higashi N (1967) Purification and chemical composition of reticulate bodies of the meningopneumonitis organisms. *J Bacteriol* **93**: 2003-2008.
Thalmann J, Janik K, May M, Sommer K, Ebeling J, Hofmann F, Genth H & Klos A (2010) Actin re-organization induced by Chlamydia trachomatis serovar D--evidence for a critical role of the effector protein CT166 targeting Rac. *PLoS One* **5**: e9887.
Tomishige N, Kumagai K, Kusuda J, Nishijima M & Hanada K (2009) Casein kinase I{gamma}2 down-regulates trafficking of ceramide in the synthesis of sphingomyelin. *Mol Biol Cell* **20**: 348-357.
van der Sluijs P, Hull M, Webster P, Male P, Goud B & Mellman I (1992) The small GTP-binding protein rab4 controls an early sorting event on the endocytic pathway. *Cell* **70**: 729-740.
van Meer G, Voelker DR & Feigenson GW (2008) Membrane lipids: where they are and how they behave. *Nat Rev Mol Cell Biol* **9**: 112-124.
van Ooij C, Apodaca G & Engel J (1997) Characterization of the Chlamydia trachomatis vacuole and its interaction with the host endocytic pathway in HeLa cells. *Infect Immun* **65**: 758-766.
van Ooij C, Kalman L, van I, Nishijima M, Hanada K, Mostov K & Engel JN (2000) Host cell-derived sphingolipids are required for the intracellular growth of Chlamydia trachomatis. *Cell Microbiol* **2**: 627-637.
Vonderheit A & Helenius A (2005) Rab7 associates with early endosomes to mediate sorting and transport of Semliki forest virus to late endosomes. *PLoS Biol* **3**: e233.
Walter P & Ron D (2011) The unfolded protein response: from stress pathway to homeostatic regulation. *Science* **334**: 1081-1086.
Wei JH, Zhang ZC, Wynn RM & Seemann J (2015) GM130 Regulates Golgi-Derived Spindle Assembly by Activating TPX2 and Capturing Microtubules. *Cell* **162**: 287-299.
WHO (2012) Global incidence and prevalence of selected curable sexually transmitted infections – 2008. *WHO Press, World Health Organization, Geneva* 2; 3.
Wolf K & Hackstadt T (2001) Sphingomyelin trafficking in Chlamydia pneumoniae-infected cells. *Cell Microbiol* **3**: 145-152.
Wolfert MA & Boons GJ (2013) Adaptive immune activation: glycosylation does matter. *Nat Chem Biol* **9**: 776-784.
Wong M & Munro S (2014) Membrane trafficking. The specificity of vesicle traffic to the Golgi is encoded in the golgin coiled-coil proteins. *Science* **346**: 1256898.
Wood DO, Wood RR & Tucker AM (2014) Genetic systems for studying obligate intracellular pathogens: an update. *Curr Opin Microbiol* **17**: 11-16.
Wuppermann FN, Hegemann JH & Jantos CA (2001) Heparan sulfate-like glycosaminoglycan is a cellular receptor for Chlamydia pneumoniae. *J Infect Dis* **184**: 181-187.
Yadav S, Puri S & Linstedt AD (2009) A primary role for Golgi positioning in directed secretion, cell polarity, and wound healing. *Mol Biol Cell* **20**: 1728-1736.
Yamaji T & Hanada K (2015) Sphingolipid metabolism and interorganellar transport: localization of sphingolipid enzymes and lipid transfer proteins. *Traffic* **16**: 101-122.
Yao J, Dodson VJ, Frank MW & Rock CO (2015) Chlamydia trachomatis Scavenges Host Fatty Acids for Phospholipid Synthesis via an Acyl-Acyl Carrier Protein Synthetase. *J Biol Chem* **290**: 22163-22173.
Yao J, Cherian PT, Frank MW & Rock CO (2015) Chlamydia trachomatis Relies on Autonomous Phospholipid Synthesis for Membrane Biogenesis. *J Biol Chem* **290**: 18874-18888.
Yao J, Abdelrahman YM, Robertson RM, Cox JV, Belland RJ, White SW & Rock CO (2014) Type II fatty acid synthesis is essential for the replication of Chlamydia trachomatis. *J Biol Chem* **289**: 22365-22376.
Yasuda S, Kitagawa H, Ueno M, Ishitani H, Fukasawa M, Nishijima M, Kobayashi S & Hanada K (2001) A novel inhibitor of ceramide trafficking from the endoplasmic reticulum to the site of sphingomyelin synthesis. *J Biol Chem* **276**: 43994-44002.
Yatomi Y, Ruan F, Ohta J, Welch RJ, Hakomori S & Igarashi Y (1995) Quantitative measurement of sphingosine 1-phosphate in biological samples by acylation with radioactive acetic anhydride. *Anal Biochem* **230**: 315-320.
Ying S, Pettengill M, Ojcius DM & Hacker G (2007) Host-Cell Survival and Death During Chlamydia Infection. *Curr Immunol Rev* **3**: 31-40.

Ying S, Fischer SF, Pettengill M, Conte D, Paschen SA, Ojcius DM & Hacker G (2006) Characterization of host cell death induced by Chlamydia trachomatis. *Infect Immun* **74**: 6057-6066.
Yudowski GA, Puthenveedu MA, Henry AG & von Zastrow M (2009) Cargo-mediated regulation of a rapid Rab4-dependent recycling pathway. *Mol Biol Cell* **20**: 2774-2784.
Zeidler H & Hudson AP (2014) New insights into Chlamydia and arthritis. Promise of a cure? *Ann Rheum Dis* **73**: 637-644.
Zerial M & McBride H (2001) Rab proteins as membrane organizers. *Nat Rev Mol Cell Biol* **2**: 107-117.
Zhang K & Kaufman RJ (2008) From endoplasmic-reticulum stress to the inflammatory response. *Nature* **454**: 455-462.
Zheng L, Baumann U & Reymond JL (2004) An efficient one-step site-directed and site-saturation mutagenesis protocol. *Nucleic Acids Res* **32**: e115.
Zhong G, Liu L, Fan T, Fan P & Ji H (2000) Degradation of transcription factor RFX5 during the inhibition of both constitutive and interferon gamma-inducible major histocompatibility complex class I expression in chlamydia-infected cells. *J Exp Med* **191**: 1525-1534.
Zimmermann P, Zhang Z, Degeest G, Mortier E, Leenaerts I, Coomans C, Schulz J, N'Kuli F, Courtoy PJ & David G (2005) Syndecan recycling [corrected] is controlled by syntenin-PIP2 interaction and Arf6. *Dev Cell* **9**: 377-388.
Zungu MM, Brown M & Downs CT (2013) Seasonal thermoregulation in the burrowing parrot (Cyanoliseus patagonus). *J Therm Biol* **38**: 47-54.

6 Appendix

6.1 Supplementary figure

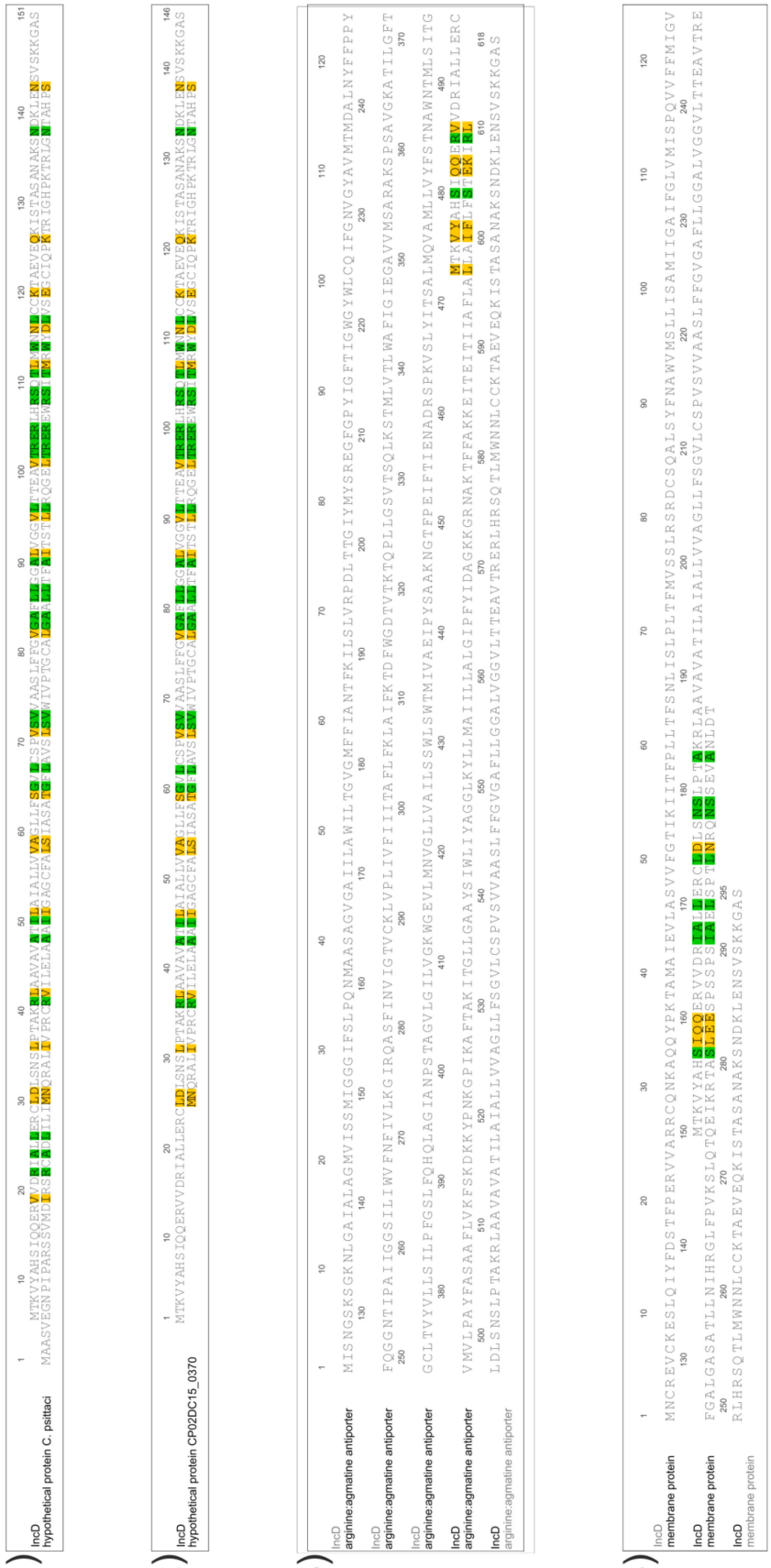

Figure 6.1 *C. trachomatis* IncD shares sparse gene sequence homologies with *C. psittaci*.
Schematic sequence alignment of IncD and hits identified with blast. Sequences were aligned via Geneious multiple alignment, using the cost matrix blosum62. Color codes: green = identical, yellow = similar, white = not similar

6.2 Abbrevations

Table 6.1Abbrevations

Abbreviation	
(E)CFP	(enhanced) cyan fluorescent protein
(E)GFP	(enhanced) green fluorescent protein
(E)YFP	(enhanced) yellow fluorescent protein
(M)OMP	(major) outer membrane protein
.FASTA	File format
aa	Amino acid
AB	aberrant body
ACTB	Actin beta
ADP	Adenosine diphosphate
APS	Ammonium persulfate
ATCC	American Type Culture Collection
ATP	Adenosine triphosphate
BCA	bicinchoninic acid
BFA	Brefeldin A
BLAST	Basic Local Alignment Search Tool
BSA	Bovine serum albumin
BzgA	*'Bundeszentrale für gesundheitliche Aufklärung'*
C_6-NBD-Cer	6-[*N*-(7-nitrobenzo-2-oxa-1,3-diazol-4-yl)amino]caproyl-d-*erythro*-sphingosine
Ca^{2+}	calcium ion
CDC	Centers for Disease Control and Prevention
cDNA	complementary DNA
cer	ceramide
CERT	Ceramide transfer protein
CK1γ2	Casein Kinase Iγ 2
CO_2	carbon dioxide
COG	conserved oligomeric Golgi complex
CPAF	*Chlamydia* protease-like activity factor
DAG	diacylglycerole
DAPI	4',6-diamidino-2-phenylindole
DEAE	diethylaminoethyl
DMEM	Dulbecco's modified Eagle's medium
DMSO	Dimethyl sulfoxide
DNA	Deoxyribonucleic acid

DTT	Dithiothreitol
EB	Elementary body
ECL	Enhanced chemoluminescence
EDTA	(Ethylenedinitrilo)tetraacetic acid
EE	early endosome
ER	Endoplasmic reticulum
ERES	ER exit sites
ERGIC	ER – Golgi intermediate compartment
ESI	electrospray ionization
et al.	et alia
FCS	fetal calf serum
FRAP	Fluorescence Recovery After Photobleaching
FW	forward
G	ghost
GA	Golgi apparatus
GAP	GTPase-activating protein
GCN	genome copy number
GDI	guanosine nucleotide dissociation inhibitor
GEF	guanine nucleotide exchange factor
GM	Golgi matrix (protein)
GMAP	Golgi microtubule-associated protein
GRASP	Golgi reassembly stacking protein
GST	Glutathione S-transferase
GTP	Guanosine triphosphate
H_2O	water
HBS	Hepes buffered saline
HCl	hydrochloric acid
HeLa	Henrietta Lacks
HEPES	4-(2-hydroxyethyl)-1-piperazineethanesulfonic acid
HPA-12	*N*-(3-Hydroxy-1-hydroxymethyl-3-phenylpropyl)dodecanamide
HRP	Horseradish peroxidase
Hsp	Heat shock protein
IC_{50}	half maximal inhibitory concentration
IF	immunofluorescence
IFN- γ	interferon-γ
IFU	inclusion forming units
Inc	Inclusion protein

KCl	potassium chloride
LB	Luria-Bertani
LC-MS/MS	liquid chromatography coupled to tandem mass spectrometry
LCV	*Legionella* containing vacuole
LD	lipid droplet
LDH	lactate dehydrogenase
LE	late endosome
LE	late endosome
LGV	Lymphogranuolma venereum
MCS	membrane contact sites
MHC	Major histocompatibility complex
MOI	multiplicity of infection
MTOC	microtubule organizing center
MVB	multivesicular body
NaCl	sodium chloride
OmcA	Small cystein-rich outer membrane protein A
OmcB	Small cystein-rich outer membrane protein B
P, P(2), P(3)	mono-, bis-, triphosphate
p.i.	post infectionem
PAGE	polyacrylamide gel electrophoresis
PBS	phosphate buffered saline
PC	phosphatiylcholine
PCR	Polymerase chain reaction
PFA	Paraformaldehyde
PH	pleckstrin homology
PI	phosphatidylinositol
PKD	protein kinase D
PM	plasma membrane
Pmp	polymorphic membrane protein
PVDF	polyvinylidene difluoride
PX	phox homology
qPCR	quantitative PCR
Rab	Ras-like protein from rat brain
RB	Reticulate body
RE	recycling endosome
RKI	Robert Koch Institute
RNA	Ribonucleic acid

RNAi	RNA interference
rpm	Revolutions per minute
RPMI	Roswell Park Memorial Institute medium
rRNA	ribosomal RNA
RV	reverse
SDS	sodium dodecyl sulfate
SI	*Le Système international d'unités*
siRNA	short inhbiting RNA
SM	sphingomyelin
SMS	sphingomyelin synthase
SNARE	Soluble NSF attachment factor receptor
SPG	accharose phosphate glutamic acid
spp	species
SR	serine rich domain
START	StAR-related lipid-transfer
T3SS	type three secretion system
Tarp	translocated actin-recruiting phosphoprotein
TBE	Tris/Borate/EDTA
TBS	tris buffered saline
TBS-T	tris buffered saline supplemented with tween
TEM	transmission electron microscopy
TEM	transmission electron microscopy
TEMED	Tetramethylethylenediamine
TGN	trans Golgi network
UTP	Uridine-5'-triphosphate
UV/Vis	ultraviolet/ visible
VAP	vesicle-associated membrane-protein-associated proteins
WB	Western Blot
WHO	World Health Organization
WT	wild type

Table 6.2 Units

Symbol	Name	Unit
µm	micrometer	10^{-6} m
nm	Nanometer	10^{-9} m
A	Absorbance	Relative unit
Da	Dalton	$1.660538921(73)\times10^{-27}$ kg
x g	times gravity (relative centrifugal force)	9.81 m/s^2
h	hour	3600 s
G	gauge	see EN ISO 6009
mg	milli gram	10^{-6} kg
min	minute	60 s
ml	milli liter	10^{-6} m^3
mM	milli molar	mol/m^3
pH	-	$-\log_{10}([H^+])$
RT	room temperature	25 °C (as defined by IUPAC)
S	Svedberg	10^{-13}
V	Volt	SI unit
°C	degree Celsius	SI unit

6.3 List of Figures

6.4 List of Tables

Publications

Articles

The proteome of isolated Chlamydia trachomatis containing vacuole reveals a complex trafficking platform enriched for retromer components.

Lukas Aeberhard , Sebastian Banhart , Martina Fischer, Nico Jehmlich, Laura Rose, Sophia Koch, Michael Laue, Bernhard Y. Renard, Frank Schmidt and Dagmar Heuer

PLoS Pathog. 2015 Jun 4;11(6):e1004883

Chlamydia psittaci: New insights into genomic diversity, clinical pathology, host-pathogen interaction and anti-bacterial immunity

Michael R. Knittler, Angela Berndt, Selina Böcker, Pavel Dutow, Frank Hänel, Dagmar Heuer, Danny Kägebein, Andreas Klos, Sophia Koch, Elisabeth Liebler-Tenorio, Carola Ostermann, Petra Reinhold, Hans Peter Saluz, Gerhard Schöfl, Philipp Sehnert and Konrad Sachse

Int J Med Microbiol. 2014 Oct 304(7):877-893

Improved plaque assay identifies a novel anti-Chlamydia ceramide derivative with altered intracellular localization.

Sebastian Banhart, Essa M. Saied, Andrea Martini, Sophia Koch, Lukas Aeberhard, Kazimierz Madela, Christoph Arenz and Dagmar Heuer.

Antimicrob Agents Chemother 2014 Jul 58(9):5537-5546

Chlamydia psittaci induce Golgi fragmentation in human cells and interact with a reduced set of Golgi-related Rab proteins and depend on CERT function

Sophia Edelmann, Sebastian Banhart, Essa M. Saied, Andrea Martini, Lukas Aeberhard, Laura Rose and Dagmar Heuer

Pathogens and Disease, in preparation

Quantitative sphingolipids reveal the species-specific sphingolipid composition of elementary bodies from human and zoonotic Chlamydia species

Sophia Edelmann, Sebastian Banhart, Andrea Martini, Lukas Aeberhard, Laura Rose, Lukasz Japtok, Burkard Kleuser and Dagmar Heuer

Cellular Microbiology, in preparation

Talks

Blocking CERT-dependent ceramide transport leads to species-specific reduction of Chlamydia progeny formation.

Sophia Koch, Sebastian Banhart, Sophie Buerkle, Laura Rose, Lukas Aeberhard, Essa M. Saied, Lukasz Japtok, Burkhard Kleuser and Dagmar Heuer

67th Annual Meeting of the German Society of Hygiene and Microbiology, Münster 2015

Int J Med Microbiol. 2015 Sept 305(S1):165

Comparative analysis of Golgi structure in C. trachomatis and C. psittaci infections.

Sophia Koch, Sebastian Banhart, Andrea Martini, Lukas Aeberhard and Dagmar Heuer

12th German Chlamydia Workshop, Berlin 2014

Poster presentations

Characterizing the interaction of Chlamydia psittaci with the Golgi apparatus – a comparative analysis of a human and a zoonotic pathogen

Sophia Koch, Sebastian Banhart, Lukas Aeberhard, Sophie Bürkle, Anke Herrmann, Essa M. Saied and Dagmar Heuer

National German Symposium on Zoonoses Research 2014 & 7th International Conference on Emerging Zoonoses, Berlin 2014

Chlamydia interacts with the Golgi apparatus - understanding the underlying molecular mechanisms

Sophia Koch, Sebastian Banhart, Lukas Aeberhard, Frank Schmidt and Dagmar Heuer

SPP1580 Internal Meeting, Bonn 2015

Chlamydia trachomatis recruits the Golgi matrix protein golgin-84 - analyzing domains essential for recruitment of cellular proteins to the chlamydial inclusion

Sophia Koch, Sebastian Banhart, Lukas Aeberhard, Julia Heymann and Dagmar Heuer

SPP1580 International Meeting, Glashütten 2013

Chlamydia interacts with the Golgi apparatus - understanding the role of the cellular factors golgin-84, Rab6A and Rab11A

Sophia Koch, Sebastian Banhart, Lukas Aeberhard, Julia Heymann and Dagmar Heuer

2nd International Symposium for PhD Students on Protein Trafficking in Health and Disease, Hamburg 2012

Curriculum vitae

-- Aus datenschutzrechtlichen Gründen in der Online-Version nicht enthalten. --

Acknowledgements

First of all, I would like to express my sincere gratitude to my supervisor Dr. Dagmar Heuer, for the exciting project, for her enthusiasm, her motivation and her continuous support even in *extraordinary* situations. Dagmar provided great guidance and was always open for discussions thereby still giving me the right amount of freedom to explore and develop ideas on my own.

Besides my advisor, I would like to thank Prof. Dr. Markus Wahl for taking his time to serve as my second reviewer. Moreover, I want to thank Dr. Toni Aebischer for his insightful comments and for critical questions which helped to consider this project and methodologies from different perspectives.

My sincere thanks also go to Prof. Dr. Christoph Arenz and Dr. Essa Saied for the excellent cooperation and for synthesizing plenty of lipid analogues. I also owe thanks to Prof. Dr. Burkhard Kleuser and Dr. Lukasz Japtok for sharing their expertise and providing the opportunity to perform sphingolipid analytics.

I want to thank Dr. Kazimierz Madela for his great and vivid introduction into the RKI imaging facility and his friendly and skilled advices during many sessions at the microscope. I also thank Dr. Michael Laue and Gudrun Holland for their professional expertise and for valuable electron micrographs. I would further like to thank the RKI sequencing team for their quick and excellent sequencing service.

I owe special thanks to Dr. Sebastian Banhart, not only for reviewing almost every text fragment that I gave to him, but for sharing his experience and giving great support in applying imaging methods, for fruitful discussions and for “rectangular” thoughts that always helped to arrange my own ideas. I thank my fellow labmates Dr. Lukas Aeberhard and Laura Rose for the positive and inspiring atmosphere and for all the fun we have had in the last years. Andrea Martini, Anke Herrmann, Verena Keil you have always been great helps in all technical and practical lab issues – thank you!

I would like to thank my family for their encouragement and their continuous support during this thesis and my entire life.

And I thank Nicola for her patience, her open ears and open arms.

Selbständigkeitserklärung

Ich erkläre, dass ich die vorliegende Arbeit selbständig und nur unter Verwendung der angegebenen Literatur und Hilfsmittel angefertigt habe. Wurden Ergebnisse in Kooperation produziert, ist dies entsprechend angegeben.

Berlin, Januar 2016 Sophia Edelmann